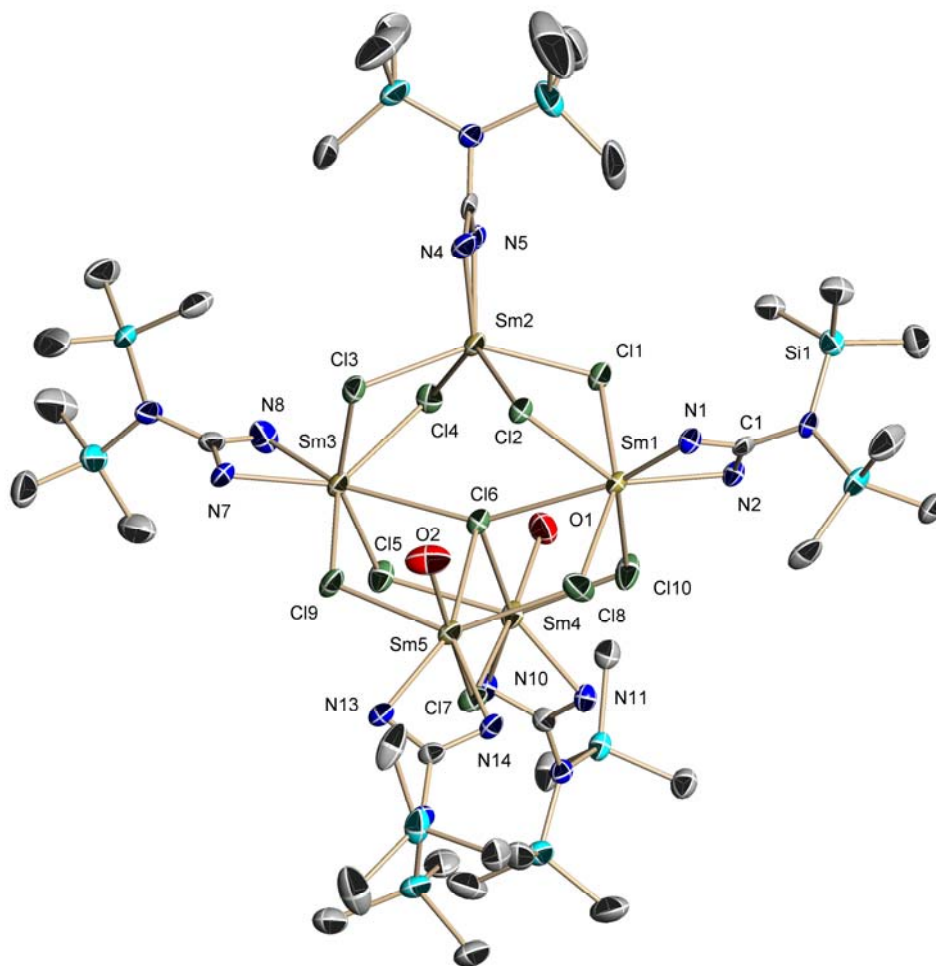


Zhensheng Zhang

---

**Oxygen Bridged Metal Systems:  
Heterometallic Compounds Containing Main Group  
Metal, Transition Metal and f-Elements**

---



**Oxygen Bridged Metal Systems:  
Heterometallic Compounds Containing Main Group  
Metal, Transition Metal and f-Elements**

Dissertation

zur Erlangung des Doktorgrades

der Mathematisch–Naturwissenschaftlichen Fakultäten

der Georg–August–Universität zu Göttingen

vorgelegt von

**Zhensheng Zhang**

aus Tianjin

(V. R. China)

Göttingen 2010

**D7**

**Referent: Professor Dr. Dr. h.c. mult. H. W. Roesky**

**Korreferent: Professor Dr. Dietmar Stalke**

**Tag der mündlichen Prüfung:**

*Dedicated to my parents  
For their love and affection*

## Acknowledgement

The work described in this doctoral dissertation has been carried out under the guidance and supervision of Professor Dr. Dr. h.c. mult. Herbert W. Roesky at the Institute of Inorganic Chemistry of the Georg-August-University in Göttingen between April 2005 and October 2010.

My sincere thanks and gratitude are due to

### **Professor Dr. Dr. h.c. mult. Herbert W. Roesky**

for his constant advice, guidance, motivation, suggestions, and discussions throughout this work. I would like to thank him for his personal attention and the freedom I enjoyed during my stay in Göttingen.

I would like to thank Prof. Dr. Dietmar Stalke, Prof. Carola Schulzke, Dr. R. Herbst-Irmer, Dr. T. Schulz, Prof. G. M. Sheldrick and Dr. B. Dittrich for their kind help in X-ray crystallographic studies. I could not have finished my research work without the help from technical and non technical staff from our institute. I thank Mr. W. Zolke, Mr. R. Schöne, and Dr. M. John (NMR spectra), Mr. T. Schuchardt (mass spectra), Mr. M. Hesse (IR spectra), the staff of the Analytical Laboratories and Werkstatt for their timely support during this research work.

I thank Mr. M. Schlote for his full collaboration with chemicals supporting.

I am thankful to Frau H. Tappe and Dr. A. C. Stückl for their kind help.

I thank all my colleagues for creating a lively work atmosphere and for having good support with me. I am grateful to Dr. H. Zhu, Dr. Z. Yang, Mr. Y. Yang and Dr. P. M. Gurubasavaraj for numerous fruitful discussions and their help during this work. I am thankful to Dr. S. Nagendran, Dr. S. K. Mandal, Dr. S. Singh, Dr. U. N. Nehete, Dr. L. Pineda, Dr. V. M. Jimenez-Perez, Dr. G. Nikiforov, Dr. C.-W. So, Dr. D. Ghoshal, Dr. N. D. Reddy, Dr. S. Nembenna, Dr. R. S. Ghadwal, Dr. Gasper Tavčar, Dr. A. Jana, Dr. B. Nekoueishahraki, Dr. Sarish Sankar, Dr. J. Li, Dr. S. Khan, Dr. R. Azhakar, Mr. S. S. Sen, Dr. C. Ene for their friendliness and for providing friendly work atmosphere.

I also thank Dr. X. Ma, Dr. Q. Zhang, Dr. K. Starke, Mr. A. Döring, M. Han for

their friendliness.

The full support and encouragement from my parents, and my family made this work possible.

## Abbreviations

$\delta$	chemical shift
$\lambda$	wavelength
$\mu$	bridging
$\nu$	wave number
A	activity
Ar	aryl
atm	atmosphere
br	broad
<i>n</i> Bu	<i>n</i> -butyl
°C	Celsius
calcd.	calculated
Cp	cyclopentadienyl
Cp*	pentamethyl cyclopentadienyl
d	doublet
decomp.	decomposition
DSC	differential Scanning Calorimetry
EI	electron impact ionization
Et	ethyl
equiv.	equivalents
eV	electron volt
g	grams
Hz	Hertz
<i>i</i> Pr	isopropyl
IR	infrared
<i>J</i>	coupling constant
K	Kelvin
L	ligand
M	metal

m	multiplet
MAO	methylaluminumoxane
$m/z$	mass/charge
M.p.	melting point
$M^+$	molecular ion
Me	methyl
min.	minutes
MS	mass spectrometry, mass spectra
NMR	nuclear magnetic resonance
Ph	phenyl
ppm	parts per million
q	quartet
R, R', R''	organic substituent
s	singlet
sept	septet
t	triplet
THF	tetrahydrofuran
$T_m$	melting points of polymers
TMS	tetramethylsilane
$V$	volume
$Z$	number of molecules in the unit cell
Ln	4f elements



<b>1. Introduction.....</b>	<b>1</b>
1.1. Multinuclear Metal Center Complexes as Polymerization Catalysts.....	1
1.2. Metal Hydroxides, Heterobi- and Heterotrimetallic Oxygen Bridged Complexes.....	2
1.3. Oxygen Bridged Rare Earth Complexes with Ln-O-M Moiety.....	5
1.4. Scope and Aim of the Present Work.....	6
<b>2. Result and Discussion.....</b>	<b>8</b>
2.1. Synthesis and Structural Characterization of Monomeric Heterobimetallic Oxides with an Al-O-M Skeleton.....	8
2.1.1. Synthesis, Structural Characterization, and Reactivity of the Ethyl Substituted Aluminum Hydroxide and Catalytic Properties of Its Derivative.....	8
2.1.1.1. Synthesis of LAIEt(Cl) (1) and LAIEt(OH) (2).....	9
2.1.1.2. Synthesis of LAIEt( $\mu$ -O)ZrMeCp <sub>2</sub> (3).....	10
2.1.1.3. X-ray Structural Analysis of LAIEt(OH) (2) and LAIEt( $\mu$ -O)ZrMeCp <sub>2</sub> (3).....	11
2.1.1.4. Ethylene Polymerization Studies.....	15
2.1.1.5. Polymer Properties.....	17
2.1.1.6. Synthesis of LAIEt( $\mu$ -O)M(THF)Cp <sub>2</sub> (M = Yb, 4; Er, 5; Dy, 6; Y, 7).....	17
2.1.2. Synthesis and Characterization of LAIPh( $\mu$ -O)M(THF)Cp <sub>2</sub> (M=Yb, 8; Er, 9).....	18
2.1.3. Synthesis of LAI Me( $\mu$ -O)Zr( <i>n</i> BuCp) <sub>2</sub> (10).....	19
2.2. Synthesis and Structural Characterization of Monomeric Heterobimetallic Oxides with a Ge(II)-O-M Skeleton (M=Yb, 11; Y, 12).....	21
2.3. Synthesis and Structural Characterization of [CH(C(Me)NH-2,6- <i>i</i> Pr <sub>2</sub> C <sub>6</sub> H <sub>3</sub> ) <sub>2</sub> ] <sup>+</sup> [(C <sub>6</sub> F <sub>5</sub> ) <sub>3</sub> B( $\mu$ -OH)B(C <sub>6</sub> F <sub>5</sub> ) <sub>3</sub> ] <sup>-</sup> (13).....	29
2.4. Synthesis and Characterization of (Cp <sup>*</sup> <sub>2</sub> ZrMeOLi) <sub>2</sub> (THF) <sub>2</sub> (14) and	

Cp* <sub>2</sub> PrN(SiMe <sub>3</sub> ) <sub>2</sub> (15).....	34
2.4.1. Synthesis and Characterization of (Cp* <sub>2</sub> ZrMeOLi) <sub>2</sub> (THF) <sub>2</sub> (14)...	34
2.4.2. Synthesis and Characterization of Cp* <sub>2</sub> PrN(SiMe <sub>3</sub> ) <sub>2</sub> (15).....	35
2.5. Synthesis and Characterization of (9-Oxidophenalenone) <sub>3</sub> Yb (16).....	38
2.6. Synthesis and Characterization of Organo-lanthanide Compounds with Guanidinato Ligand.....	40
2.6.1. Synthesis and Characterization of L' <sub>2</sub> SmBr (BrLi) (THF) <sub>2</sub> (17) and L' <sub>2</sub> Sm(THF)(μ-O)MeAIL ( L'=(Me <sub>3</sub> Si) <sub>2</sub> NC(NCy) <sub>2</sub> ) (18).....	40
2.6.1.1. Synthesis of [(Me <sub>3</sub> Si) <sub>2</sub> NC(NCy) <sub>2</sub> ] <sub>2</sub> SmBr <sub>2</sub> Li(THF) <sub>2</sub> (17).....	40
2.6.1.2. Synthesis of [(Me <sub>3</sub> Si) <sub>2</sub> NC(NCy) <sub>2</sub> ] <sub>2</sub> Sm(THF)(μ-O)MeAIL (18).....	41
2.6.2. Synthesis and Structural Characterization of L'LnCl <sub>2</sub> (LiCl) <sub>n</sub> (THF) <sub>m</sub> .....	43
2.6.2.1. Synthesis of [(Me <sub>3</sub> Si) <sub>2</sub> NC(NCy) <sub>2</sub> SmCl <sub>2</sub> ] <sub>5</sub> (THF) <sub>2</sub> (19).....	44
2.6.2.2. Synthesis of [(Me <sub>3</sub> Si) <sub>2</sub> NC(NCy) <sub>2</sub> YbCl <sub>2</sub> ] <sub>2</sub> (LiCl) <sub>2</sub> (THF) <sub>4</sub> (20)....	49
2.6.3 Synthesis of Heterotrimetallic Oxides.....	53
<b>3. Summary and Outlook.....</b>	<b>55</b>
3.1. Summary.....	55
3.2. Outlook.....	60
<b>4. Experimental Section.....</b>	<b>61</b>
4.1. General Procedures.....	61
4.2. Physical Measurements.....	61
4.3 Starting Materials.....	62
4.4 Syntheses of Compounds 1-20.....	62
4.4.1 Synthesis of LAIEt(Cl) (1).....	63
4.4.2 Synthesis of LAIEt(OH) (2).....	63
4.4.3 Synthesis of LAIEt(μ-O)ZrMeCp <sub>2</sub> (3).....	64
4.4.4 Synthesis of LAIEt(μ-O)Yb(THF)Cp <sub>2</sub> (4) .....	65
4.4.5 Synthesis of LAIEt(μ-O)Er(THF)Cp <sub>2</sub> (5).....	66

4.4.6 Synthesis of LAIEt( $\mu$ -O)Dy(THF)Cp <sub>2</sub> (6).....	66
4.4.7 Synthesis of LAIEt( $\mu$ -O)Y(THF)Cp <sub>2</sub> (7).....	67
4.4.8 Synthesis of LAIPh( $\mu$ -O)Yb(THF)Cp <sub>2</sub> (8).....	68
4.4.9 Synthesis of LAIPh( $\mu$ -O)Er(THF)Cp <sub>2</sub> (9).....	69
4.4.10 Synthesis of LAIME( $\mu$ -O)Zr( <i>n</i> BuC <sub>5</sub> H <sub>4</sub> ) <sub>2</sub> (10).....	69
4.4.11 Synthesis of LGe( $\mu$ -O)Yb(THF)Cp <sub>2</sub> (11).....	70
4.4.12 Synthesis of LGe( $\mu$ -O)Y(THF)Cp <sub>2</sub> (12).....	71
4.4.13 Synthesis of [CH(C(Me)NH-2,6- <i>i</i> Pr <sub>2</sub> C <sub>6</sub> H <sub>3</sub> ) <sub>2</sub> ] <sup>+</sup> [(C <sub>6</sub> F <sub>5</sub> ) <sub>3</sub> B( $\mu$ -OH)B (C <sub>6</sub> F <sub>5</sub> ) <sub>3</sub> ] <sup>-</sup> (13).....	71
4.4.14 Synthesis of (Cp <sup>*</sup> <sub>2</sub> ZrMeOLi) <sub>2</sub> (THF) <sub>2</sub> (14).....	72
4.4.15 Synthesis of Cp <sup>*</sup> <sub>2</sub> PrN(SiMe <sub>3</sub> ) <sub>2</sub> (15).....	73
4.4.16 Synthesis of (9-Oxidophenalenone) <sub>3</sub> Yb (16).....	73
4.4.17 Synthesis of [(Me <sub>3</sub> Si) <sub>2</sub> NC(NCy) <sub>2</sub> ] <sub>2</sub> SmBr <sub>2</sub> Li(THF) <sub>2</sub> (17).....	74
4.4.18 Synthesis of [(Me <sub>3</sub> Si) <sub>2</sub> NC(NCy) <sub>2</sub> ] <sub>2</sub> Sm(THF)( $\mu$ -O)MeAIL (18).....	75
4.4.19 Synthesis of [(Me <sub>3</sub> Si) <sub>2</sub> NC(NCy) <sub>2</sub> SmCl <sub>2</sub> ] <sub>5</sub> (THF) <sub>2</sub> (19).....	75
4.4.20 Synthesis of [(Me <sub>3</sub> Si) <sub>2</sub> NC(NCy) <sub>2</sub> YbCl <sub>2</sub> ] <sub>2</sub> (LiCl) <sub>2</sub> (THF) <sub>4</sub> (20).....	76
4.5. Polymerization of ethylene.....	76
4.6. Polymer characterization.....	77
<b>5. Handling and Disposal of Solvents and Residual Wastes.....</b>	<b>78</b>
<b>6. Crystal Data and Refinement Parameters.....</b>	<b>79</b>
<b>7. References.....</b>	<b>85</b>

## 1. Introduction

### 1.1. Multinuclear Metal Center Complexes As Polymerization Catalysts

Since the discovery of the catalytic olefin polymerization by Ziegler and Natta, transition metal oxides have been one of the hot topics in various academic and industrial fields.<sup>[1]</sup>

These oxides, which are commonly used as polyfunctional catalysts and precursors for the preparation of bi- and trimetallic heterogeneous catalysts, also can act as catalysts themselves and serve as models for the catalyst-substrate interaction.<sup>[2-5]</sup> The widespread research interest in this field of organometallic oxides is initiated by the remarkable properties of methylaluminoxane (MAO) as activator for metallocene catalysts in olefin polymerization<sup>[6,7]</sup> and the valuable catalytic properties of organorhenium oxides.<sup>[8]</sup> Investigations by Sinn and Kaminsky<sup>[9]</sup> indicated that soluble metallocene catalysts in combination with methylaluminoxane achieve extremely high activities in the polymerization of olefins.

These investigations are accompanied by an increased understanding of the factors that are important for stabilizing polymerization active metal centers and controlling their activity and selectivity. The design and synthesis of new transition metal precursors and main group organometallic cocatalysts became a very important subject which could provide high catalytic activity with low cocatalyst to catalyst precursor ratio. It also allows unprecedented control over the polymer microstructure generating new polymers with improved properties. Well-defined single-site metallocene catalysts are replacing the conventional heterogeneous Ziegler-Natta catalysts gradually. It has been one of the most attractive subjects in organometallic chemistry.<sup>[10-25]</sup>

Particularly, immense interest has been taken in the synthesis of multinuclear complexes for olefin polymerization which exhibit cooperative effects between their active metal centers. Marks *et al.*<sup>[26]</sup> reported that the binuclear compounds exhibit higher catalytic activity than the mononuclear complexes.

Another approach is using “tandem catalysis” for olefin polymerization.<sup>[27-38]</sup> In this type of catalysis, two separate single site olefin polymerization catalysts of zirconium and later transition metals were used in the same system to catalyze the polymerization reaction. The first single site catalytic center produces oligomers, which are subsequently incorporated into high molecular weight polymers by the second metallic center.

Since this type of polymerization requires intermolecular processes, it was speculated that the spatial proximity between two metallic centers might perform such functions more efficiently.<sup>[26]</sup> For single site olefin polymerization catalysts two connectivity strategies have been pursued to achieve cooperative effects via multinuclear complexes.<sup>[39]</sup> It was assumed that the dicationic bimetallic framework might exhibit enhanced comonomer binding affinity. Therefore the attractive possibility of bringing two catalytic centers in close constrained proximity offers the potential for significantly enhanced catalytic efficiency. By changing the environments on the ligands surrounding the metal centers (e.g. by introducing the bulky substituents on the Cp ring or by an intramolecular bridge), stereoregularity and molecular weight of the polymers can be controlled as the result of the different specifications of the active species.<sup>[40]</sup> Some heterobimetallic complexes are known to use as olefin polymerization catalysts in which transition metals are connected to other metals via cyclopentadienyl, phosphido, nitrogen ligands, and some alkoxide groups.<sup>[41]</sup>

## **1.2. Metal Hydroxides, Heterobi- and Heterotrimetallic Oxygen Bridged Complexes**

There is immense interest in the synthesis and characterization of novel main

group metal and transition metal hydroxide complexes due to their potential applications as precursor for the synthesis of heterobi- and heteropolymetallic compounds which can find application as catalysts, cocatalysts and models for fixation of the catalysts on oxide surfaces.<sup>[42]</sup>

Recently, H. W. Roesky *et al.* have successfully reported the synthesis of several unique molecular hydroxides bearing  $\beta$ -diketiminato ligands e.g. on aluminum (LMeAl(OH),  $\text{LAl(OH)}_2$ , and  $[\text{LAl(OH)}]_2\text{O}$ ),<sup>[43]</sup> gallium (LMeGa(OH), and  $\text{LGa(OH)}_2$ ),<sup>[44]</sup> germanium (LGe(OH)),<sup>[45]</sup> magnesium (LMg(OH)) and calcium (LCa(OH))<sup>[46]</sup> and strontium (LSr(OH)).<sup>[47]</sup> Also two transition metal hydroxides were reported bearing Cp\* on zirconium ( $\text{Cp}^*_2\text{Zr(Me)OH}$ ).<sup>[48]</sup> (Chart 1)

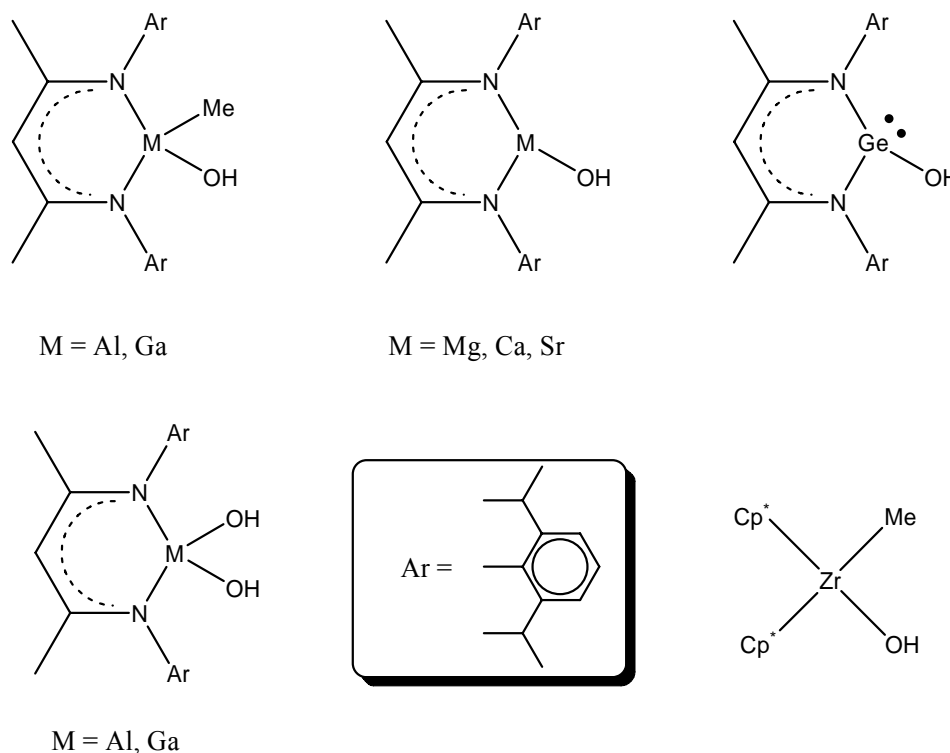


**Chart 1.** Main group and transition metal hydroxides.

Using these unprecedented hydroxide precursors, H. W. Roesky *et al.* reported a series of bimetallic complexes, some of which were tested as catalysts for the polymerization reactions.<sup>[43-51]</sup> (Chart 2) These oxygen bridged bimetallic complexes exhibit high activity in presence of a cocatalyst to give polymer with tunable



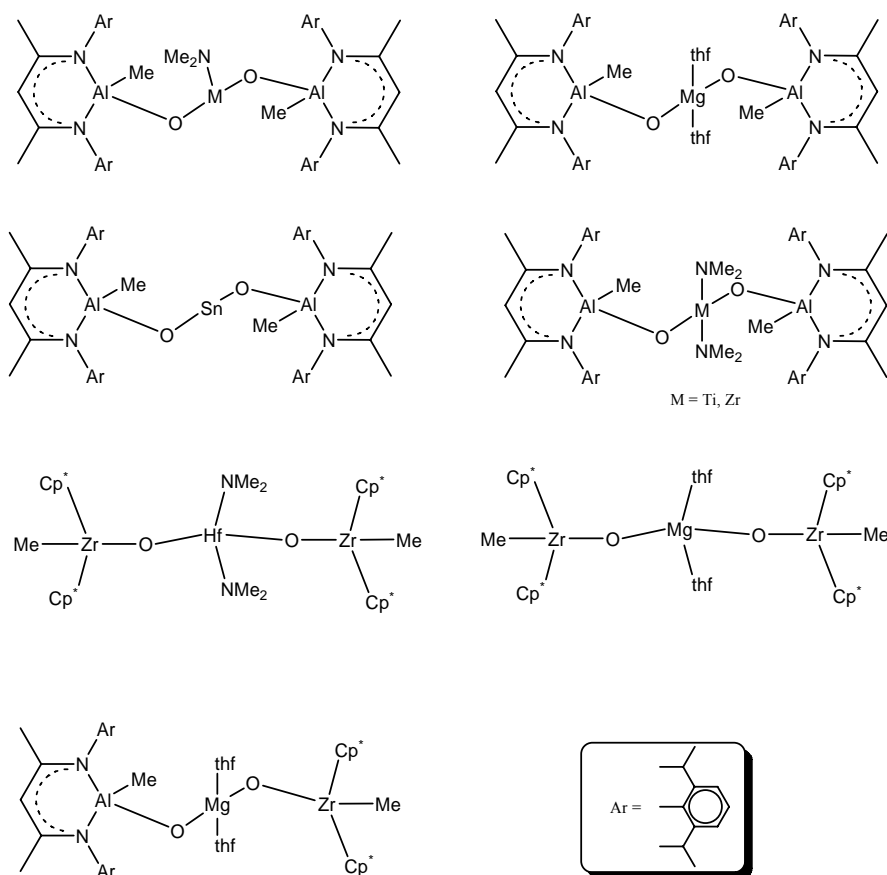


**Chart 3.** Heterotrimetallic oxygen bridged complexes.

### 1.3. Oxygen Bridged Rare Earth Complexes with Ln-O-M Moiety

Lanthanides offer a new frontier in organometallic chemistry. It is of wide interest to develop the chemistry of lanthanides containing heterometal atoms.<sup>[60]</sup> One aspect is the synthesis of mixed-metal solid-state materials with unusual physical properties.<sup>[61]</sup> The other is the fact that lanthanide aluminum heterobimetallic complexes are good catalysts for the polymerization of olefinic monomers, methyl methacrylate (MMA), lactones, and cyclic carbonates.<sup>[62]</sup> It is analogous to the development of group 4 metal and aluminum bimetallic olefin polymerization catalysts.<sup>[63]</sup> A variety of structural types and compositions have been identified under the work of Evans<sup>[60a, 64]</sup> and Yasuda<sup>[62, 65]</sup> on the synthesis and catalytic properties of the lanthanide aluminum heterometallic complexes. However, the majority of them are aluminum alkyl adducts formed through OR or OAr bridges.<sup>[60, 65]</sup>

H. W. Roesky *et al.* developed a synthetic strategy to incorporate rare-earth



metals on Al-O systems to generate compounds containing the Ln-O-Al unit,<sup>[66]</sup> where the oxygen atom is not bonded to alkyl or aryl groups (Chart 4).

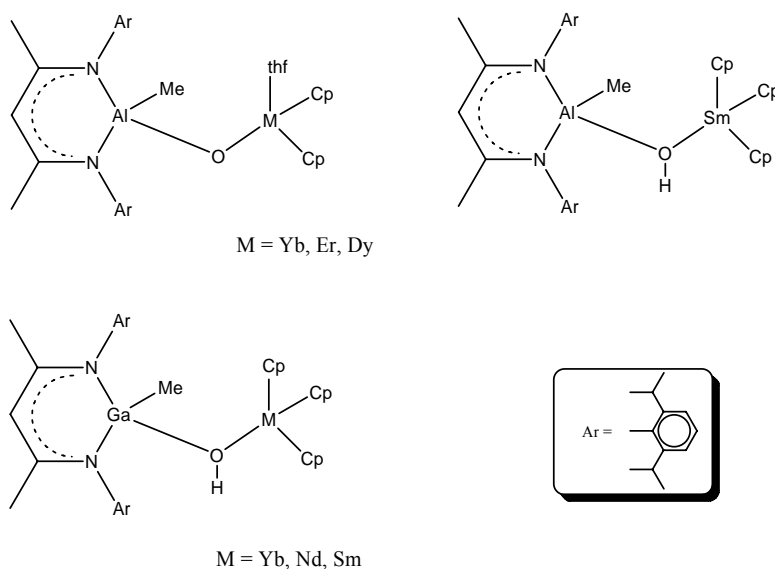


**Chart 4.** Heterobimetallic oxygen bridged complexes containing the M-O-Ln unit

We were encouraged with the result that the Ln-O-Al unit provided a stable framework to assemble new complexes of practical application such as catalysts. It is believed that the study of heterobimetallic lanthanide is not only an attractive subject of academic research but also relevant to the applied aspects of their chemistry.

It is of significant interest to introduce various metal hydroxides forming novel M-O-Ln or M-O-Ln-O-M units and to modify the fundamental properties of the individual metal atoms.

Another challenge is to prepare bimetallic complexes with Ln-O-Ln moieties. Although a few structures containing Ln-O-Ln have been reported so far,<sup>[67]</sup> most of them were obtained under unforeseen conditions.

#### 1.4. Scope and Aim of the Present Work

The above discussion shows that the heterometallic complexes have remarkable properties and can exhibit functional catalysts for olefin polymerization, especially for the heterobi- and trimetallic complexes with oxygen-bridged M-O-M' motif. Furthermore, well-defined oxygen-bridged rare earth complexes which are rationally

prepared by using the metal-hydroxide precursors are exhibiting higher catalytic activity and have been one of the most attractive subjects in organometallic chemistry. Based on these premises, the objectives of the present work are:

1. To develop new synthetic strategies for the preparation of oxygen bridged heterobi- and trimetallic complexes.
2. To find new effective ligands to modify the stability and reactivity of lanthanide complexes.
3. To introduce different metal hydroxides to lanthanide complexes to form novel M-O-Ln or M-O-Ln-O-M moieties.
4. To prepare new molecules of lanthanides that can be used as catalysts with high efficiency.

## 2. Results and Discussion

### 2.1. Synthesis and Structural Characterization of Monomeric Heterobimetallic Oxides with an Al–O–M Skeleton

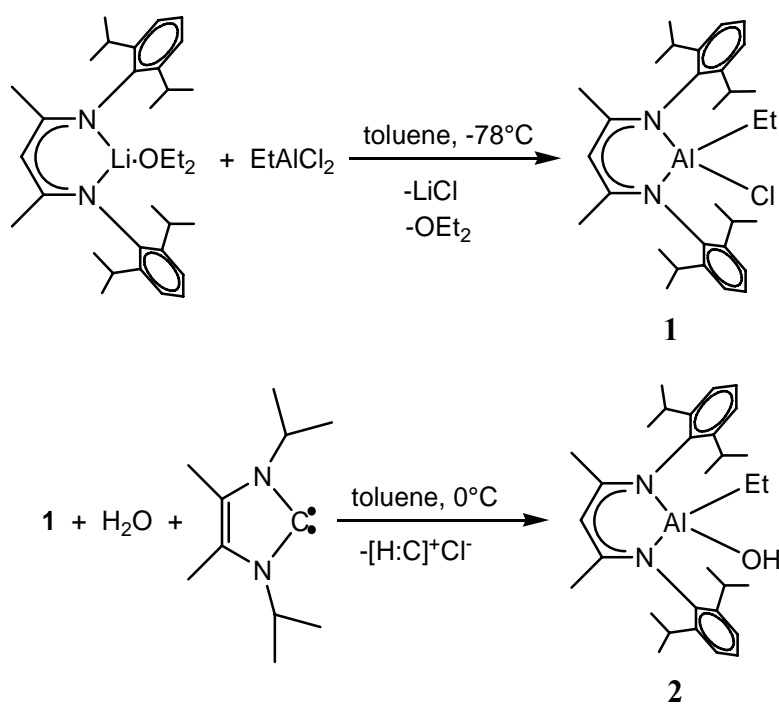
#### 2.1.1. Synthesis, Structural Characterization, and Reactivity of the Ethyl Substituted Aluminum Hydroxide and Catalytic Properties of Its Derivative

Well-defined heterobimetallic oxides have attracted extensive attention to acquire structurally unusual materials or potentially good catalysts.<sup>[50, 68]</sup> So far, various approaches were proposed both in chemistry and material science,<sup>[69]</sup> among which an elaborate strategy via organometallic hydroxides distinguished itself to be a facile route to form the M–O–M' unit in compounds without bridging OR or OAr arrangements. Especially in the course of design and synthesis of single-site homogeneous catalysts containing Al–O–M' (M' = Zr, Ti, Ln) moiety, our laboratory developed the unprecedented aluminum monohydroxide with a terminal OH group, LAI Me(OH),<sup>[43]</sup> supported by the sterically hindered  $\beta$ -diketiminato ligand (L = HC[C(Me)N(Ar)]<sub>2</sub>, Ar = 2,6-*i*Pr<sub>2</sub>C<sub>6</sub>H<sub>3</sub>). LAI Me(OH) turned out to be a suitable synthon to successfully prepare a series of new compounds LAI Me( $\mu$ -O)ZrRCp<sub>2</sub> (R = Me, Cl) and LAI Me( $\mu$ -O)Ln(THF)Cp<sub>2</sub> (Ln = Yb, Er, Dy) with well-defined structures and noticeable catalytic activity.<sup>[43, 66]</sup> Recent ab initio calculations showed that in the M–O–M' system the oxygen is responsible for the depletion of the electron density at the metal centers.<sup>[48, 50]</sup> Furthermore, our interest was intrigued by varying the group R on the aluminum site to extend the perspective of LAIR(OH). In this regard, we report on the preparation and structural characterization of ethyl substituted aluminum hydroxide LAIEt(OH) (**2**). The reactivity of this OH group was examined by the reactions with Cp<sub>2</sub>ZrMe<sub>2</sub> and Cp<sub>3</sub>M (M = Yb, Er, Dy, Y) to form the desired oxo bridged heterobimetallic oxides. The catalytic activity of the zirconium derivative

$\text{LAIEt}(\mu\text{-O})\text{ZrMeCp}_2$  (**3**) was preliminarily investigated in ethylene polymerization.

### 2.1.1.1. Synthesis of $\text{LAIEt}(\text{Cl})$ (**1**) and $\text{LAIEt}(\text{OH})$ (**2**)

Compound **1** was obtained in high yield by the reaction of  $\text{LLi}\cdot\text{OEt}_2$  with 1 equiv. of  $\text{EtAlCl}_2$  in toluene (Scheme 1). Subsequent hydrolysis of compound **1** was carried out with 1 equiv. of  $\text{H}_2\text{O}$  in the presence of 1,3-diisopropyl-4,5-dimethylimidazol-2-ylidene (abbreviated as  $:\text{C}$ ) as a  $\text{HCl}$  acceptor<sup>[70]</sup> in toluene at  $0^\circ\text{C}$  to afford compound **2** as a white solid. Compound  $[\text{H}:\text{C}]^+\text{Cl}^-$  is nearly insoluble in toluene and can be removed by filtration.



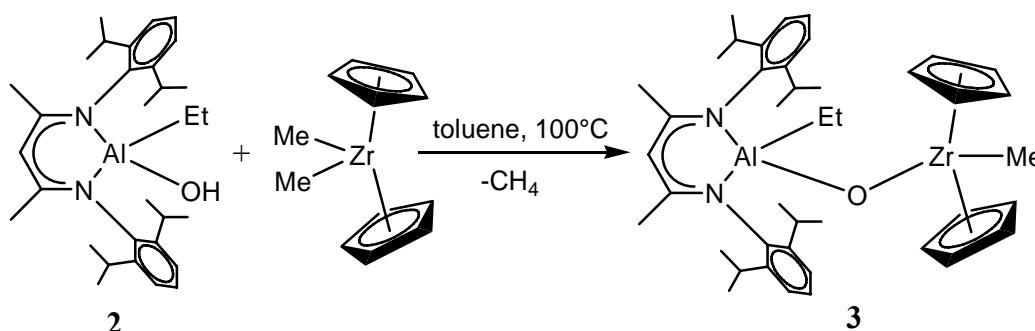
**Scheme 1.**

The composition of both compounds was confirmed by analytical and spectroscopic methods. The  $^1\text{H}$  NMR spectrum of **1** shows one quartet ( $\delta$  -0.04 ppm) and one triplet ( $\delta$  0.80 ppm) corresponding to methylene and methyl proton resonances of the ethyl group on aluminum, while in the  $^{13}\text{C}$  NMR spectrum the resonances of these groups are assigned to  $\delta$  -1.0 and 8.5 ppm. In contrast, in the  $^1\text{H}$  NMR spectrum of **2** the methylene and methyl proton resonances of the ethyl group

on aluminum show upfield shifts ( $\delta$  -0.23 and 0.71 ppm) relative to those of **1**, whereas the corresponding  $^{13}\text{C}$  NMR resonances are shifted apart ( $\delta$  -2.4 and 9.2 ppm). The singlet ( $\delta$  0.63 ppm) in the  $^1\text{H}$  NMR spectrum of **2** is assigned to the OH proton resonance, while for  $\text{LAlMe}(\text{OH})$  this resonance was observed at  $\delta$  0.53 ppm.<sup>[43]</sup> This downfield shift is probably due to the electronic effect of the substituent changing from methyl to ethyl on aluminum. In the IR spectrum of **2**, the OH stretching frequency is found at  $3729\text{ cm}^{-1}$ . The mass spectrum of **2** indicates the monomeric composition with  $m/z$  (%) 473 (24)  $[\text{M}^+-\text{OH}]$  and 461 (100)  $[\text{M}^+-\text{Et}]$ .

### 2.1.1.2. Synthesis of $\text{LAlEt}(\mu\text{-O})\text{ZrMeCp}_2$ (**3**)

Reaction of **2** with 1 equiv. of  $\text{Cp}_2\text{ZrMe}_2$  in toluene at  $100\text{ }^\circ\text{C}$  afforded the  $\mu\text{-O}$  bridged  $\text{LAlEt}(\mu\text{-O})\text{ZrMeCp}_2$  (**3**) (Scheme 2) accompanied by methane evolution.



**Scheme 2.**

The mass spectrum of **3** exhibits a peak at  $m/z$  (%) 709 (88) representing the fragment  $[\text{M}^+-\text{Me}]$ . In the  $^{13}\text{C}$  NMR spectrum of **3** the characteristic Cp resonances appear at  $\delta$  109.9 ppm. The  $^1\text{H}$  NMR spectrum displays the Cp resonances as singlet ( $\delta$  5.30 ppm). At high field, one singlet ( $\delta$  -0.32 ppm) is assigned to the Me protons of  $\text{ZrMe}$ , while one quartet ( $\delta$  -0.14 ppm) and one triplet ( $\delta$  1.14 ppm) are attributed to the methylene and methyl proton resonances of the  $\text{AlEt}$  group. No hydroxyl proton resonance is observed in the expectable range, which is consistent with the absence of any OH absorption in the range  $3600\text{--}3800\text{ cm}^{-1}$  in the IR spectrum.<sup>[43]</sup>

### 2.1.1.3. X-ray Structural Analysis of $\text{LAlEt(OH)}$ (**2**)<sup>[71]</sup> and $\text{LAlEt}(\mu\text{-O})\text{ZrMeCp}_2$ (**3**)

Keeping the THF solution of **2** at 4 °C overnight resulted in colorless X-ray quality crystals. The structure of **2** is depicted in Figure. 1. Compound **2** crystallizes in the orthorhombic space group  $P2_12_12_1$  and shows a mononuclear composition with an aluminum center in a distorted tetrahedral geometry coordinated to the chelating  $\beta$ -diketiminato ligand, an ethyl, and an OH group. Selected bond lengths and angles are listed in Table 1. On the one hand the  $\text{N}(1)\text{-Al-N}(2)$  angle ( $95.32(8)^\circ$ ) is even smaller than that of  $\text{LAlMe(OH)}$  ( $96.3(1)^\circ$ )<sup>[43]</sup>, on the other the  $\text{Al-O}$  bond length ( $1.7409(17)\text{\AA}$ ) is slightly longer than those of  $\text{LAlMe(OH)}$  ( $1.731(3)\text{\AA}$ ) and  $\text{LAl(OH)}_2$  ( $1.695(15)$ ,  $1.711(16)\text{\AA}$ ),<sup>[43b]</sup> and comparable to the terminal ones of  $[\text{LAl(OH)}]_2(\mu\text{-O})$  ( $1.738(3)$ ,  $1.741(3)\text{\AA}$ ).<sup>[43c]</sup>

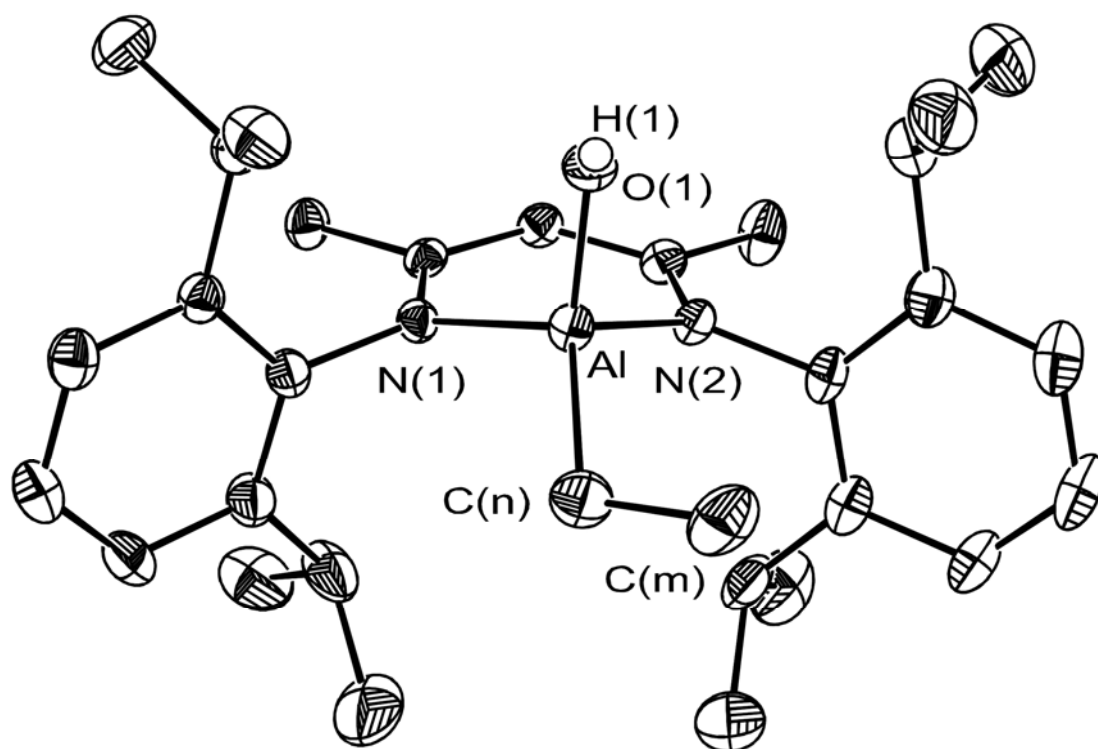


**Figure. 1.** Molecular structure of **2**. Thermal ellipsoids are drawn at the 50% level, and the hydrogen atoms of the ligand and the two THF molecules are omitted for clarity.

Compound **3** crystallizes in the orthorhombic space group  $Pnma$  (Figure. 2). Table

CD1 and table CD2 show the crystal data and structure refinement for compounds **2**·(THF)<sub>2</sub> and **3**. The ethyl group on Al and the methyl group on Zr are located in the same Al–O–Zr plane and stay away from each other in a *trans* conformation. The Al–O bond length (1.7285(10)Å) falls in between those of LAlMe( $\mu$ -O)ZrMeCp<sub>2</sub> (1.711(2) Å)<sup>[43]</sup> and of **2** (1.7409(17)Å), while the Al–C distance (1.9688(14)Å) is comparable to that of **2** (1.965(3) Å). The Zr–O bond separation (1.9424(10)Å) is slightly longer than that of LAlMe( $\mu$ -O)ZrMeCp<sub>2</sub> (1.929(2) Å)<sup>[43]</sup>, because of more steric repulsion by the ethyl group compared to its methyl counterpart. The Al–O–Zr angle (144.41(6)°) is obviously narrower than that of LAlMe( $\mu$ -O)ZrMeCp<sub>2</sub> (158.2(1)°)<sup>[43]</sup>. Selected bond distances and bond lengths for compounds **2** and **3** are shown in Table 1.

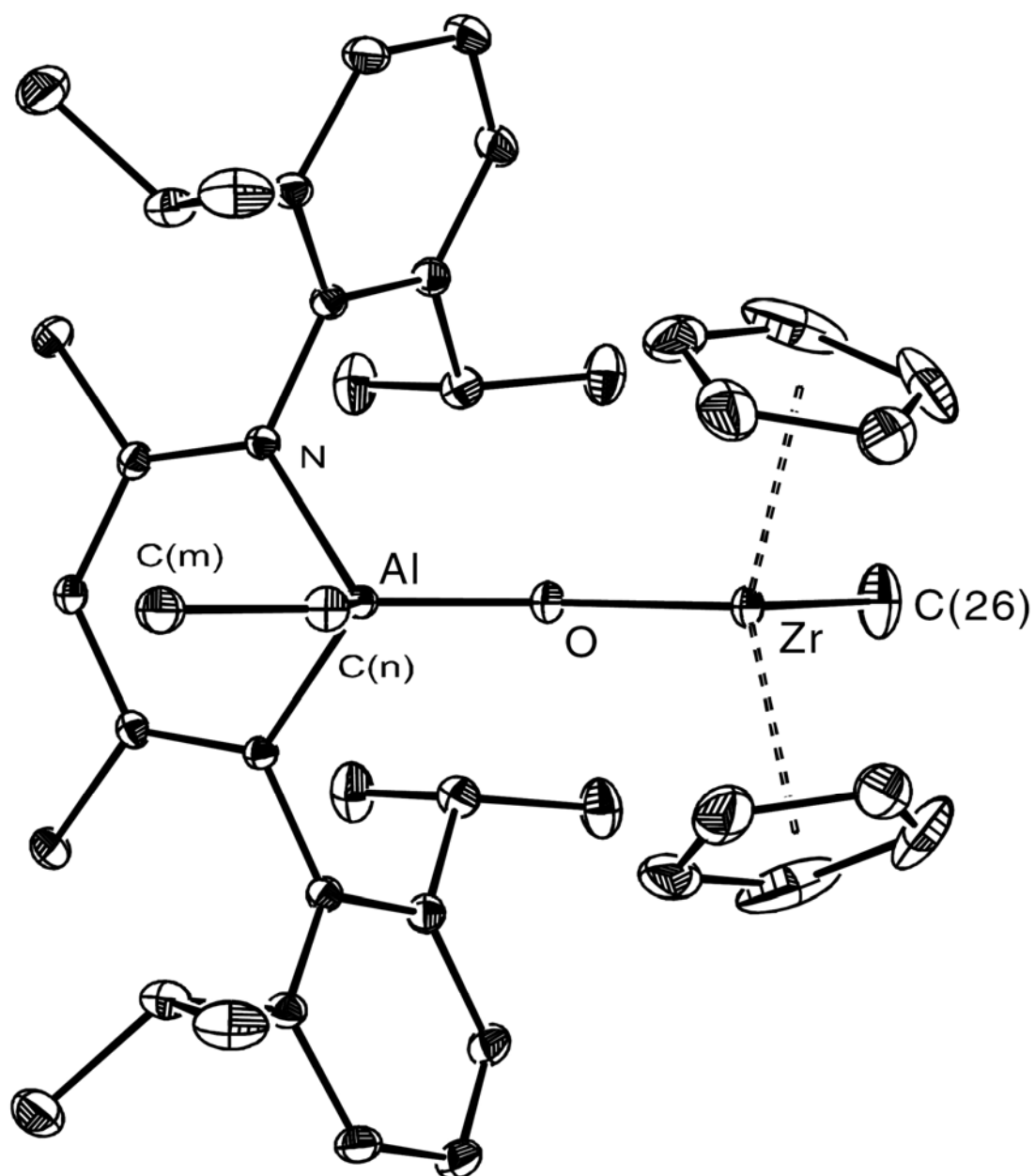


**Figure 2.** Molecular structure of **3**. Hydrogen atoms are omitted for clarity.



**Table 1.** Selected bond distances (Å) and angles (°) for compounds **2** and **3**

	<b>2</b>	<b>3</b>
Al–O	1.7409(17)	1.7285(10)
Al–N(1)	1.9047(18)	1.9213(8)
Al–N(2)	1.9147(19)	1.9213(8)
Al–C	1.965(3)	1.9688(14)
C(m)–C(n) <sup>a</sup>	1.533(4)	1.528(2)
Zr–O		1.9424(10)
Zr–X <sub>Cp</sub>		2.267
O–Al–N(1)	109.42(8)	112.68(3)
O–Al–N(2)	105.80(9)	112.68(3)
N(1)–Al–N(2)	95.32(8)	96.59(5)
O–Al–C	115.70(11)	109.34(5)
N(1)–Al–C	113.60(10)	112.58(3)
N(2)–Al–C	114.95(10)	112.58(3)
C(m)–C(n)–Al <sup>a</sup>	115.04(19)	121.35(10)
Al–O–Zr		144.41(6)
X <sub>Cp1</sub> –Zr–X <sub>Cp2</sub>		127.73

<sup>a</sup> C(m) and C(n) stand for the methyl and methylene carbon of AlEt group.

In both cases, the Al and  $\gamma$ -C atoms are arranged out of the NCCN plane to exhibit a boat conformation as shown in the simplified side view of **2** and **3** (Figure. 3). Interestingly, the direction of this arrangement turns upside down when a more bulky substituent than a proton is attached to the oxygen atom, while the angles of N(1)–Al–N(2) and N–Al–C remain almost the same. This property of the ligand ensures both stability and flexibility in such a system.

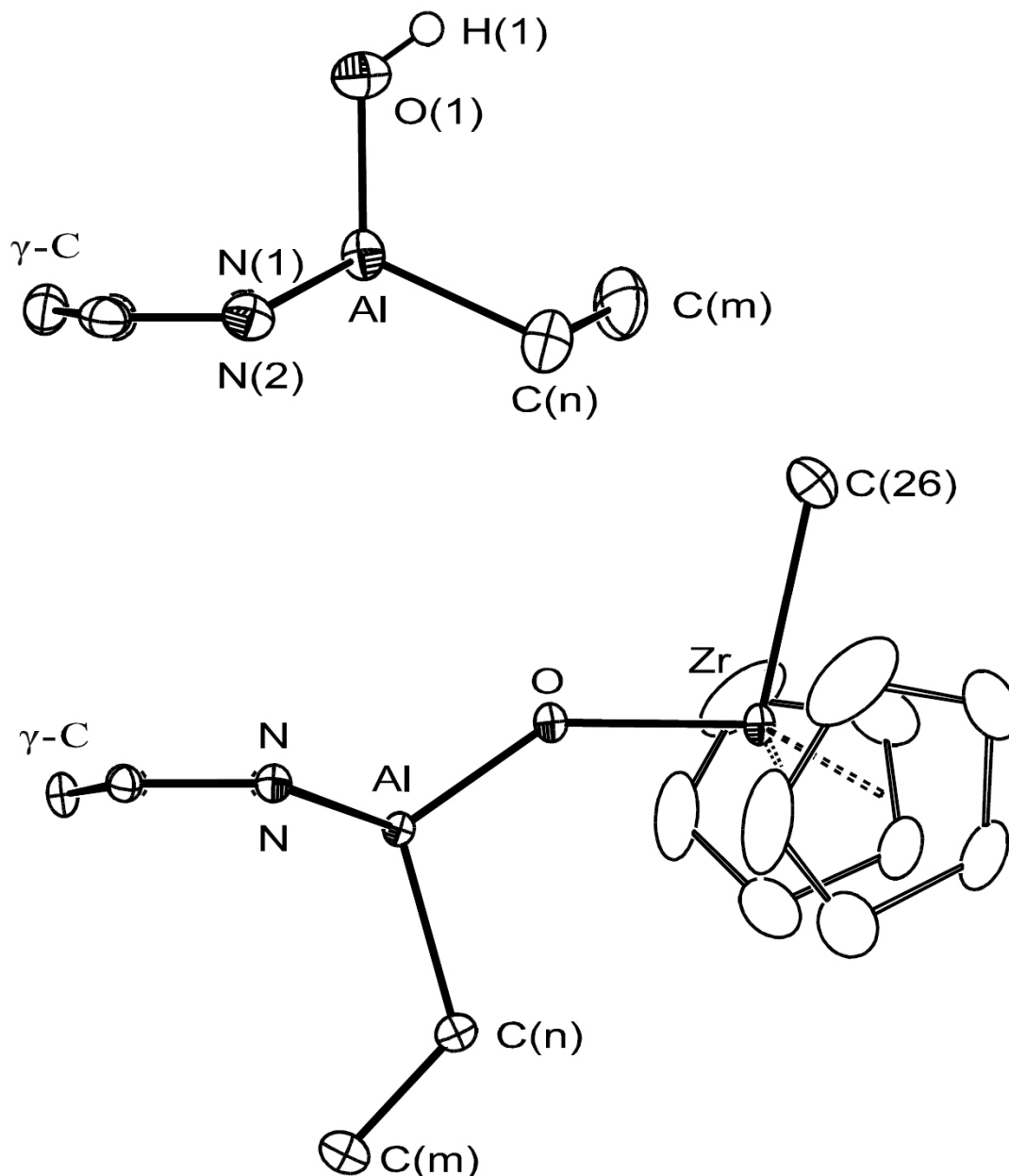


**Figure 3.** Side view of compounds **2** and **3**. Only selected atoms are included for clarity.

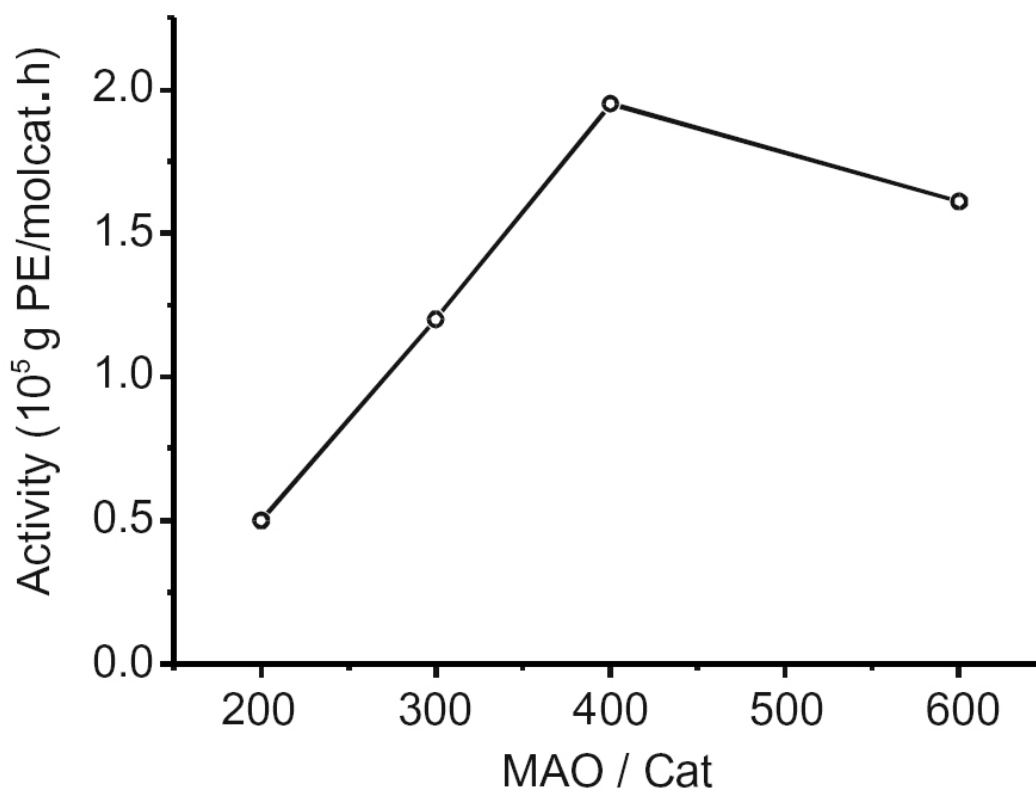
#### 2.1.1.4. Ethylene Polymerization Studies.

Table 2 summarizes the polymerization results of catalyst **3**. All polymeric materials were isolated as white powders. Under comparable polymerization conditions, the methylalumoxane (MAO)/**3** catalyst system shows lower activity compared to that of MAO/LAlMe( $\mu$ -O)ZrMeCp<sub>2</sub>.<sup>[43]</sup> However, the MAO activated

compound **3** still exhibits good catalytic activity for the polymerization of ethylene. Figure. 4 visualizes the MAO/**3** ratio dependence activity, which reveals a gradual increase in the activity with the MAO/**3** till to 400, followed by a slow decrease as the MAO/**3** ratio is raised further.

Table 2. Ethylene polymerization for compound **3** (12.4  $\mu$ mol) in 100 mL of toluene under 1 atm ethylene pressure at 25 °C

Catalyst	MAO/ <b>3</b>	t(min)	PE(g)	Activity	
				(10 <sup>5</sup> g PE/molcat.h)	T <sub>m</sub> (°C)
3	200	30	0.31	0.50	123
3	300	30	0.75	1.20	127
3	400	30	1.21	1.95	121
3	600	30	1.01	1.61	119

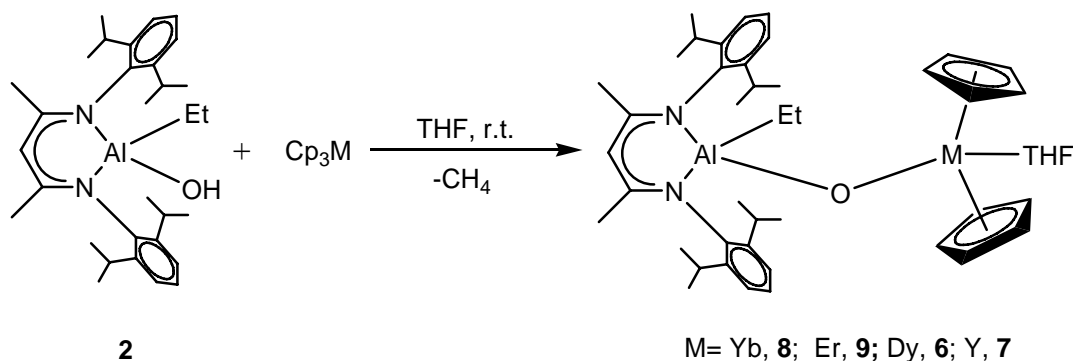


**Figure 4.** Activity against MAO to catalyst ratio of **3**.**2.1.1.5. Polymer Properties.**

DSC measurements show that the melting points ( $T_m$ ) of the polyethylene produced by MAO activated **3** are in the range of 119–127 °C, somewhat lower than the typical range for linear polyethylene. The  $^{13}\text{C}$  NMR data exhibit a resonance ( $\delta$  29.81 ppm) corresponding to the backbone carbon of the linear polyethylene.

**2.1.1.6. Synthesis of  $\text{LA}(\text{Et})(\mu\text{-O})\text{M}(\text{THF})\text{Cp}_2$  ( $\text{M} = \text{Yb}$ , **4**;  $\text{Er}$ , **5**;  $\text{Dy}$ , **6**;  $\text{Y}$ , **7**)**

In contrast to the previous elimination of  $\text{CH}_4$ , the reaction of compound **2** with 1 equiv. of  $\text{Cp}_3\text{M}$  in THF at room temperature resulted in an intermolecular elimination of  $\text{HCp}$  to render the yttrium and rare earth metal derivatives  $\text{LA}(\text{Et})(\mu\text{-O})\text{M}(\text{THF})\text{Cp}_2$  ( $\text{M} = \text{Yb}$ , **4**;  $\text{Er}$ , **5**;  $\text{Dy}$ , **6**;  $\text{Y}$ , **7**) (Scheme 3).

**Scheme 3.**

The melting points of **4**, **6**, and **7** are in the range from 208 to 210 °C, and for **5** it is 235 °C. In an average they are 40 °C lower compared to those of the corresponding methyl analogues,<sup>[66]</sup> which could be attributed to the different alkyl group on aluminum. IR spectra of **4**, **5**, **6**, and **7** are free of any OH absorption in the expected range. The mass spectra of **4**, **5**, and **6** exhibit the most intense peak  $[\text{M}^+ \text{-THF-Et}]$  with isotopic pattern, followed by  $[\text{M}^+ \text{-THF-Et-Cp}]$ . In the mass spectrum of **7**, the base peak is assigned to the fragment  $[\text{M}^+ \text{-Et-Y}(\text{THF})\text{Cp}_2]$ .

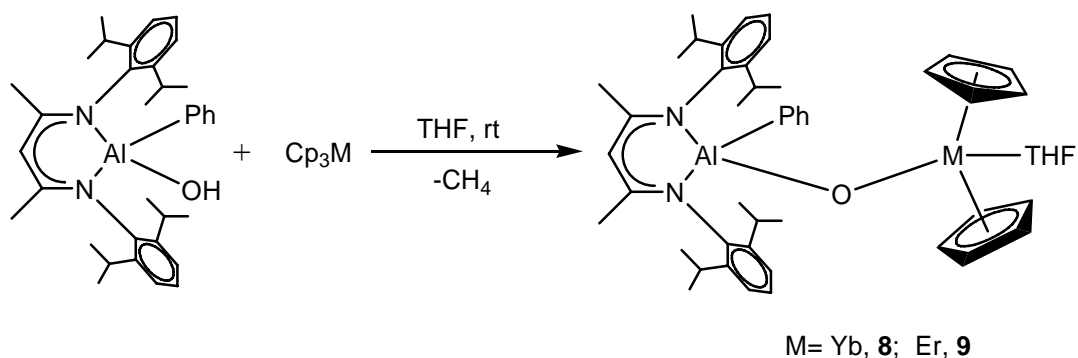
Because of the paramagnetic properties of the three lanthanide elements, it is not

meaningful to describe the detailed NMR spectra of **4**, **5**, and **6** in solution, whereas the data of the yttrium analogue LAIEt( $\mu$ -O)Y(THF)Cp<sub>2</sub> (**7**) could be helpful for characterizing these systems. In the <sup>13</sup>C NMR spectrum of **7** the Cp resonances are found at  $\delta$  110.0 ppm. In the <sup>1</sup>H NMR spectrum, the Cp resonances appear as singlet ( $\delta$  5.85 ppm), while one quartet ( $\delta$  0.40 ppm) and one triplet ( $\delta$  1.60 ppm) are assigned to the methylene and methyl proton resonances of the AlEt group. Two broad resonances ( $\delta$  1.34 and 3.08 ppm) correspond to those of the protons of the coordinated THF. The absence of a hydroxyl proton resonance additionally confirms the formation of **7** by intermolecular elimination of HCp. It is worth mentioning that all <sup>1</sup>H and <sup>13</sup>C resonances of the substituents on the metal centers of **7** exhibit a downfield shift when compared with those of **3**, which may be related to the change of the chemical environment.

### 2.1.2. Synthesis and Characterization of LAIPh( $\mu$ -O)M(THF)Cp<sub>2</sub> (M=Yb, Er)

Previously the successful application of methyl-substituted aluminum hydroxide LAiMe(OH) and ethyl-substituted aluminum hydroxide LAiEt(OH) ( L=HC[C(Me)N(Ar)]<sub>2</sub>, Ar=2,6-*i*Pr<sub>2</sub>C<sub>6</sub>H<sub>3</sub> ) with Cp<sub>3</sub>Ln to prepare the  $\mu$ -oxygen bridged M-O-Ln unit ( Ln=lanthanide ) encouraged us to extend these investigations with a variety of functionalized aluminum compounds. Further efforts were made to use phenyl-substituted aluminum hydroxide LAIPh(OH)<sup>[72]</sup> to prepare the corresponding derivatives.

The reaction of compound LAIPh(OH) with 1 equiv. of Cp<sub>3</sub>Ln in THF at room temperature resulted in an intermolecular elimination of HCp to afford rare earth metal derivatives LAIEt( $\mu$ -O)Ln(THF)Cp<sub>2</sub> (Ln = Yb, **8**; Er, **9**). (Scheme 4)



Scheme 4

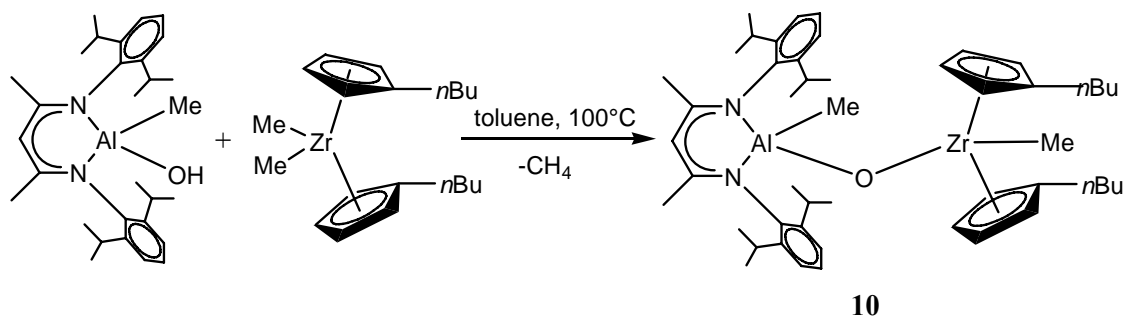
The melting point measurements resulted in decomposition which might be attributed to the bulky phenyl group on aluminum. In contrast to the increasing melting point, **8** and **9** obtained a better solubility in organic solvents. IR spectra of **8** and **9** are free of OH absorption in the expected range. The mass spectra of **8** and **9** exhibit the basic unit as  $[M^+ \text{-THF-Ph}]$ . Due to the paramagnetic properties of the Yb and Er elements, it is not meaningful to describe the detailed NMR spectra of **8** and **9**.

### 2.1.3. Synthesis of $LAlMe(\mu\text{-O})Zr(nBuC_5H_4)_2(10)$

As we know, most of the efforts being made to produce the  $LAlR(\mu\text{-O})\text{-MR}'Cp_2$  ( $M=\text{Zr, Ln}$ ,  $R'=\text{Me}$  or  $\text{THF}$ ) are focussed on varying the group R on the aluminum site to improve the activity and thermal stability of catalysts containing the M-O-M' moiety.

Herein, a flexible group was introduced to the Cp ligand on Zr with a further step to prepare the oxo-bridged heterobimetallic systems intending to explore its reactivity.

$(nBuC_5H_4)_2ZrMe_2$  was prepared according to the literature procedure<sup>[73]</sup> from MeLi and  $(nBuC_5H_4)_2ZrCl_2$ . Because of its stickiness, it reacted with 1 equiv. of  $LAlMe(OH)$  directly in situ to afford  $LAlMe(\mu\text{-O})\text{-ZrMe}(nBuC_5H_4)_2$  as expected.



Scheme 5

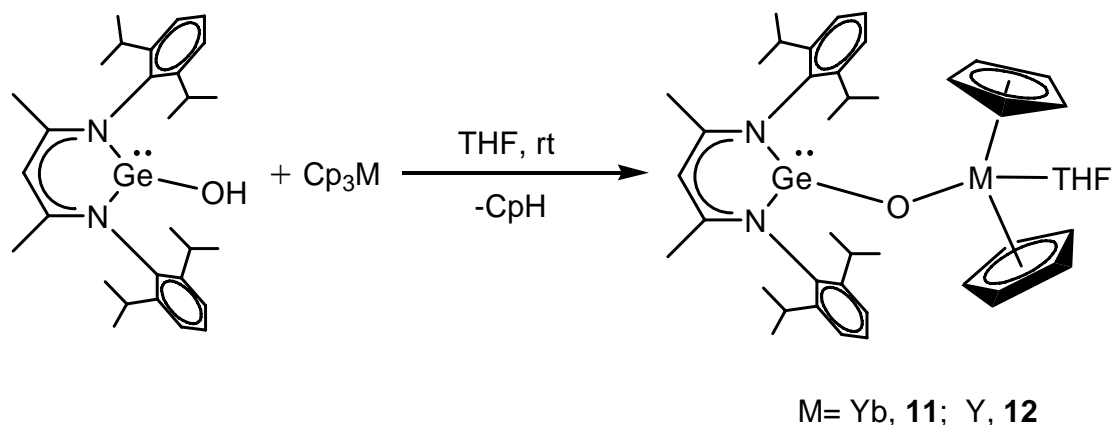
The IR spectra indicated that no hydroxyl absorption is observed in the expected range, which is consistent with the absence of any OH band. Mass spectrum exhibits a ion of  $m/z$  (%) 809(82) which represents the fragment  $[\text{M}^+-\text{Me}]$ . The  $^1\text{H}$  NMR spectrum of **10** shows four resonances at lower field ( $\delta$  5.05, 5.11, 5.26, 5.57 ppm) corresponding to  $n\text{BuC}_5\text{H}_4$  proton resonances. It is obvious from the singlet resonance of  $\text{LAIEt}(\mu\text{-O})\text{ZrMeCp}_2$  that the Cp group is flexible on the nmr time scale.

## 2.2. Synthesis and Structural Characterization of Monomeric Heterobimetallic Oxides with a Ge(II)–O–M Skeleton (M=Yb, Y)

Well-defined heterobimetallic oxides not only involve synthetic challenges in chemistry but also potentially provide prolific precursors for practical application.<sup>[1, 5]</sup> In recent years, several organometallic hydroxides have been developed with the purpose of preparing structurally characterized oxides containing the M-O-M' moiety.<sup>[50]</sup> Starting from the monomeric aluminum hydroxide  $\text{LAl}(\text{Me})\text{OH}$  ( $\text{L}=\text{HC}[\text{C}(\text{Me})\text{N}(\text{Ar})]_2$ ,  $\text{Ar}=2,6\text{-}i\text{Pr}_2\text{C}_6\text{H}_3$ ), compound  $\text{LAl}(\text{Me})(\mu\text{-O})\text{Zr}(\text{Me})\text{Cp}_2$  was first obtained (with high activity for ethylene polymerization<sup>[43a]</sup>), followed by a series of new compounds containing Al-O-M (M = Ln,<sup>[66]</sup> Mg,<sup>[59]</sup> Ti, Hf<sup>[55]</sup>) units. Organometallic hydroxides of group 14 were also employed, among which the silanols as alcohol analogues were used to prepare metallasiloxanes.<sup>[74]</sup> Subsequently, the use of the germanium(II) hydroxide  $\text{LGeOH}$ ,<sup>[45]</sup> which is considered as a congener of a low-valent carbon analogue, gave oxo-bridged complexes  $\text{LGe}(\mu\text{-O})\text{M}(\text{Me})\text{Cp}_2$  (M=Zr, Hf).<sup>[49]</sup> However, until now there is still no reported Ge-O-lanthanide linkage of a monomeric germanium(II) compound. In view of the extensive interest in the chemistry of lanthanide compounds containing heterometallic atoms,<sup>[75, 60b, 60c]</sup> we describe herein the preparation and characterization of  $\text{LGe}(\mu\text{-O})\text{M}(\text{THF})\text{Cp}_2$  (M = Yb, **11**; Y, **12**).

Organometallic hydroxides have proven to be facile precursors of M-O-M' moieties by the intermolecular elimination of  $\text{CH}_4$ ,<sup>[43a, 49, 55]</sup>  $\text{HN}(\text{SiMe}_3)_2$ ,<sup>[59, 74]</sup> and  $\text{HCp}$ ,<sup>[66]</sup> respectively. In a previous report,  $\text{LGeOH}$  exhibited its affinity to the methyl group,<sup>[49]</sup> although Cp groups coexist at the same metal center. Accordingly, further experimental evidence is required to explore its activity with respect to homoleptic complexes where only Cp is available as leaving group.





Scheme 6.

The reaction of LGeOH with 1 equiv of Cp<sub>3</sub>Yb was carried out smoothly in THF at room temperature (Scheme 6). The color of the solution changed from dark green to yellow, providing an indication of the reaction progress. After the removal of all the volatiles under vacuum, the absence of the OH stretching frequency of LGe( $\mu$ -O)Yb(THF)Cp<sub>2</sub> (**11**) was confirmed by IR. In the mass spectrum of **11**, the most intense peak ( $m/z$  491) is assigned to the fragment [M<sup>+</sup>-OYb(THF)Cp<sub>2</sub>] with an isotopic pattern that is consistent with the presence of low-valent germanium coordinated by the ligand. The <sup>1</sup>H NMR spectrum of **11** comprises a series of broad resonances due to the paramagnetism of ytterbium. These resonances still can be tentatively attributed to the backbone of the ligand but without precise assignments.

To elucidate the structure of **11** in solution, diamagnetic LGe( $\mu$ -O)Y(THF)Cp<sub>2</sub> (**12**) was prepared by the same procedure (Scheme 6). Although there is no noticeable change in the solution color, the elimination of HCp occurs readily in this reaction. The IR spectrum of **12** provides direct evidence for the absence of the OH group. The mass spectrum of **12** shows the base peak corresponding to the fragment [M<sup>+</sup>-OY(THF)Cp<sub>2</sub>]. The <sup>1</sup>H NMR spectrum of **12** can be fully interpreted. The characteristic Cp resonance is present as a singlet ( $\delta$  5.90 ppm), and two broad resonances ( $\delta$  1.41 and 3.31 ppm) are assigned to the protons of the coordinated THF. Other resonances correspond to the backbone of the ligand assuming an unsymmetrical environment. The composition of both compounds was further confirmed by elemental analysis.

From the concentrated THF extract at 4 °C, pale-yellow crystals of **11** and **12** of X-ray quality are recovered in relatively low yield. They are stable in the solid state under an inert atmosphere at room temperature. The decomposition of **11** and **12** is observed when the solids are heated at moderately high temperature (218 °C for **11**; 210 °C for **12**). Crystallographic data for the structural analyses of **11** and **12** are shown in Table CD3 and CD4. The compounds crystallize isotypically in the triclinic space group *P*-1. In the asymmetric unit, two crystallographically independent molecules are found with minor differences in their dimensions, as shown in Table 3 for selected bond parameters.

**Table 3.** Selected Bond Lengths (Å) and Angles (°) of **11** and **12** <sup>a</sup>

	<b>11</b> <sup>a</sup>	<b>11</b> <sup>b</sup>	<b>12</b> <sup>a</sup>	<b>12</b> <sup>b</sup>
M-O(1)	2.018(5)	2.048(5)	2.066(5)	2.059(5)
Ge-O(1)	1.769(5)	1.762(5)	1.758(5)	1.763(4)
Ge-N(1)	2.057(5)	2.089(5)	2.056(5)	2.081(5)
Ge-N(2)	2.061(5)	2.063(5)	2.073(5)	2.059(5)
X <sub>Cp1</sub> -M	2.328	2.337	2.380	2.390
X <sub>Cp2</sub> -M	2.358	2.365	2.382	2.417
O(1)-Ge-N(1)	102.2(2)	101.3(2)	100.5(2)	100.5(2)
O(1)-Ge-N(2)	101.4(2)	100.0(2)	101.3(2)	101.7(2)
N(1)-Ge-N(2)	87.0(2)	85.9(2)	86.5(2)	86.34(19)
Ge-O(1)-M	153.7(3)	151.3(4)	152.8(3)	152.0(3)
X <sub>Cp1</sub> -M-X <sub>Cp2</sub>	127.44	127.08	126.79	127.42

<sup>a</sup> a and b are the two independent molecules.

The molecular structure of **11** is depicted in Figure 5. The germanium atom is located in a distorted pyramidal geometry involving the chelating  $\beta$ -diketiminato ligand and one bridging oxygen atom (and a stereochemically active lone pair of electrons). Two Cp groups and two oxygen atoms comprise the pseudotetrahedral coordination environment of the ytterbium atom. The deviation of germanium and  $\gamma$ -C

from the NCCN ligand plane gives a boat conformation with germanium and  $\gamma$ -C out-of-plane (Figure 7). This is consistent with previous observations.<sup>[49]</sup> **1** also features a bent Ge-O-Yb ( $153.7(3)$ ,  $151.3(4)^\circ$ ) arrangement. The Ge-O bond length ( $1.769(5)$ ,  $1.762(5)$  Å) is even shorter than those in Ge-O-Zr ( $1.797(2)$  Å) and Ge-O-Hf ( $1.799(3)$  Å) species,<sup>[49]</sup> whereas the Yb-O ( $2.018(5)$ ,  $2.048(5)$  Å) separation is comparable to that of  $\text{LAIme}(\mu\text{-O})\text{Yb}(\text{THF})\text{Cp}_2$  ( $2.020(1)$  Å).<sup>[66]</sup> The Ge-N bond lengths ( $2.057(5)$ - $2.089(5)$  Å) and the N-Ge-N bond angle ( $87.0(2)$ ,  $85.9(2)^\circ$ ) are close to those reported in literature.<sup>[76]</sup> The Yb- $X_{\text{Cp}}$  distances ( $2.328$ - $2.365$  Å) are comparable with those of Al-O-Yb compounds, with or without coordinated THF ( $2.37$  and  $2.34$  Å, respectively), whereas the  $X_{\text{Cp1}}\text{-Yb-}X_{\text{Cp2}}$  angle ( $127.44$ ,  $127.08^\circ$ ) is narrower when compared with those in Al-O-Yb compounds ( $129.1(3)$  and  $129.6(3)^\circ$ ).<sup>[66]</sup>

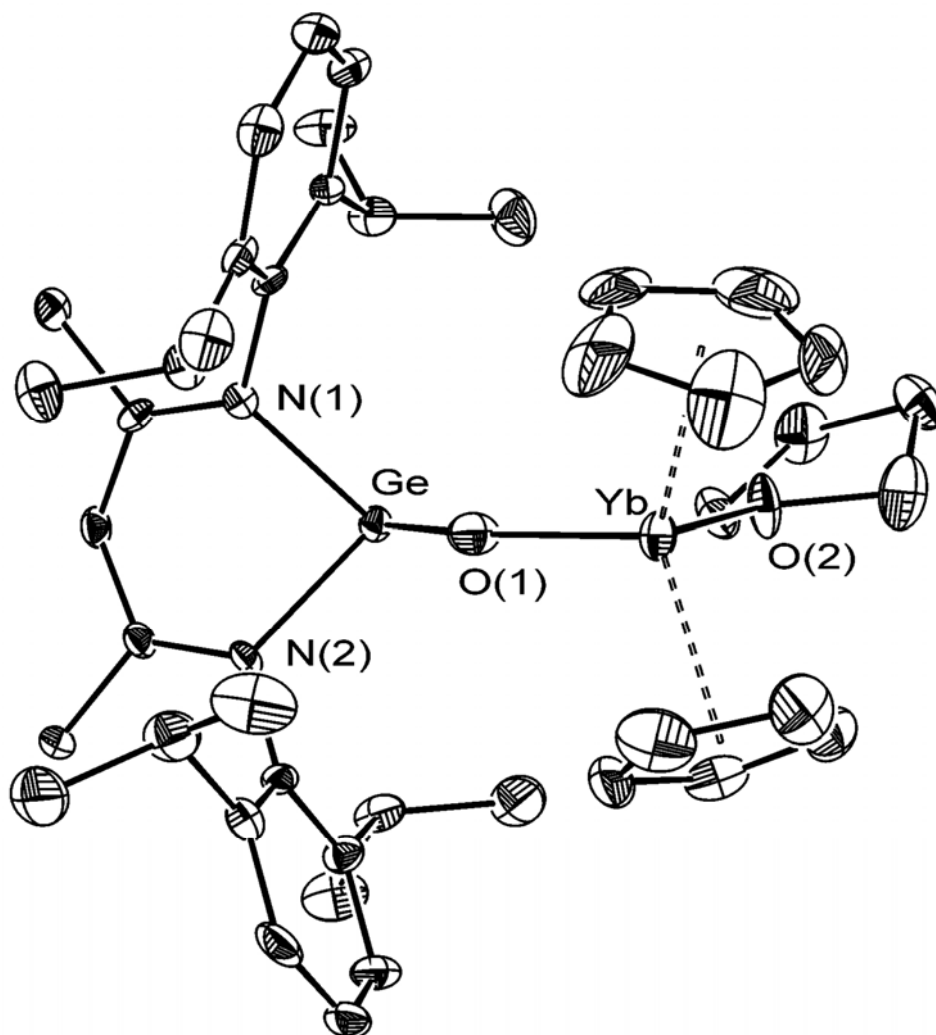


**Figure 5.** Molecular structure of **11**. Thermal ellipsoids are drawn at the 50% level, and the hydrogen atoms are omitted for clarity.

The isotopic structure of **12** is shown in Figure 6; it involves an obtuse Ge-O-Y (152.8(3), 152.0(3)°) angle and a shorter Ge-O (1.758(5), 1.763(4) Å) and a longer Y-O (2.066(5), 2.059(5) Å) bond distance. Simplified side views of the molecular structure of **11** and **12** are shown in Figure 7. The boat conformation of the C<sub>3</sub>N<sub>2</sub>Ge six-membered ring and the bent Ge-O-M skeleton can be clearly recognized.

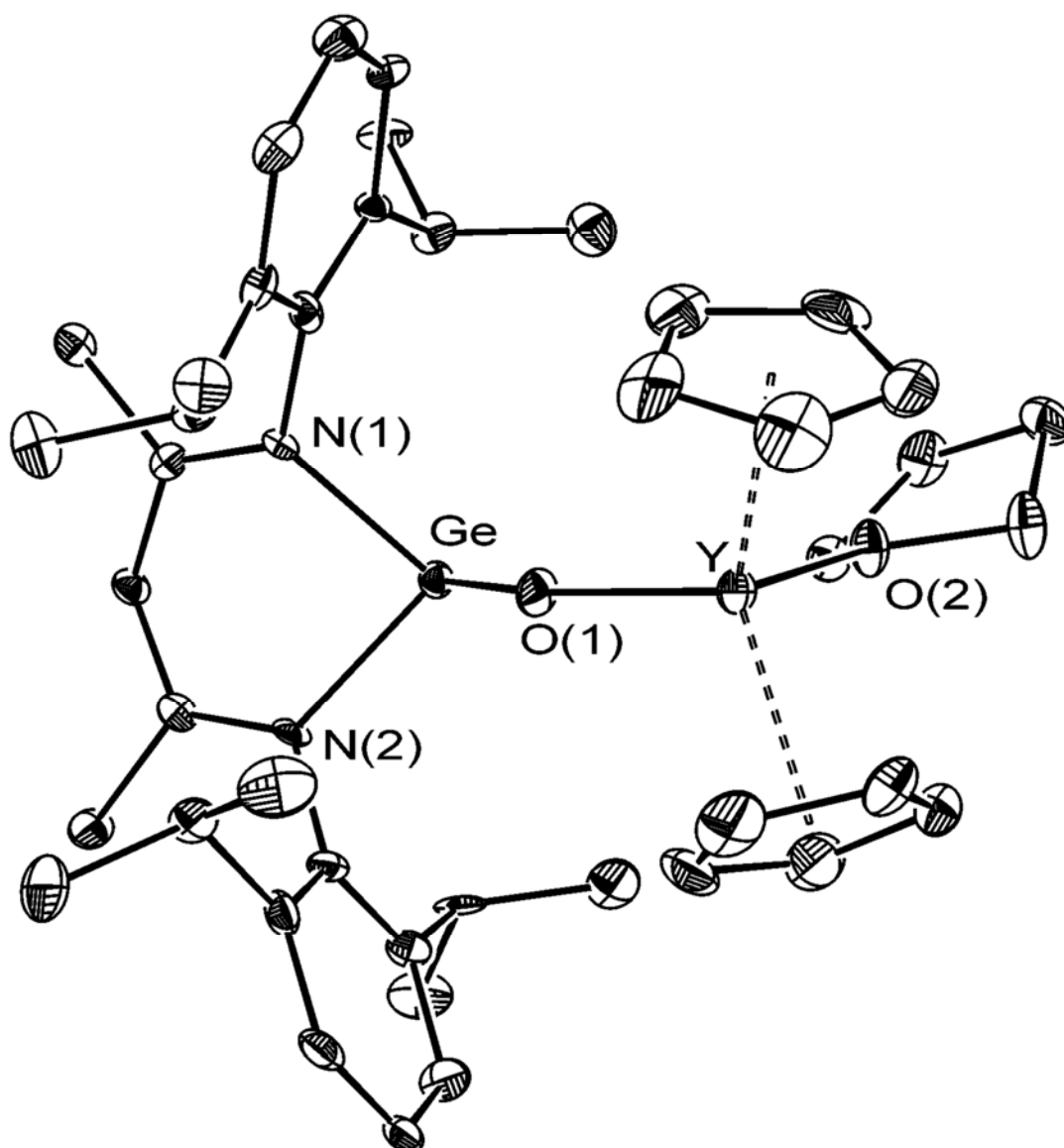


**Figure 6.** Molecular structure of **12**. Thermal ellipsoids are drawn at the 50% level, and the hydrogen atoms are omitted for clarity.

It is worth mentioning that the Ge-O bond lengths in **11** and **12** (1.758-1.769 Å) are shorter than those reported in germanium(II) aryloxides (1.8-1.9 Å).<sup>[77]</sup> This structural feature is attributable to the formation of strong bonds between the high Lewis acidic ytterbium and yttrium elements and the hard donor oxygen, which in turn strengthens the interaction between the germanium atom and the oxygen donor.<sup>[45]</sup> The same trend is also observed in the aluminum derivatives containing the Al-O-Ln skeleton (Ln =lanthanide).<sup>[43a, 55, 66]</sup>

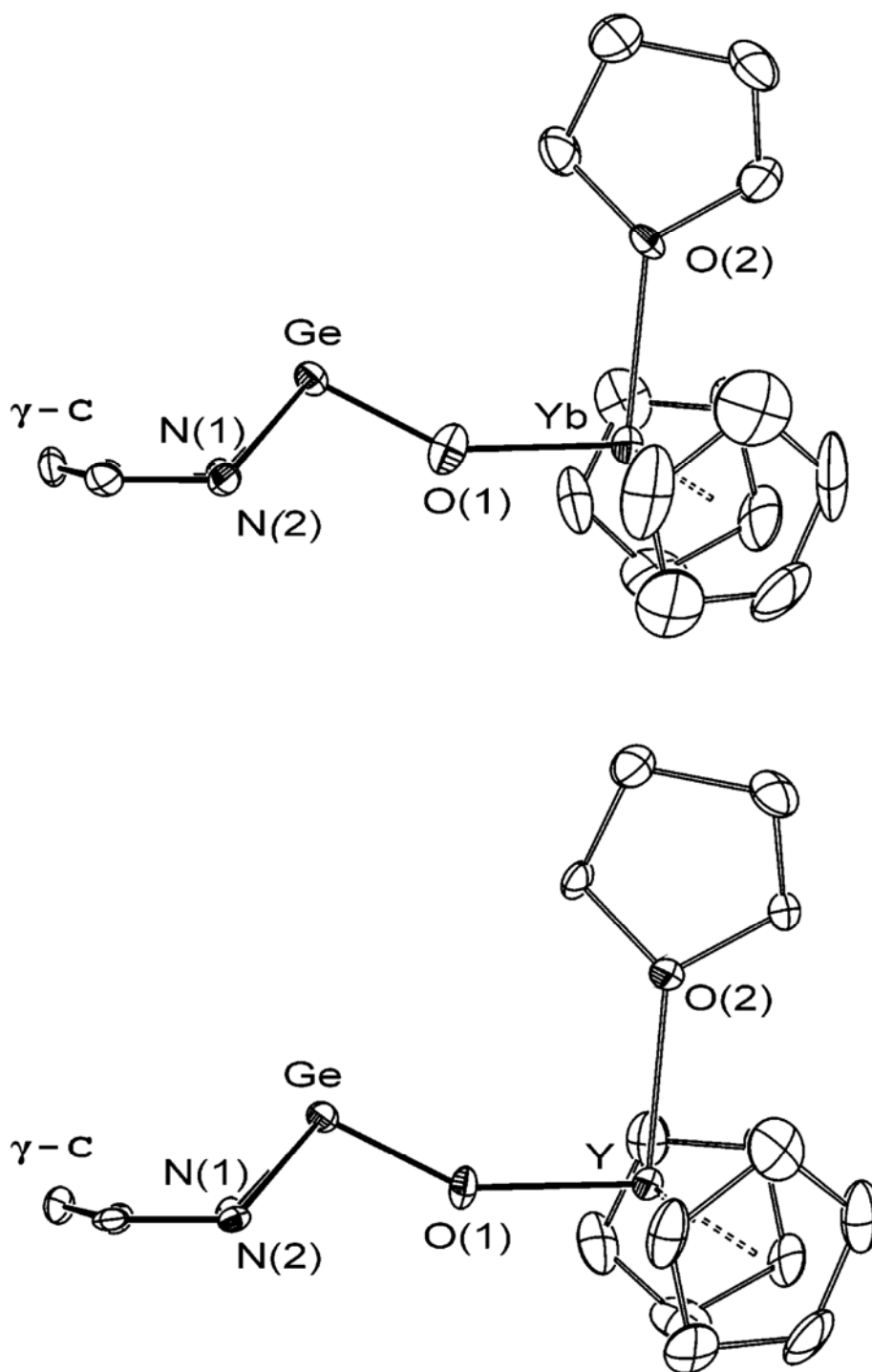


**Figure 7.** Side view of the molecular structures of **11** and **12**. The Ar and methyl groups of the ligand and all of the hydrogen atoms are omitted for clarity.

### *Special Features.*

The structure of **11** was originally solved and refined with one independent molecule in the monoclinic space group  $P2_1/n$ , but the refinement displayed some

unusual and unsatisfactory features; the R1 value was high (7%) and many systematically absent reflections had significant intensity. Assuming the structure to be pseudosymmetric, the symmetry was lowered to  $P2_1$ , whereupon the R1 value was lowered to 4%. However, an analysis of the geometry showed no significant deviations from  $P2_1/n$ , and the Flack twinning parameter refined to 0.5. Following a suggestion from Dr. Regine Herbst-Irmer (University of Göttingen), an alternative model was tested that involved a triclinic space group with  $\alpha$  and  $\gamma$  angles close to  $90^\circ$ , plus pseudo-merohedral twinning by  $180^\circ$  rotation about the  $y$  axis. This model refined satisfactorily. The structure of **12** showed an  $\alpha$  angle differing significantly from  $90^\circ$ . This necessarily led to lower data quality because the twinning components were not completely overlapped but did at least provide further evidence for the triclinic symmetry.

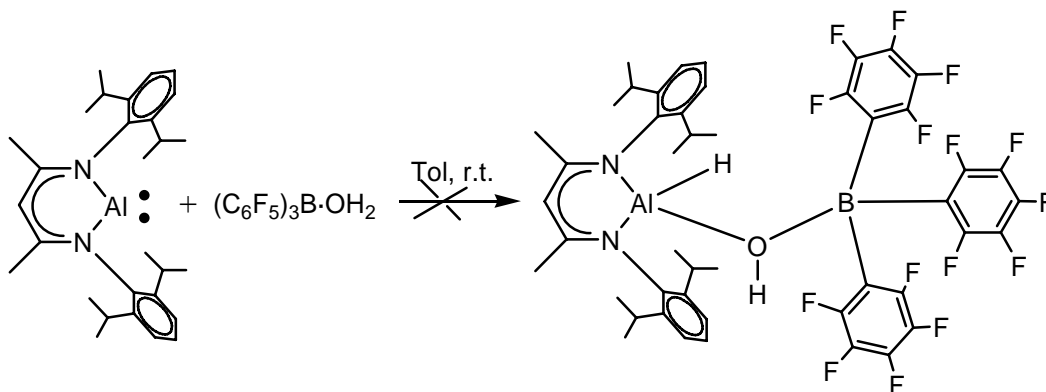
The exact nature of the pseudosymmetry/twinning cannot be determined with total confidence, and molecular dimensions of both compounds should therefore be treated with caution. The triclinic cells are presented in a nonstandard manner to emphasize their pseudo-monoclinic nature.

### 2.3. Synthesis and Structural Characterization of $[\text{CH}(\text{C}(\text{Me})\text{NH}-2,6\text{-}i\text{Pr}_2\text{C}_6\text{H}_3)_2]^+[(\text{C}_6\text{F}_5)_3\text{B}(\mu\text{-OH})\text{B}(\text{C}_6\text{F}_5)_3]^-$ (**13**)

Tris(pentafluorophenyl)borane is currently extensively used as a strong Lewis acid, particularly as an activator for metallocene polymerization catalysts.<sup>[79]</sup> Water coordinated to the strong Lewis acid  $\text{B}(\text{C}_6\text{F}_5)_3$  is known to behave as a strong Brønsted acid which is able to protonate alkyl groups bound to metal centers.<sup>[80]</sup>

In our lab,  $(\text{C}_6\text{F}_5)_3\text{B}\cdot\text{OH}_2$  has been successfully used to prepare and stabilise an  $\text{Al}=\text{O}$  containing structure.<sup>[81]</sup> But the attempt to react  $(\text{C}_6\text{F}_5)_3\text{B}\cdot\text{OH}_2$  with  $\text{Cp}_3\text{Ln}$  resulted in a failure. Cp ligand cannot be eliminated even under heating.

However, the purpose to obtain a  $\text{B}(\mu\text{-OH})\text{-Al}$  unit from  $(\text{C}_6\text{F}_5)_3\text{B}\cdot\text{OH}_2$  and LAl: (Scheme 7) led to an ionic compound of composition  $[\text{CH}(\text{C}(\text{Me})\text{NH}-2,6\text{-}i\text{Pr}_2\text{C}_6\text{H}_3)_2]^+[(\text{C}_6\text{F}_5)_3\text{B}(\mu\text{-OH})\text{B}(\text{C}_6\text{F}_5)_3]^-$  (**13**).



**Scheme 7**

$(\text{C}_6\text{F}_5)_3\text{B}\cdot\text{OH}_2$  was prepared from  $(\text{C}_6\text{F}_5)_3\text{B}$  with 1 equiv. of water at  $-20\text{ }^\circ\text{C}$  in pentane as a white powder. Further reaction with 1 equiv. of LAl: ( $\text{L} = \text{CH}(\text{C}(\text{Me})\text{N}-2,6\text{-}i\text{Pr}_2\text{C}_6\text{H}_3)_2$ ) in toluene at room temperature afforded a colorless crystal of **13** which was determined by X-ray diffraction. The structure of **13** is depicted in Figure 8.



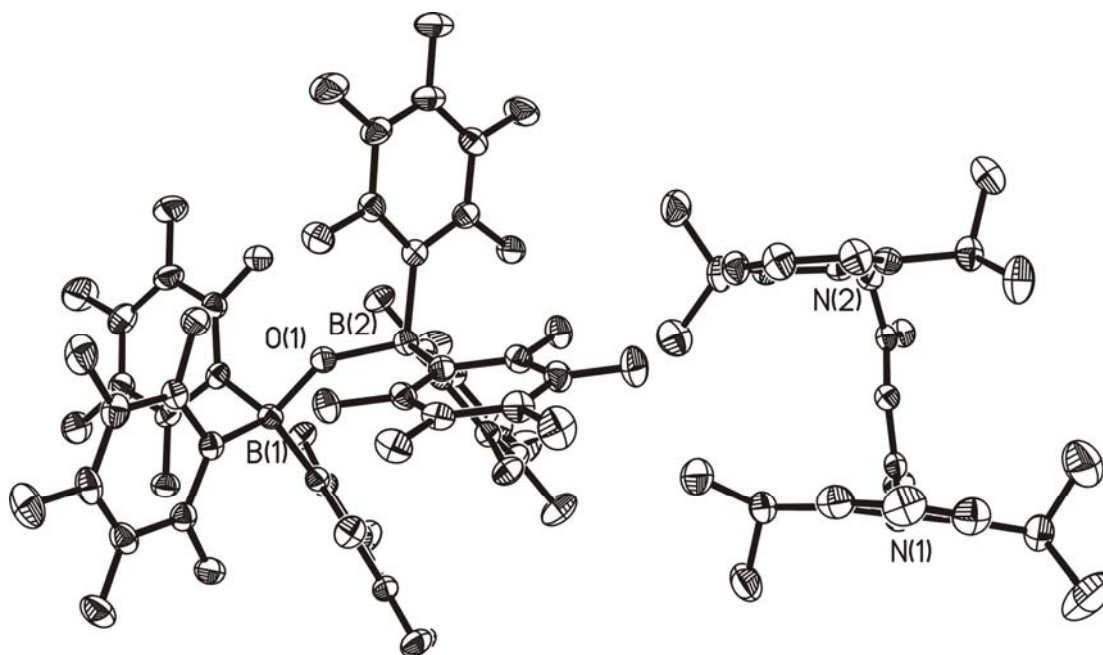


**Figure 8.** Molecular structure of **13**. Thermal ellipsoids are drawn at the 50% level, and the hydrogen atoms are omitted for clarity.

Compound **13** crystallized in the monoclinic space group  $P21/c$  (Table CD5) and shows a composition with an anion as  $[(C_6F_5)_3B(\mu-OH)B(C_6F_5)_3]^-$  (Figure 9.) and a cation as  $[CH(C(Me)NH-2,6-iPr_2C_6H_3)_2]^+$  (Figure 10.).

Selected bond lengths and angles are listed in Table 4.

According to Figure 10, the cation has an inversion of configuration comparing with the  $L^-$  ligand in LAIR(OH) and its derivatives.

The bond lengths of C(14)-C(15) (1.391(3)Å) and C(15)-C(16) (1.394(3)Å) are much shorter than those of C(13)-C(14) (1.498(3)Å) and C(16)-C(17) (1.504(3)Å), as well as the N(1)-C(14) (1.331(3) Å) and N(2)-C(16) (1.329(3) Å) are much shorter than N(1)-C(1) (1.446(3) Å) and N(2)-C(18) (1.441(3) Å).

The angle of B(1)-O(1)-B(2) exhibits as  $141.28(16)^\circ$ . Bond lengths of B-O average as 1.561 Å. It is shorter than the B-O bond length within  $[(C_6F_5)_3B \cdot OH_2] \cdot (H_2O)_2$  (1.5769(14) Å).<sup>[80a]</sup>

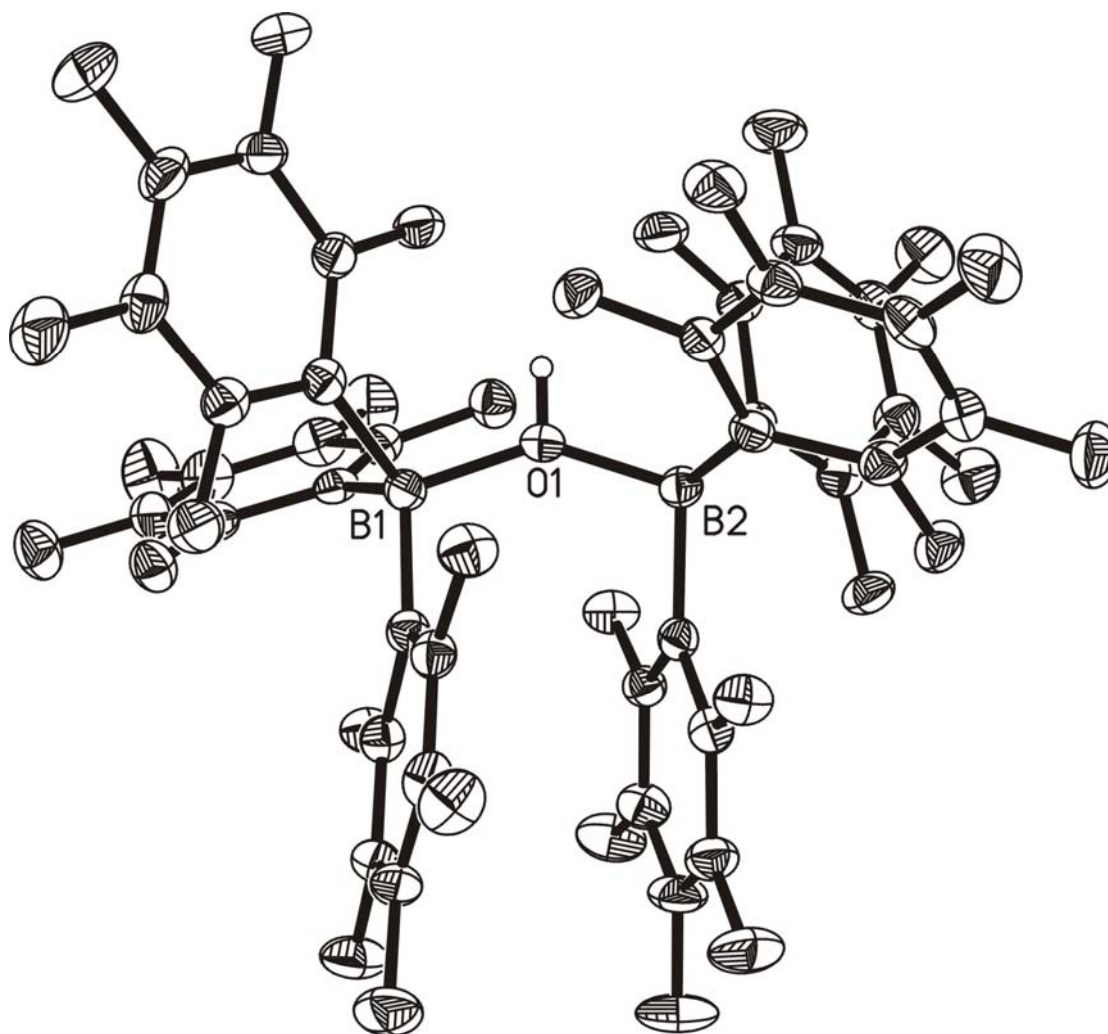
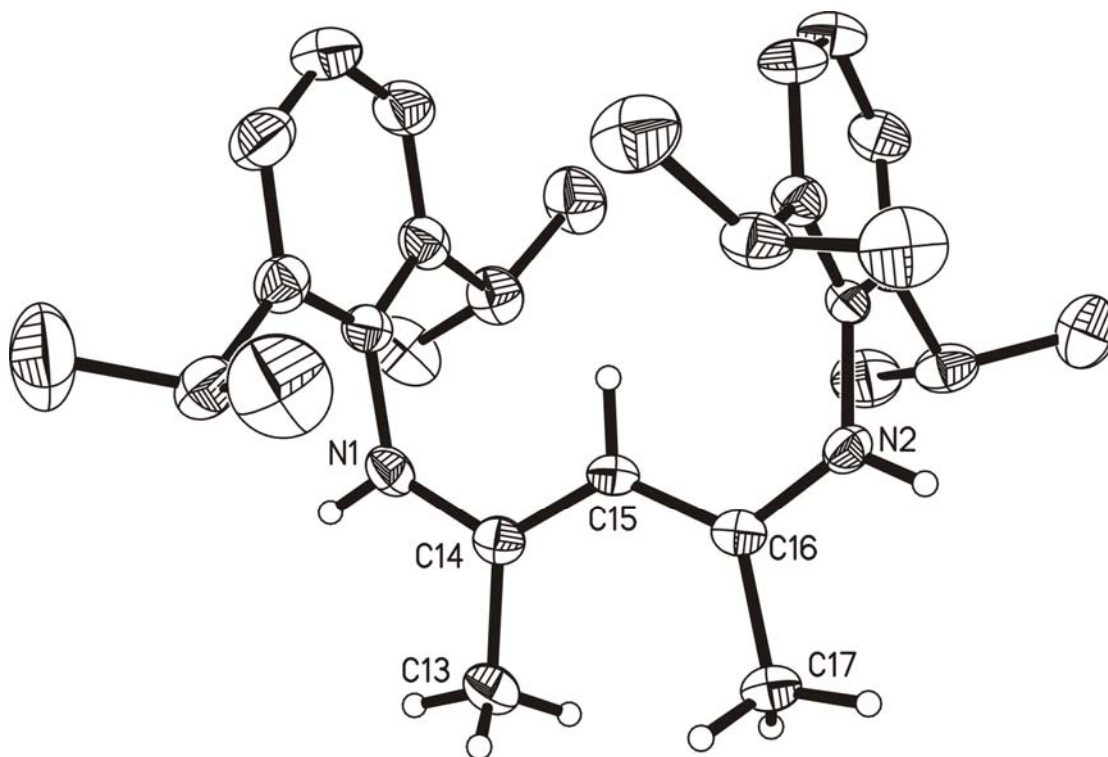


**Figure 9.** The anion structure of **13**  $[(\text{C}_6\text{F}_5)_3\text{B}-(\mu\text{-OH})\text{-B}(\text{C}_6\text{F}_5)_3]^-$ . Thermal ellipsoids are drawn at the 50% level, and the hydrogen atoms are omitted for clarity.

**Table 4.** Selected Bond lengths [ $\text{\AA}$ ] and angles [ $^\circ$ ] for **13**.

B(1)-O(1)	1.565(3)	N(2)-C(18)	1.441(3)
B(2)-O(1)	1.557(2)	C(13)-C(14)	1.498(3)
N(1)-C(14)	1.331(3)	C(14)-C(15)	1.391(3)
N(1)-C(1)	1.446(3)	C(15)-C(16)	1.394(3)
N(2)-C(16)	1.329(3)	C(16)-C(17)	1.504(3)
O(1)-B(1)-C(48)	108.66(15)	C(30)-B(2)-C(36)	104.71(16)
O(1)-B(1)-C(60)	109.49(16)	C(14)-N(1)-C(1)	126.26(19)
C(48)-B(1)-C(60)	113.38(16)	C(16)-N(2)-C(18)	124.17(18)

O(1)-B(1)-C(54)	108.30(15)	B(2)-O(1)-B(1)	141.28(16)
C(48)-B(1)-C(54)	114.59(17)	C(6)-C(1)-C(2)	123.1(2)
C(60)-B(1)-C(54)	102.18(15)	C(6)-C(1)-N(1)	118.26(18)
O(1)-B(2)-C(42)	106.40(15)	C(2)-C(1)-N(1)	118.69(19)
O(1)-B(2)-C(30)	110.26(15)	C(3)-C(2)-C(1)	117.0(2)
C(42)-B(2)-C(30)	115.82(16)	C(3)-C(2)-C(7)	122.2(2)
O(1)-B(2)-C(36)	107.82(15)	C(1)-C(2)-C(7)	120.8(2)
C(42)-B(2)-C(36)	111.64(16)	C(4)-C(3)-C(2)	121.1(2)

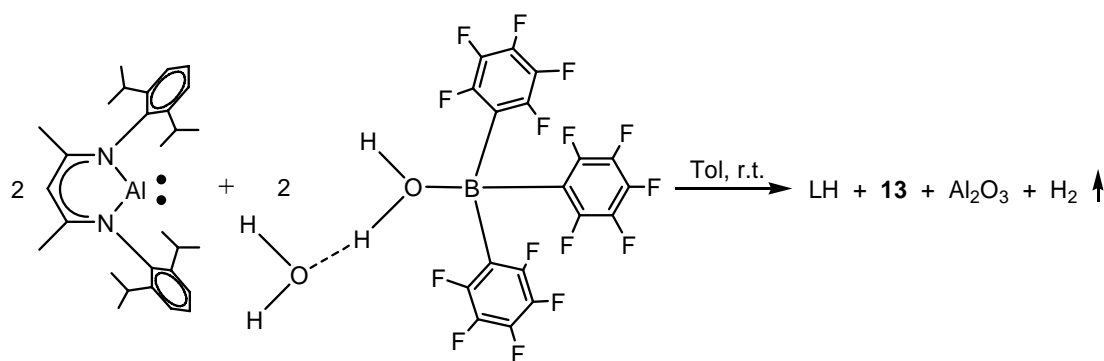


**Figure 10.** The cation structure of **13**  $[\text{CH}(\text{C}(\text{Me})\text{NH}-2,6\text{-}i\text{Pr}_2\text{C}_6\text{H}_3)_2]^+$ . Thermal ellipsoids are drawn at the 50% level, and the hydrogen atoms on 2,6-*i*PrAr are omitted for clarity.

$^1\text{H}$  NMR spectrum displays the resonance of N-H proton ( $\delta$  12.39 ppm) and O-H ( $\delta$  7.59 ppm) as singlet. The resonance of  $^{19}\text{F}$  NMR spectrum of **13** appears in three groups which are assigned to *p*-, *m*-, *o*-F elements separately on the aryl ring. A singlet for  $^{11}\text{B}$  NMR appears at  $\delta$  -3.79 ppm. In the IR spectrum of **13**, O-H stretching

frequency is found at  $3699\text{ cm}^{-1}$ , as well as the N-H stretching frequency at  $3542\text{ cm}^{-1}$ . The mass spectrum exhibits peaks at  $m/z$  (%) 512 (100), 403(88), 418(30), representing the fragments of  $[(\text{C}_6\text{F}_5)_3\text{B}^+]$ ,  $[\text{NacNac}^+-\text{Me}]$ , and  $[\text{NacNac}^+]$  respectively. Due to the low solubility in  $\text{CDCl}_3$ ,  $^{13}\text{C}$  NMR has not been performed.

Further investigation indicates that this reaction proceeds according to the procedure given in Scheme 8. The  $(\text{C}_6\text{F}_5)_3\text{B}\cdot\text{OH}_2$  transformed slowly into the adduct of  $(\text{C}_6\text{F}_5)_3\text{B}\cdot(\text{OH}_2)_2$  owing to the water in the system, which reacted with  $\text{LAl}$ : following an oxidation-reduction step. As a result,  $\text{Al}^{+1}$  is oxidized to  $\text{Al}^{+3}$  and  $\text{H}^+$  is reduced to  $\text{H}_2$ .

**Scheme 8**

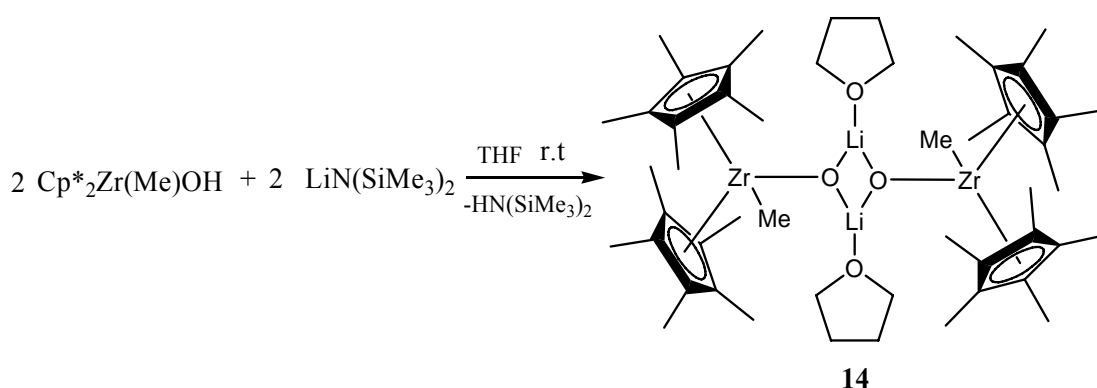
## 2.4. Synthesis and Characterization of $(Cp^*ZrMeOLi)_2(THF)_2$ and $Cp^*ZrN(SiMe_3)_2$ .

### 2.4.1. Synthesis and Characterization of $(Cp^*ZrMeOLi)_2(THF)_2$ (**14**)

Since the first  $LiAlMe(\mu-O)Ln Cp_2 \cdot THF$  was prepared, a series of analogue compounds and derivatives were obtained.<sup>[66]</sup> However, to react other organometallic-hydroxides with rare earth compounds needs further efforts.

$Cp^*Zr(Me)OH$  has been proved to be an active reagent to produce heterobimetallic compounds with Ti, Hf, and other moieties.<sup>[48]</sup> Nevertheless, no reaction occurred when  $Cp^*Zr(Me)OH$  was treated with  $Cp_3Ln$ . It acts not as active as the  $LiAlMeOH$  in this case. To build up a Zr-O-Ln structure,  $Cp^*Zr(Me)OLi$  (**14**) was prepared to improve the reactivity.

Compound **14** was obtained by the reaction of  $Cp^*Zr(Me)OH$  with 1 equiv. of  $LiN(SiMe_3)_2$  in THF. (Scheme 9) Suitable crystals were afforded for X-ray diffraction. Unfortunately, the quality of the data for compound **14** was not good enough to be published. The rough structure is shown in Figure 11.



Scheme 9

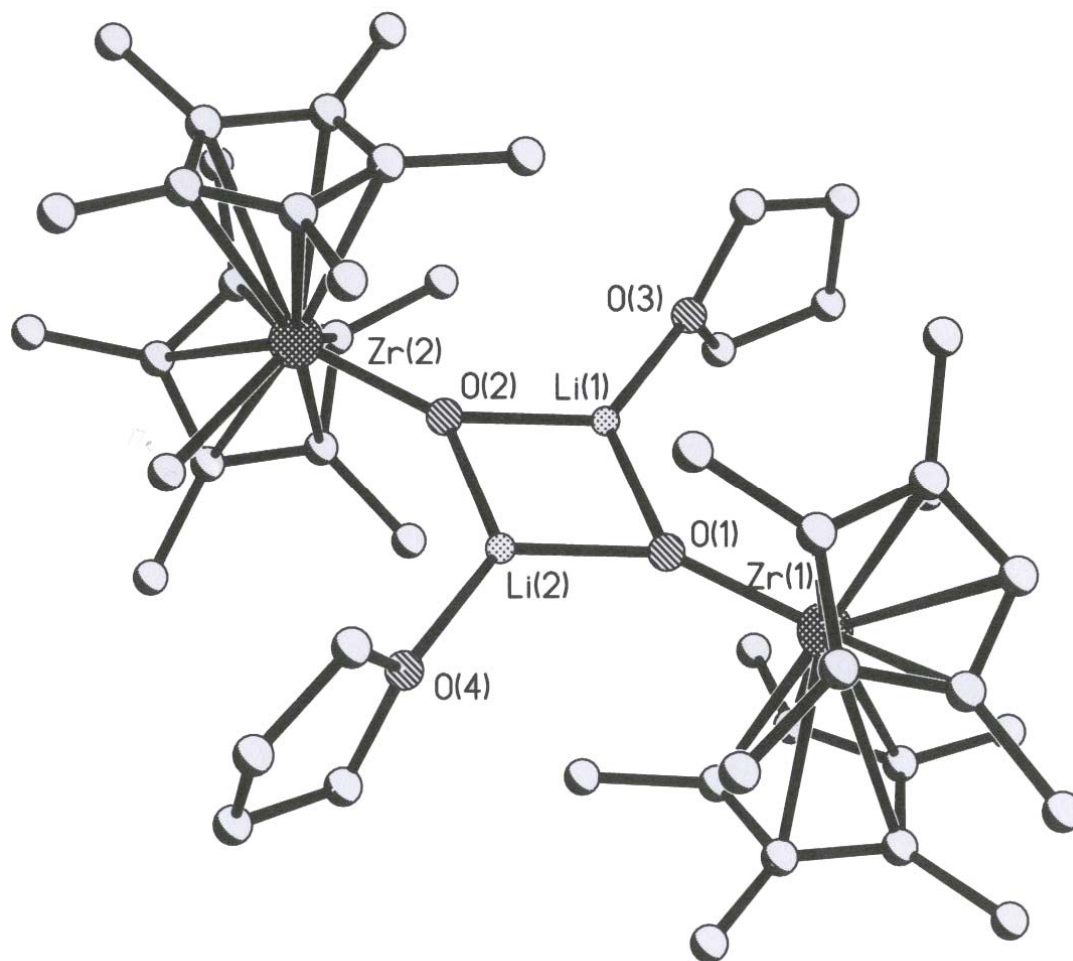


**Figure.11.** The rough structure of compound **14**

$^1\text{H}$  NMR spectrum exhibits the singlet for  $\text{Cp}^*(\text{Me})$  ( $\delta$  1.8 ppm) and a singlet of  $\text{Zr-Me}$  ( $\delta$  -0.22 ppm). No resonance for the OH proton was observed. Moreover in the IR spectrum no -OH absorption in the OH region was observed. Mass spectrum exhibits a fragment of  $m/z(\%)$  377(100) representing  $[1/2 \text{M}^+ - \text{Me} - \text{OLi}]$ .

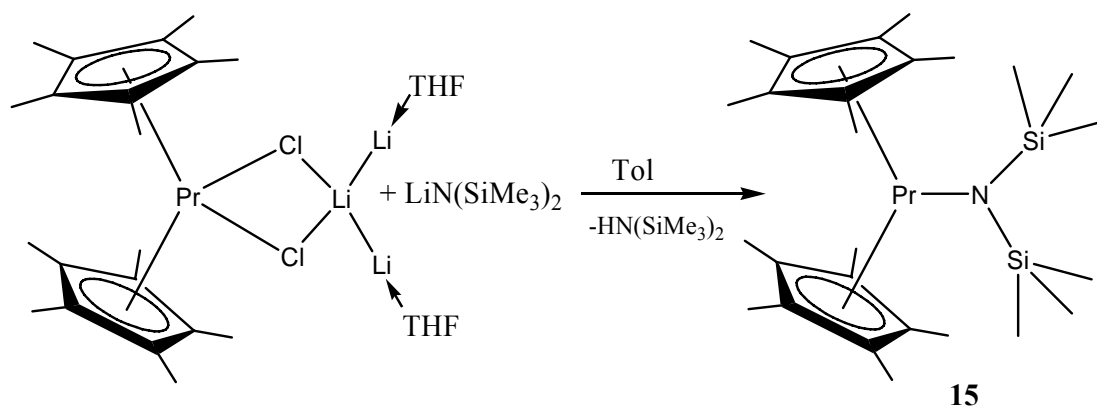
Reactions of complex **14** with  $\text{LnCl}_3$  did not lead to an appropriate result.

#### 2.4.2. Synthesis and Characterization of $\text{Cp}^*_2\text{PrN}(\text{SiMe}_3)_2$ (**15**)

The bulky pentamethylcyclopentadienyl ligand is particularly popular in the organometallic chemistry of rare earth compounds.<sup>[78, 82]</sup> Considerable success in the synthesis of highly reactive organolanthanide species can be attributed to the favorable chemical properties of complexes with a bis(pentamethylcyclopentadienyl) ligand environment due to the size of the pentamethylcyclopentadienyl ligand.

In order to activate the lanthanide compounds, the  $(\text{Me}_3\text{Si})_2\text{N}$ - ligand has been introduced to bis(pentamethylcyclopentadienyl)lanthanide derivatives. Supposedly it is much easier to eliminated in the presence of the bulky  $\text{Cp}^*$  ligand.

The praseodymium was chosen as the target element due to the large size of this metal.  $(\text{C}_5\text{Me}_5)_2\text{PrCl}(\text{LiCl})(\text{THF})_2$  was prepared according to the literature.<sup>[83]</sup> Due to its high sensitivity it was not separated and directly reacted with 1 equiv. of  $\text{LiN}(\text{SiMe}_3)_2$  in situ (Scheme 10). Suitable crystals of **15** were obtained for X-ray diffraction measurements. Unfortunately, due to its very high sensitivity, compound **15** slowly decomposed even under an inert gas and low temperature, which resulted in low quality of the crystallographic data. The rough structure of **15** is depicted in Figure 12.



**Scheme 10**

Compound **15** quickly decomposed during the measurement of its melting point. The same happened when the IR spectrum was done, with the result that very broad bands appeared. From the mass spectrum, only the peaks of  $m/z$  (%) 136 (100) [ $\text{Cp}^{*+}$ ] and 160 (17) [ $(\text{SiMe}_3)_2\text{N}^+$ ] can be assigned. Because of the paramagnetic properties of Pr, the  $^1\text{H}$  NMR spectrum exhibits no meaningful results.

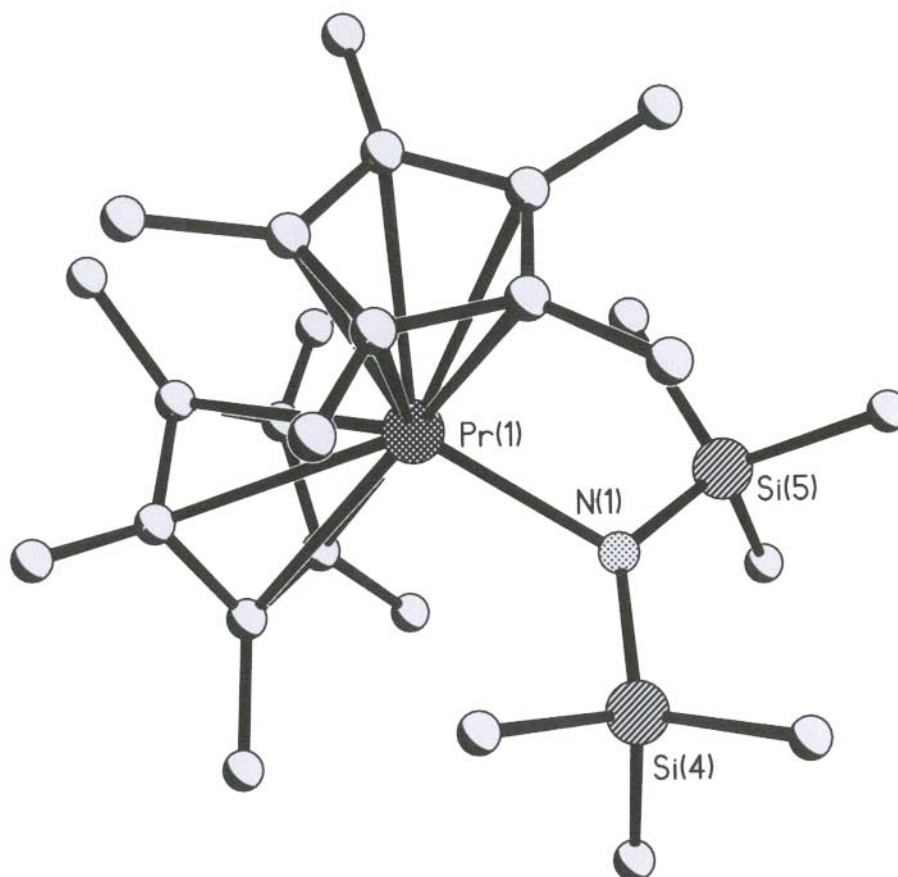


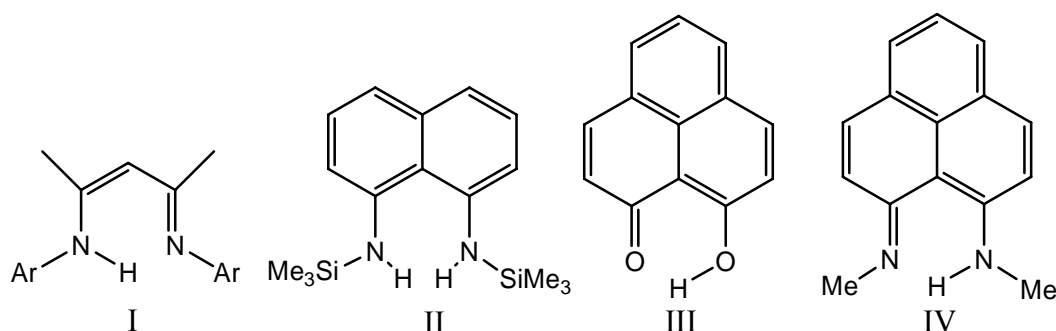
**Figure.12.** The rough structure of compound 15

The failure of building up the target structure of  $\text{Cp}^*_2\text{Zr}(\text{Me})\text{-O-LnCp}_2$  might be due to the crowded environment caused by the Cp or  $\text{Cp}^*$  ligands. To successfully obtain the Zr-O-Ln units, new effective ligands are required to modify the reactivity of lanthanide complexes which should not only be bulky enough to stabilize the lanthanides but also have enough space to accommodate the bulky part of zirconium.



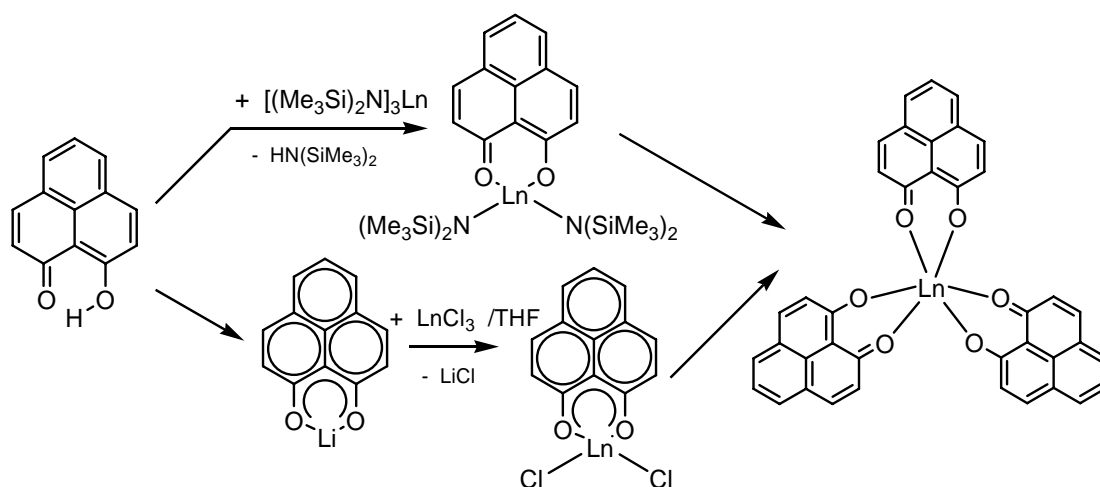
## 2.5. Synthesis and Characterization of (9-Oxidophenalenone)<sub>3</sub>Yb (16)

The  $\beta$ -diketiminato ligand (HC[C(Me)N(Ar)]<sub>2</sub>, Ar = 2,6-*i*Pr<sub>2</sub>C<sub>6</sub>H<sub>3</sub>) (I, Scheme 11) has proved to be prevalent in organometallic chemistry as well as in rare earth chemistry. Recently, research activity has been focused on other ligands such as (trimethylsilylamino)naphthalene,<sup>[84]</sup> 9-hydroxyphenalenone<sup>[85]</sup> and 1,9-dialkyldiaminophenalenone<sup>[86]</sup> which can form metal chelates (II, III, IV, Scheme 11). These ligands display unusual electron delocalization characters and are used as spectator ligands.



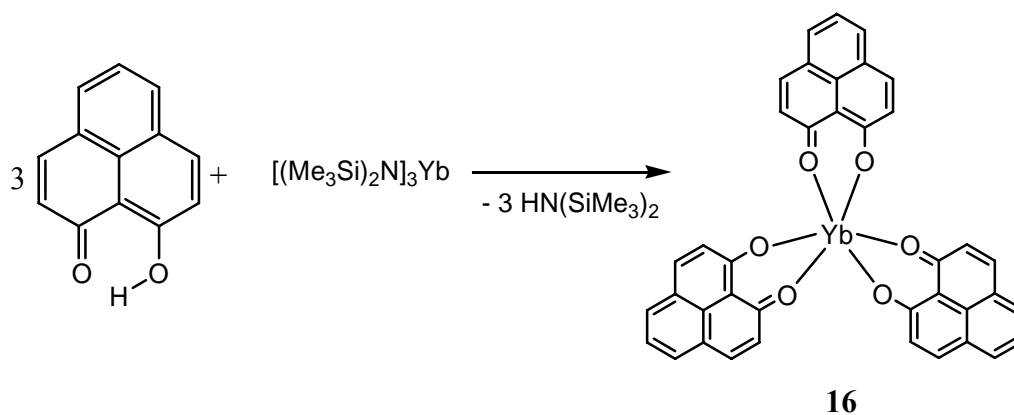
**Scheme 11**

All ligands II, III and IV have an extended plane. Attempts to react with rare earth compound in 1:1 ratio resulted in an asymmetric substitution, and finally turned into a mixture of compounds. (Scheme 12, III as an example).



**Scheme 12**

Ligand III reacts with  $[(\text{Me}_3\text{Si})_2\text{N}]_3\text{Yb}$  in 3:1 ratio to yield an insoluble yellow powder **16** from the solution which has been proved to be pure. (Scheme 13)



**Scheme 13**

IR spectrum of **16** indicates the absence of O-H absorption. The mass spectrum of **16** exhibits the ions of  $[9\text{-oxo}]^+$  and  $[M]^+$ . **16** slowly decomposes under heating.

Ligand II reacts with  $[(\text{Me}_3\text{Si})_2\text{N}]_3\text{Yb}$  in 3:1 ratio resulting in a soluble dark powder which decomposed slowly in solution to eliminate ligand II. That might be due to the bulky  $-\text{SiMe}_3$  group on N-atom which provides a crowded environment.

## 2.6. Synthesis and Characterization of Organo-lanthanide Compounds with guanidinato ligand

### 2.6.1. Synthesis and Characterization of $L'_2SmBr \cdot (BrLi) \cdot (THF)_2$ and $L'_2Sm(THF)(\mu-O)MeAll$ ( $L'=(Me_3Si)_2NC(NCy)_2$ )

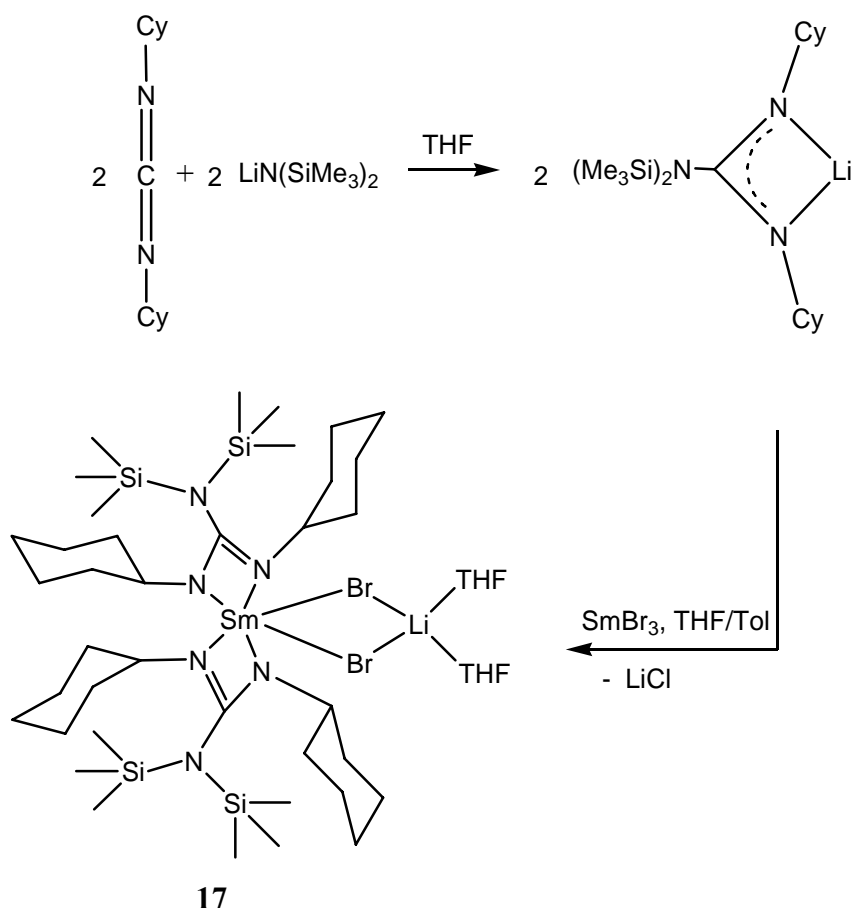
The organolanthanide chemistry has made considerable progress in the past two decades<sup>[78, 87, 88]</sup> and has been generally dominated by the synthesis of cyclopentadienyl sandwich and half-sandwich complexes.<sup>[87, 88]</sup> Recently, research activity has been directed to the substitution of cyclopentadienyl ligands by other coordinating systems in order to obtain complexes with modified structures and reactivities.

Some achievements indicate that monoanionic guanidates are highly versatile ligands which are able to bind in a variety of coordination modes to alkali, transition, lanthanide and main group metals.<sup>[90, 91]</sup> Another facet of their versatility is the opportunity to vary substituent groups which will have an effect on the properties of the complexes that are formed.

#### 2.6.1.1. Synthesis of $[(Me_3Si)_2NC(NCy)_2]_2SmBr_2Li(THF)_2$ (**17**)

Herein, we were attracted to N-substituted guanidate anions,  $[(Me_3Si)_2NC(NCy)_2]^-$ , as potential bulky supporting ligand for organolanthanide complexes.

Compound **17** was obtained in high yield as large yellow crystals by the reaction of  $SmBr_3$  with 2 equiv. of  $[(Me_3Si)_2NC(NCy)_2]Li$  which was freshly prepared from  $CyN=C=NCy$  and  $LiN(SiMe_3)_2$  in 1:1 molar ratio. (Scheme 14)



Scheme 14

Compound **17** quickly decomposed when heated to release a colorless liquid in the tube. The mass spectrum indicated a number of fragments which were difficult to assign. Only the peak of  $m/z$  (%) 160 (8)  $[(\text{SiMe}_3)_2\text{N}^+]$  could be recognized. Due to the paramagnetic properties of Sm, the NMR spectrum was not meaningful. X-ray diffraction and element analysis can prove the composition.

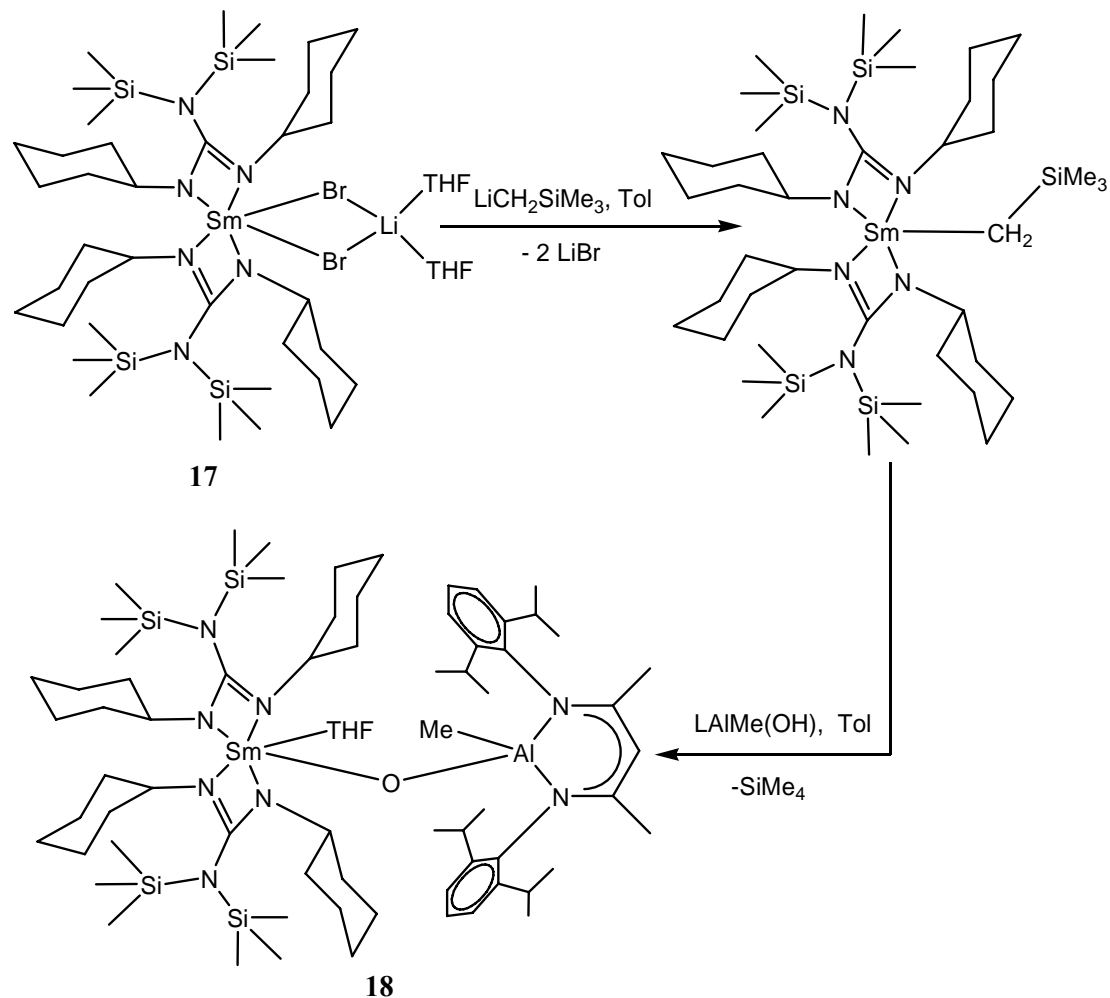
The crystals of **17** are fairly stable, even when exposed to air for a short time. That can be attributed to the perfect coordination site of Sm.

The reduction of compound **17** by K or  $\text{KC}_8$  resulted in a color change to dark red, although only the starting material **17** could be isolated.

#### 2.6.1.2. Synthesis of $[(\text{Me}_3\text{Si})_2\text{NC}(\text{NCy})_2]_2\text{Sm}(\text{THF})(\mu\text{-O})\text{MeAl}$ (**18**)

Further investigation with compound **17** was directed toward preparation of heterobimetallic compound. (Scheme 15)

Compound **17** was first modified by an alkyl group by reacting it with  $\text{LiCH}_2\text{SiMe}_3$  in 1:1 ratio. The intermediate was highly sensitive and was reacted with  $\text{LAlMe}(\text{OH})$  to result in the  $\mu\text{-O}$  bridged bimetallic complex **18** as tiny needles.



**Scheme 15**

Compound **18** decomposed quickly when heated under elimination of a colorless liquid. The IR spectrum indicates that no O-H stretching frequency is observed. Mass spectrum of **18** exhibits an ion of  $m/z$  (%) 418(70) representing the fragment  $[\text{NacNac}^+]$  of  $\text{LAlMe}(\text{OH})$ . Another peak at  $m/z$  (%) 160 (18) is assigned to  $[(\text{SiMe}_3)_2\text{N}^+]$  which is assigned to the starting material **17**. Due to the paramagnetic character of Sm, the NMR spectrum is not meaningful.

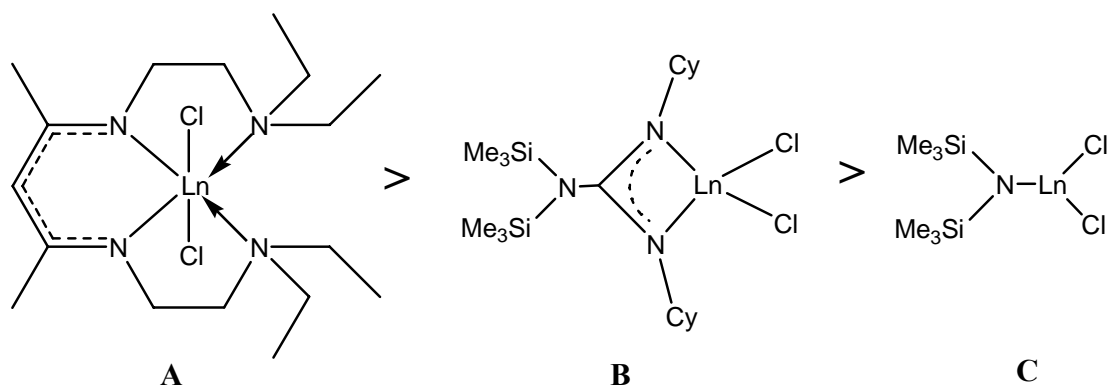
### 2.6.2. Synthesis and Structural Characterization of $L'LnCl_2(LiCl)_n(THF)_m$

Since Wilkinson synthesized the first  $Cp_3Ln$  complex in 1954,<sup>[78, 87]</sup> organolanthanide chemistry has attracted considerable attention due to its well known potential in homogeneous catalysis particularly in polymerization reactions.

Early research in this field was mostly focused on sandwich- and half-sandwich-type structures with Cp or Cp-like ligands,<sup>[88]</sup> whereas non-cyclopentadienyl ligands are known as tailor-made ligands.<sup>[88-92]</sup> It is believed that a rational design of the coordination sphere of Ln atoms might lead to the unique control of flexibility and reactivity. Nitrogen-containing ligands are considered to be of the most interesting ones, since their complexes should be fairly stable due to the coordination capability of nitrogen atoms. Nevertheless, the synthesis of those complexes is still affected by some difficulties, especially for (dichloro) $Ln^{III}$  compounds. According to the simple rule of organolanthanide chemistry, “sterically saturation” strongly affects the reactivity and stability.<sup>[93]</sup> That usually leads to compounds of composition  $[LLnCl_2]$  (L = nitrogen-containing ligand), which form adducts with LiCl, such as  $[(Me_3Si)_2NLnCl_2(THF)(LiCl)(THF)_2]_2$ .<sup>[94]</sup> Hence, complexes with the general formula  $LLnCl_2$  remain relatively rare.

However, using the  $\beta$ -diketiminato ligand we were able to isolate salt-free  $LLnX_2$  (**A**) complexes.<sup>[92]</sup> This ligand provides a planar four-membered coordination environment, which results in a perfect six-coordinate lanthanide atom (Scheme 16).

Recently, a new guanidinato ligand was synthesized, which seems to be a promising ligand system for lanthanide complexes.<sup>[90, 91]</sup> A guanidinato ligand was employed to prepare  $L'LnCl_2(LiCl)_n(THF)_m$  (**B**) compounds with the expectation that it cannot only deliver a sterically stable environment but also can modify the reactivity of the complexes. However, comparison of the number of coordinating nitrogen atoms of the guanidinato ligand with that of other nitrogen ligands results in the arrangement shown in Scheme 16. The guanidinato ligand can be placed between the  $\beta$ -diketiminato and the  $(Me_3Si)_2N$  ligand (**C**).

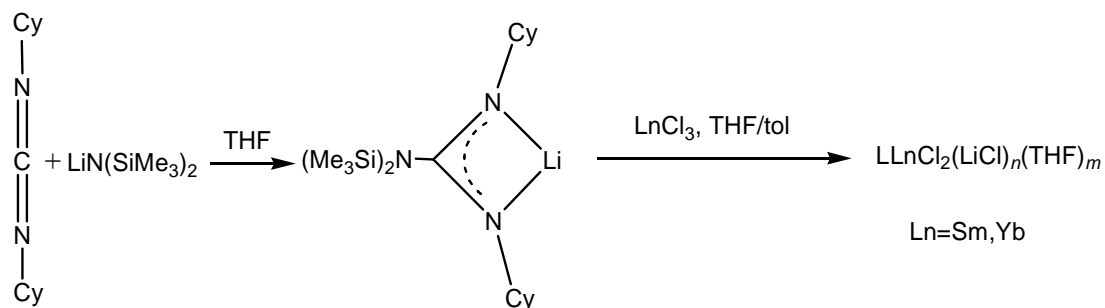


**Scheme 16.** Arrangement according to the numbers of coordinating nitrogen atoms.

We started our investigation in this area by reasoning that less bulky ligands would produce a larger unshielded surface of the molecular sphere, which might result in higher activities and new coordination sites.

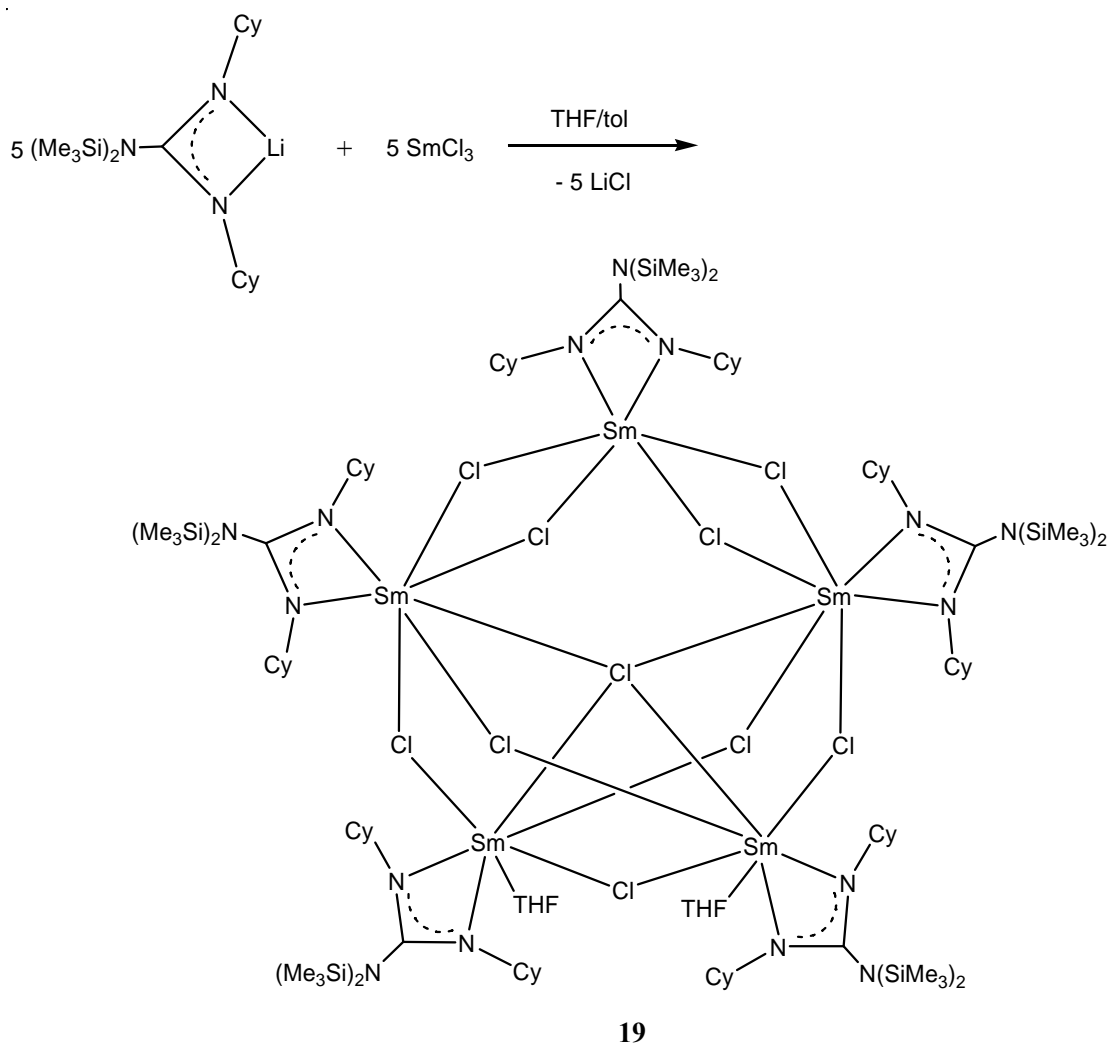
### 2.6.2.1. Synthesis of $[(\text{Me}_3\text{Si})_2\text{NC}(\text{NCy})_2\text{SmCl}_2]_5(\text{THF})_2$ (**19**)

The  $\text{LLnCl}_2(\text{LiCl})_n(\text{THF})_m$  ( $\text{L} = \text{guanidinato ligand}$ ) complexes were synthesized from anhydrous  $\text{LnCl}_3$  and  $\text{LiN}(\text{SiMe}_3)_2$  in tetrahydrofuran (Scheme 17).



**Scheme 17.** General procedure for preparation of  $\text{LLnCl}_2(\text{LiCl})_n(\text{THF})_m$  complexes.

The preparation of  $[\text{LSmCl}_2]$  from  $\text{SmCl}_3$  and  $\text{LLi}$  in a 1:1 molar ratio led to yellow crystals of  $[\text{LSmCl}_2]_5(\text{THF})_2$  (**19**), which showed a salt-free cage structure (Scheme 18).



**Scheme 18.** Synthesis of  $[LSmCl_2]_5(THF)_2$ .

Complex **19** crystallizes in the triclinic space group  $P-1$  from toluene at  $0\text{ }^\circ\text{C}$ ; **19** is stable in solvents such as tetrahydrofuran, toluene or without solvent under dry nitrogen. From X-ray structure analysis one can see that the bulky guanidinato ligands are arranged on a sphere consisting of samarium and chlorine atoms (Figure 13). Each cluster unit is composed of five  $LSmCl_2$  moieties and two THF molecules. The five  $LSmCl_2$  units are not equally arranged so that three different types can be observed.

Each guanidinato ligand coordinates to a samarium atom in a chelating fashion, with acute N–Sm–N angles [ranging from  $55.95(12)$  to  $56.51(11)^\circ$ ]. The N–Sm–N



angle is much sharper than that of a diketiminato ligand, which arranges on average around  $76^\circ$ .<sup>[89a]</sup>

The N–Sm bond lengths range from 2.356(3) to 2.384(3) Å. This is longer than the standard N–Sm bond length within the diketiminato ligand [from 2.276(3) to 2.334(3) Å],<sup>[89a]</sup> which might be due to the repulsion of the crowded guanidinato ligands (Table 6).

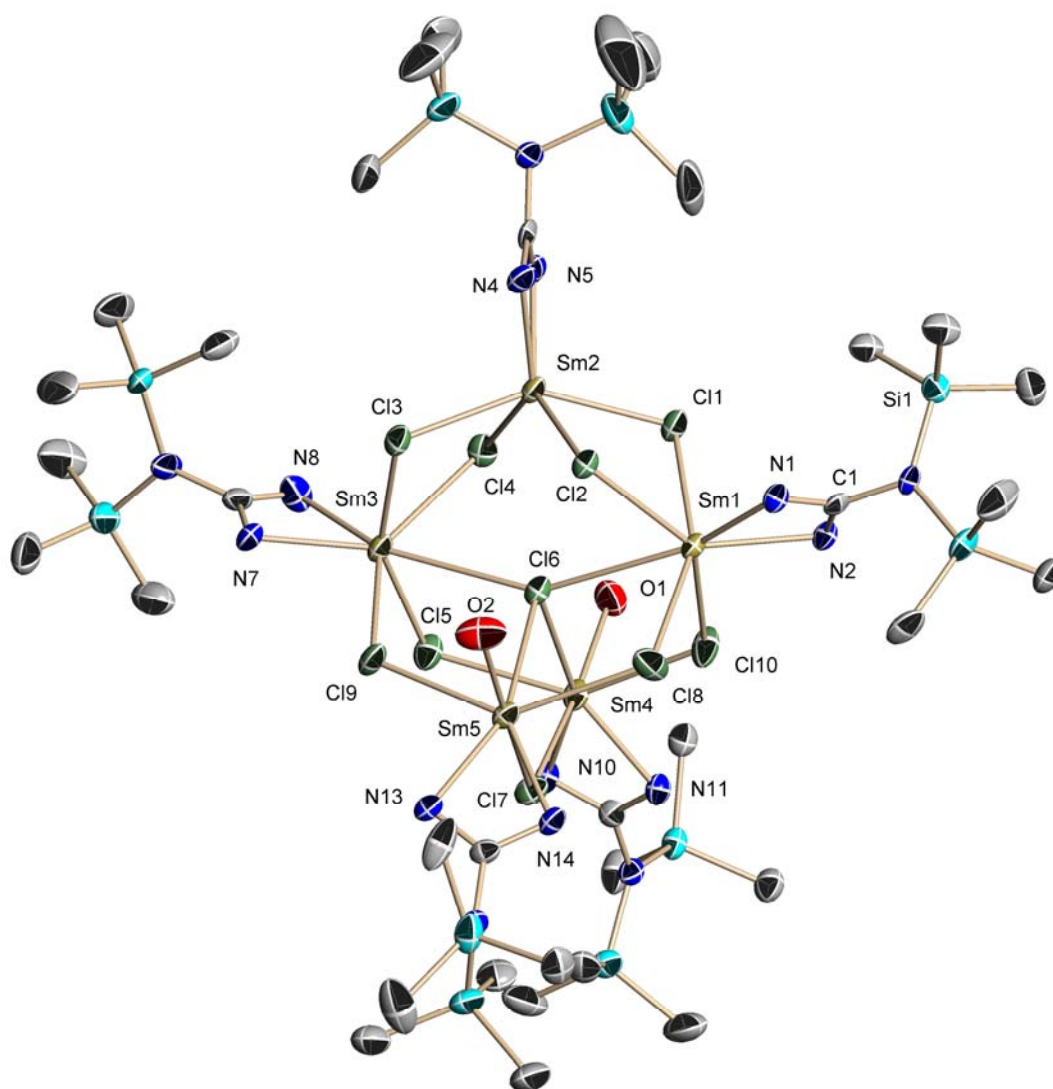


**Figure 13.** Molecular structure of **19**; thermal ellipsoids are drawn at 50% probability level; the Cy groups on nitrogen atoms are omitted for clarity.

**Table 6.** Selected Bond Lengths [ $\text{\AA}$ ] and Angles [ $^\circ$ ] of **19**

Sm(1)-N(1)	2.360(3)	Sm(3)-Cl(3)	2.7458(10)
Sm(1)-N(2)	2.384(3)	Sm(3)-Cl(9)	2.7764(10)
Sm(1)-Cl(8)	2.7160(11)	Sm(3)-Cl(4)	2.8182(10)
Sm(1)-Cl(1)	2.7584(10)	Sm(3)-Cl(6)	3.0749(10)
Sm(1)-Cl(10)	2.7592(11)	Sm(4)-N(11)	2.375(3)
Sm(1)-Cl(2)	2.7992(9)	Sm(4)-N(10)	2.375(3)
Sm(1)-Cl(6)	3.0876(10)	Sm(4)-Cl(7)	2.7199(10)
Sm(2)-N(4)	2.356(3)	Sm(4)-Cl(10)	2.7755(11)
Sm(2)-N(5)	2.370(3)	Sm(4)-Cl(5)	2.7935(10)
Sm(2)-Cl(3)	2.7223(10)	Sm(4)-Cl(6)	3.0349(10)
Sm(2)-Cl(4)	2.7293(11)	Sm(5)-N(13)	2.379(3)
Sm(2)-Cl(1)	2.7364(10)	Sm(5)-N(14)	2.383(3)
Sm(2)-Cl(2)	2.7532(9)	Sm(5)-Cl(7)	2.7282(10)
Sm(3)-N(8)	2.372(3)	Sm(5)-Cl(9)	2.7928(10)
Sm(3)-N(7)	2.373(3)	Sm(5)-Cl(8)	2.8062(11)
Sm(3)-Cl(5)	2.7171(10)	Sm(5)-Cl(6)	3.0743(10)
N(1)-Sm(1)-N(2)	56.24(10)	Sm(2)-Cl(3)-Sm(3)	97.62(3)
N(4)-Sm(2)-N(5)	56.51(11)	Sm(2)-Cl(4)-Sm(3)	95.75(3)
N(8)-Sm(3)-N(7)	55.95(12)	Sm(3)-Cl(5)-Sm(4)	113.47(4)
N(11)-Sm(4)-N(10)	56.44(10)	Sm(4)-Cl(7)-Sm(5)	111.03(4)
N(13)-Sm(5)-N(14)	56.22(10)	Sm(1)-Cl(8)-Sm(5)	114.57(4)
Sm(2)-Cl(1)-Sm(1)	96.83(3)	Sm(3)-Cl(9)-Sm(5)	118.06(4)
Sm(2)-Cl(2)-Sm(1)	95.49(3)	Sm(1)-Cl(10)-Sm(4)	118.65(4)

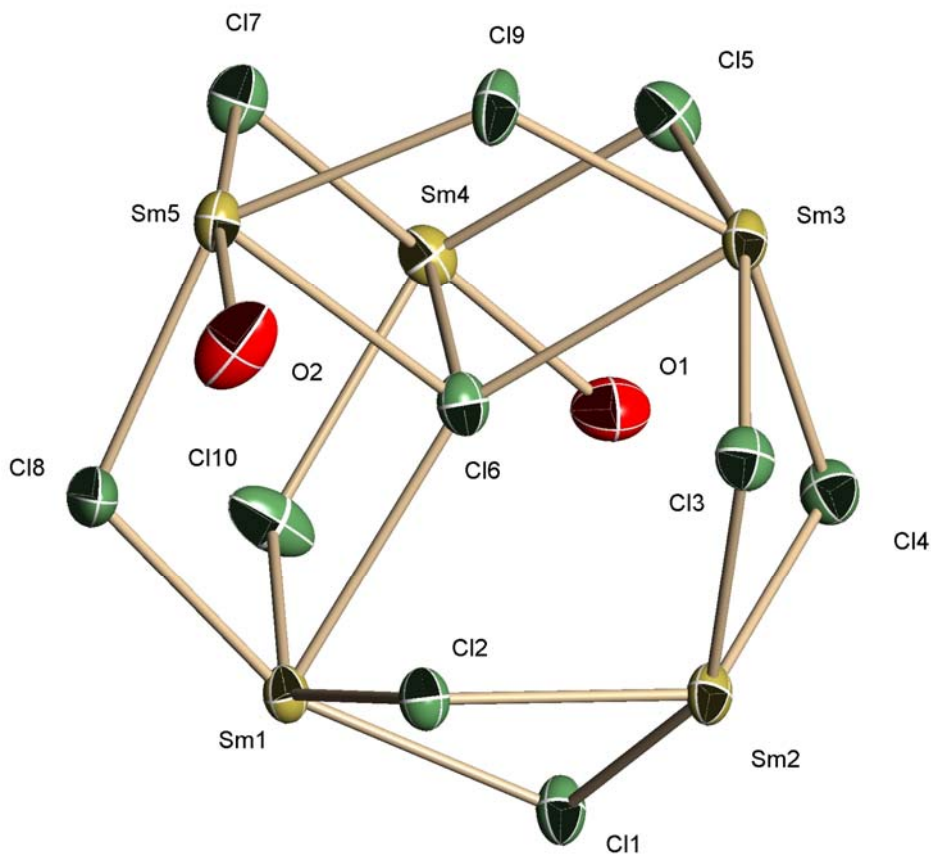


**Figure 14.** The central structure of the  $[\text{SmCl}_2]_5$  cage of **19**; thermal ellipsoids are drawn at 50% probability level.

Figure 14 shows five Sm, ten Cl atoms and two oxygen atoms of the THF molecules. The molecular sphere consists of nine  $\mu$ -chlorine atoms, each connecting to two Sm atoms. This leads to a basket-like cage.

The bridging Sm-Cl bond lengths range from 2.7160 to 2.8182 Å.

Sm(1) and Sm(3) each coordinates five chlorine atoms, whereas Sm(5) and Sm(4) coordinate four chlorine atoms and a THF molecule. An exception is Sm(2) that coordinates four chlorine atoms.

Sm(2) exhibits Sm-Cl-Sm bond angles [from 95.49(3) to 97.62(3)°] much sharper than those of the other Sm-Cl-Sm angles that range from 111.03(4) to 118.65(4)°.

Within the basket structure of the five samarium atoms, the interatomic Sm...Sm interactions are ranging from 4.110 to 4.775 Å.

Without considering the difference of the Sm–Cl bond lengths the cage has two mirror planes crossing the central Cl(6) atom with the result that Sm(1) and Sm(3) have similar surroundings, and also Sm(4) and Sm(5) are similar. However, due to the bulky ligands and the crowded environment, the mirrors are only virtually there.

An exception to the bridging chlorine atoms is Cl(6) that occupies the center of the cage, and coordinates to four Sm atoms simultaneously (Figure 14). This is an unprecedented result and has not been observed in organosamarium compounds.

When comparing the Sm–Cl(6) bond lengths with those of the bridging  $\mu$ -Cl atoms, it can be noted that the latter Sm–Cl bonds are much shorter. As shown in Table 6, the Sm–Cl(6) bond lengths are ranging from 3.0349(10) to 3.0876(10) Å, where the average Sm–( $\mu$ -Cl) bond length is 2.75 Å. The distance between Sm(2) and Cl(6) is 3.618 Å, which indicates that there is no bonding interaction between these atoms.

Compared with some other lanthanide clusters, most of them adopt a Cp-like ligand to obtain a better shielding environment, or stabilized by cations or anions.<sup>[95-100]</sup> The guanidinato ligand cluster provides a new idea to afford a less shielding environment.

Efforts to obtain a NMR spectrum of **19** led to broad resonances due to its paramagnetic character. Nevertheless, the proton resonances of the –SiMe<sub>3</sub> groups result in separated sharp signals ( $\delta$ = 0.068, 0.108, 0.173 ppm).

#### 2.6.2.2. Synthesis of [(Me<sub>3</sub>Si)<sub>2</sub>NC(NCy)<sub>2</sub>YbCl<sub>2</sub>]<sub>2</sub>(LiCl)<sub>2</sub>(THF)<sub>4</sub>(**20**)

The reaction of YbCl<sub>3</sub> with LLi in a 1:1 molar ratio in tetrahydrofuran resulted in red crystals of [LYbCl<sub>2</sub>]<sub>2</sub>(LiCl)<sub>2</sub>(THF)<sub>4</sub> (**20**) (Scheme 19). Crystals of **20** are stable in tetrahydrofuran under an inert gas. When the solvent is removed, the crystals partially

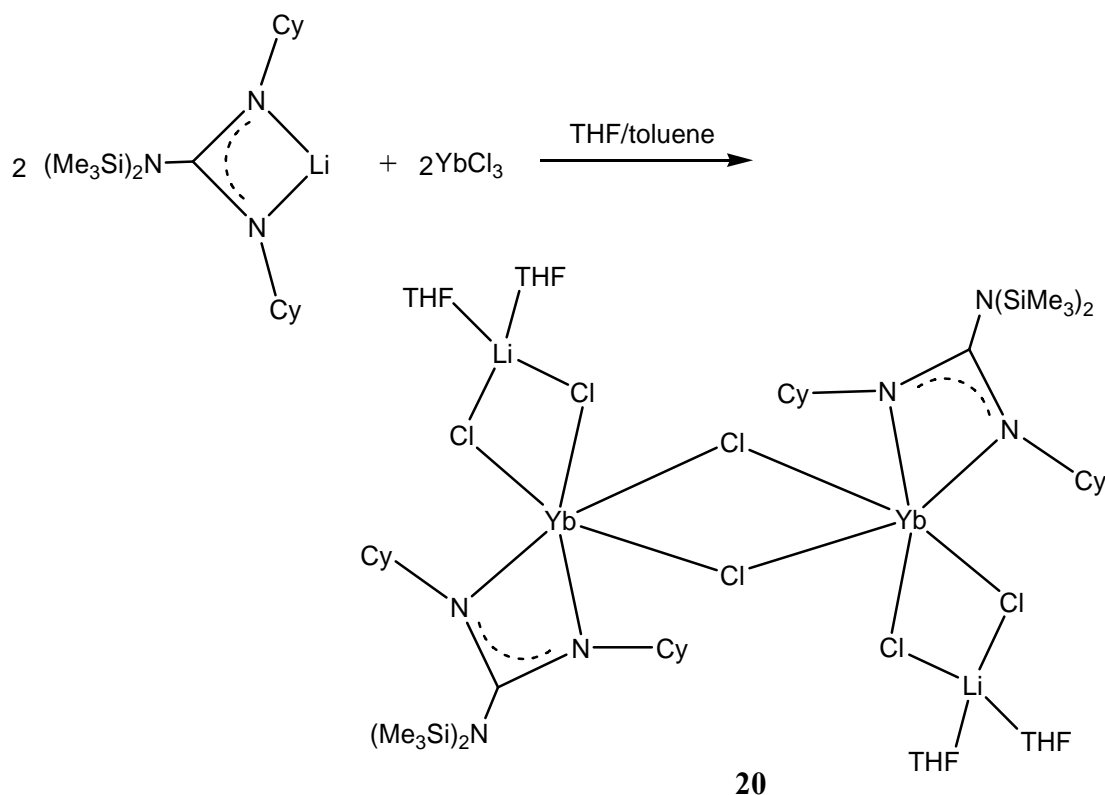
decompose to release THF and LiCl.

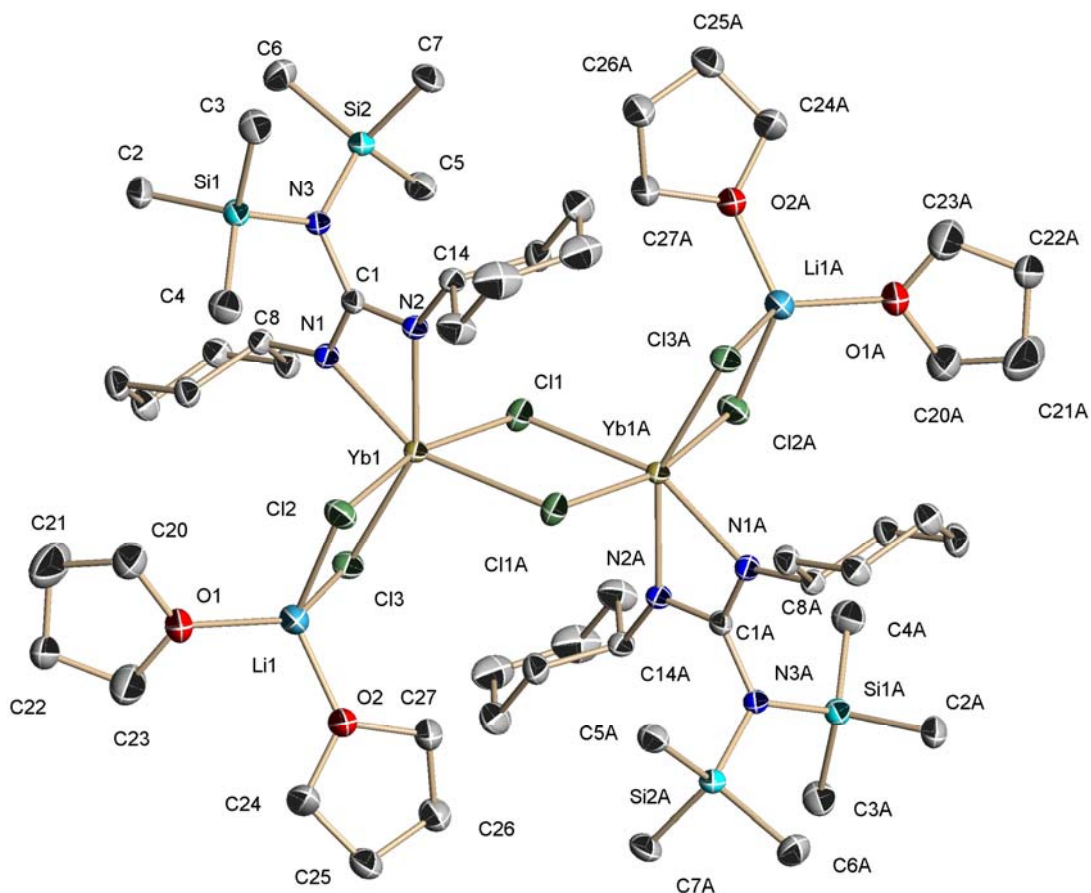
The X-ray crystal structure of **20** exhibits a stable six-coordinate lanthanide atom with cocrystallized LiCl, **20** is a dimer and consequently shows a structure that is much different from that of **19**. It crystallizes in the triclinic *P*-1 space group with an *s* center of symmetry.

Selected bond lengths and angles of **20** are listed in Table 7.

The N–Yb–N angles of the chelating guanidinato ligand average to 58.68(5)°, which are less acute than those of the corresponding ones in compound **19**. The N–Yb bond lengths range from 2.22658(15) to 2.2705(14) Å, and the Yb–Cl bond lengths within the Yb–Cl–Yb bridge [from 2.6727(7) to 2.6691(8) Å] are longer than those in the Yb–Cl–Li bridge [from 2.5944(7) to 2.5978(6) Å].

Due to its paramagnetic nature, the NMR spectrum of **20** cannot be defined in detail. Only the proton resonance of the –SiMe<sub>3</sub> groups results in a single sharp signal ( $\delta=0.062$  ppm) (Figure 15)



Scheme 19. Synthesis of  $[\text{LYbCl}_2]_2(\text{LiCl})_2(\text{THF})_4$ 

**Figure 15.** Molecular structure of **20**; thermal ellipsoids are drawn at 50% probability level.

**Table 7.** Selected Bond Lengths [ $\text{\AA}$ ] and Angles [ $^\circ$ ] for **20**

Yb(1)-N(1)	2.2658(15)	Yb(1)-Cl(2)	2.5944(7)
Yb(1)-N(2)	2.2705(14)	Yb(1)-Cl(3)	2.5978(6)
Yb(1)-Cl(1)	2.6727(7)	Yb(1)-Cl(1A)	2.6691(8)
N(1)-Yb(1)-N(2)	58.68(5)	Cl(2)-Yb(1)-Cl(3)	84.93(2)
Cl(1)-Yb(1)-Cl(1A)	78.157(17)	Yb(1)-Cl(1)-Yb(1A)	101.844(17)

The reason for the different structures of **19** and **20** might be the variation of the ionic radii from Sm to Yb (Sm: 1.132 Å; Yb: 1.042 Å).<sup>[93]</sup> Since the guanidinato ligands adopt approximately a planar configuration, the shielding angle determined along the longer edge (Figure 16) shown for **19** ranges from 129.7 to 132.8° (Table 8). Obviously, this angle for **20** is larger when compared with that of **19**.

In compound **20** the Yb atoms both have a coordination number of six, with the consequence that the ytterbium atom is arranged closer to the guanidinato ligand resulting in a better shielding, whereas in compound **19** four samarium atoms are coordinated to seven donor atoms, and only one is coordinated to six donor atoms resulting in the cage structure and a smaller shielding effect of the guanidinato ligands. It is suggested that in both reactions the same types of products are formed, but the difference in shielding effect leads to the situation that the samarium pentanuclear cluster crystallizes easier than the dinuclear one, whereas in the case of ytterbium the situation is reversed.

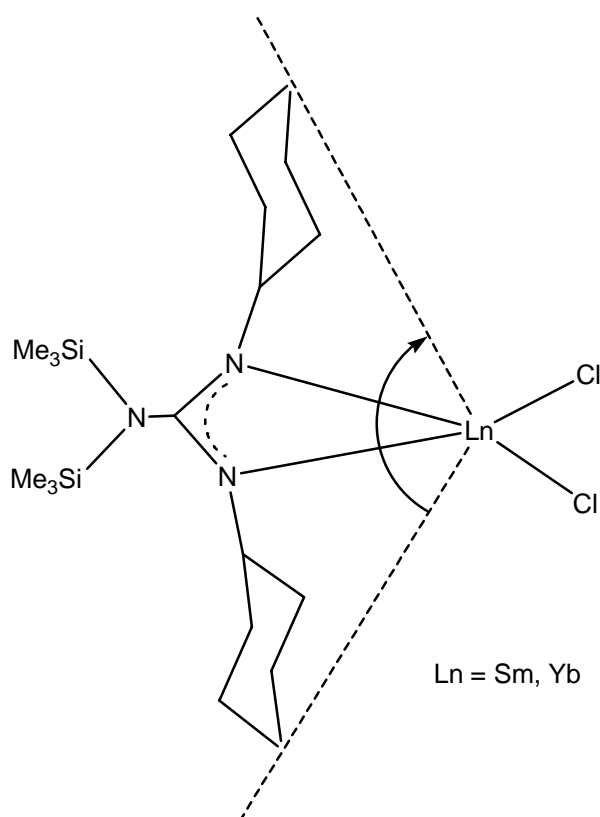


**Figure 16.** Shielding angle included by the dotted lines.

**Table 8.** Shielding Angles [°] for **19** and **20**

C(5)...Sm(1)...C(11)	129.5
C(24)...Sm(2)...C(30)	132.8
C(44)...Sm(3)...C(50)	124.7
C(64)...Sm(4)...C(70)	125.1
C(84)...Sm(5)...C(90)	125.9
In average	127.6
C(11)...Yb(1)...C(17)	135.11(3)

### 2.6.3 Attempt of Synthesis of Heterotrimetallic Oxides

Further investigations with  $L'LnCl_2(LiCl)_n(THF)_m$  were carried out with the purpose of preparing the heterotrimetallic oxides following the general procedure, LSrOH as example, in Scheme 20.

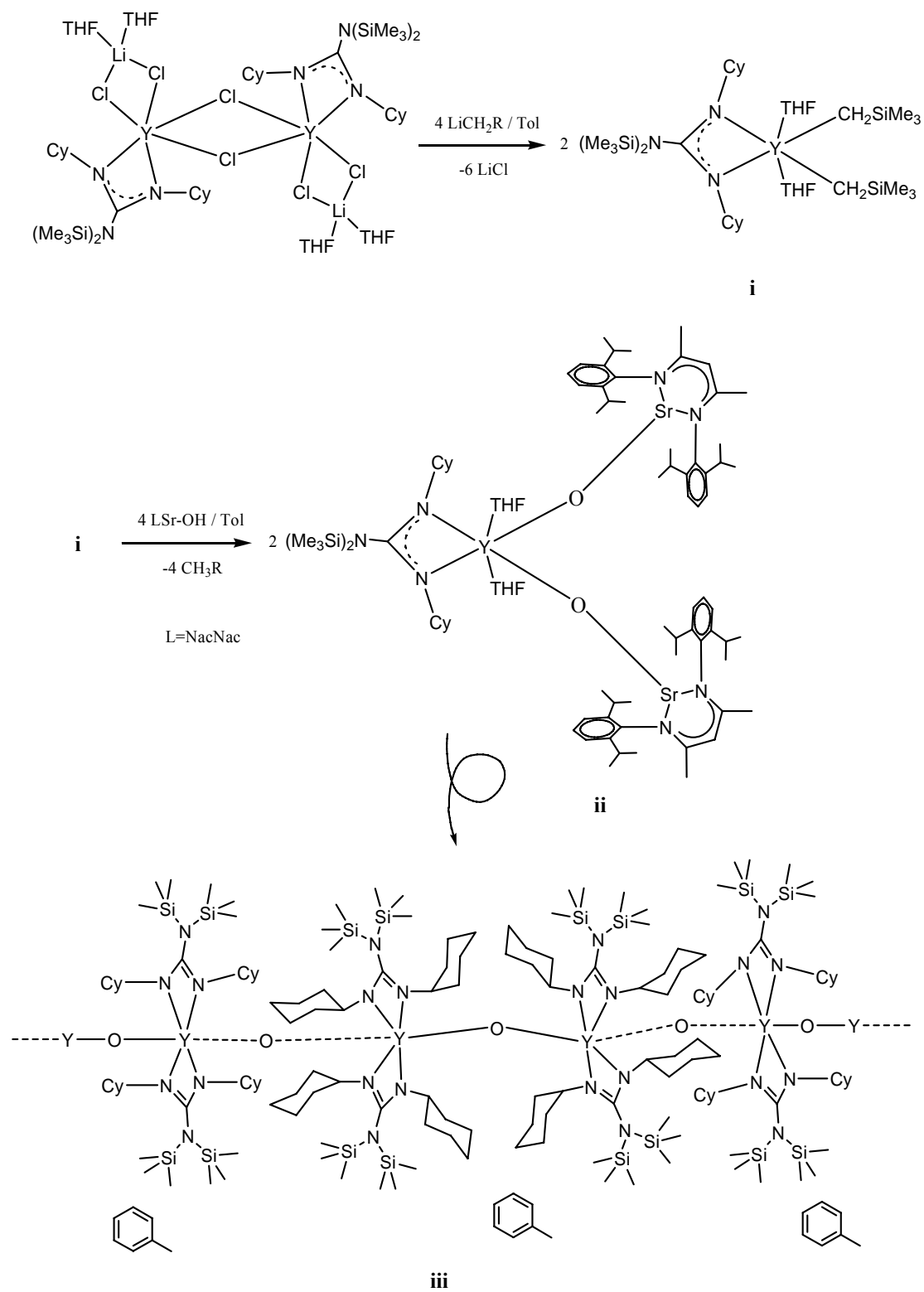
$L'LnCl_2(LiCl)_n(THF)_m$  reacting with 2 equiv.  $LiCH_2SiMe_3$  at low temperature affords a highly sensitive intermediate compound  $L'Ln(CH_2SiMe_3)_2(THF)_2$ . Then the intermediate compound reacts with 2 equiv. metal-hydroxide by eliminating  $SiMe_4$ . However, according to the results we obtained so far, the heterotrimetallic oxides are not stable. The reactions are always connected with rearrangements that result in surprising products.

The X-ray diffraction analysis with the crystals from the reaction with LMgOH and LSrOH showed that there might be different oxygen bridged metals, as shown in Scheme 20. The Mg and Sr metals are not assembled in these structures. Reactions with  $LaI_2Me(OH)$  result in similar products, but the mass spectrometric analysis from the reaction with  $Cp^*_2ZrMeOH$  showed the fragment of  $Cp^*$ . This implies there might be a Zr-O-Ln unit.

However, X-ray analysis has not defined all the details yet because of some



unusual features met during the refinement. Further efforts are still in need to establish the results.



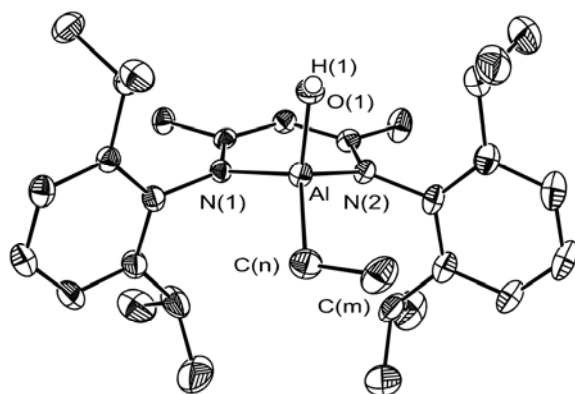
Scheme 20

### 3. Summary and Outlook

#### 3.1. Summary

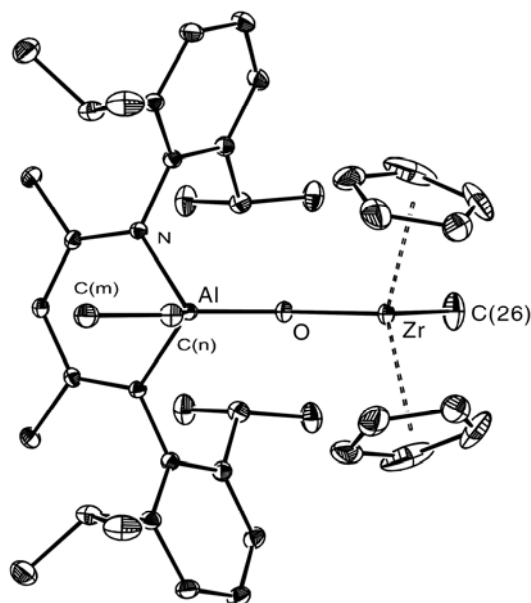
Recently, preparations of oxygen-bridged heterobi- and heterotrimetallic complexes have attracted much attention. It was found that these systems are high efficient catalysts for olefin polymerization. Many new methods have been developed, although it is still difficult to achieve, these goals with rare earth elements.

Ethyl substituted aluminum chloride (**1**) was prepared following a similar route as that of  $\text{LAlMe(OH)}$  ( $\text{L} = \text{HC}[\text{C}(\text{Me})\text{N}(\text{Ar})]_2$ ,  $\text{Ar} = 2,6\text{-}i\text{Pr}_2\text{C}_6\text{H}_3$ ). Subsequent hydrolysis of compound **1** was carried out with 1 equiv. of  $\text{H}_2\text{O}$  in the presence of 1,3-diisopropyl-4,5-dimethylimidazol-2-ylidene which resulted in the formation of ethyl substituted aluminum hydroxide (**2**). X-ray structural data for (**2**) show that the Al-O bond length is a little longer when compared with that of  $\text{LAlMe(OH)}$ .



**Structure of complex 2**

Reaction of (**2**) with 1 equiv. of  $\text{Cp}_2\text{ZrMe}_2$  in toluene afforded the  $\mu\text{-O}$  bridged  $\text{LAlEt}(\mu\text{-O})\text{ZrMeCp}_2$  (**3**). X-ray diffraction data indicated that the ethyl group on Al and the Me group on Zr stay away from each other in a trans conformation. The Zr-O bond length is also a little longer when compared with that in methyl substituted derivative.



. Structure of complex 3

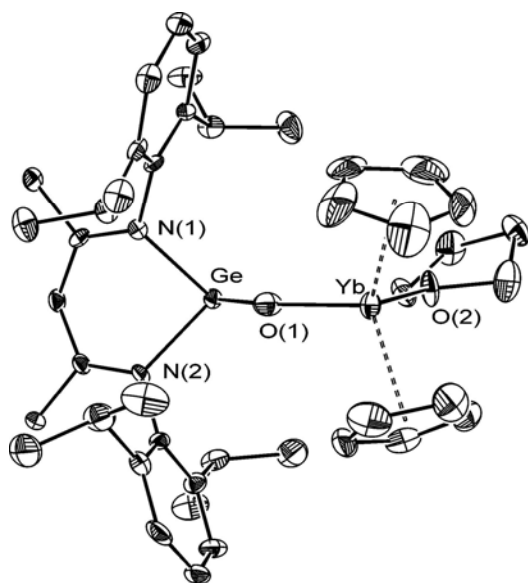
A summary of the polymerization results shows that complex (3) has lower activity than the methyl substituted one. However, it still exhibits good catalytic activity for the polymerization of ethylene.

Compound (2) reacts with  $\text{Cp}_3\text{Ln}$  to afford Al-O-Ln derivative (Ln = Yb, 4; Er, 5; Dy, 6; Y, 7). The melting points of complexes (5-7) are a little lower when compared with those of the methyl substituted ones.

The phenyl substituted Al-O-Ln derivatives (Ln = Yb, 8; Er, 9) have also been obtained.

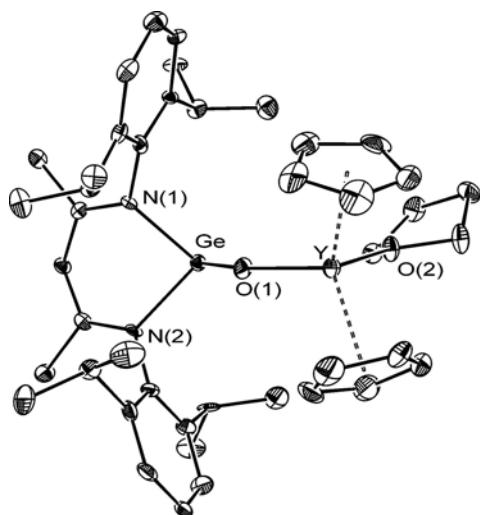
In contrast to the variation of the substituents on Al, a flexible *n*Bu group was also introduced at the Cp to afford  $\text{LAlMe}(\mu\text{-O})\text{Zr}(\text{Me})(n\text{BuC}_5\text{H}_4)_2$  (10). The  $^1\text{H}$  NMR shows that the H resonances of  $\text{C}_5\text{H}_4$  were separated into four groups. This is due to the *n*Bu group which changed the chemical environment.

The reaction of  $\text{LGeOH}$  with 1 equiv of  $\text{Cp}_3\text{Yb}$  was carried out smoothly in THF at room temperature to afford the first Ge-( $\mu\text{-O}$ )-Yb complex  $\text{LGe}(\mu\text{-O})\text{Yb}(\text{THF})\text{Cp}_2$  (11).

**Structure of complex 11**

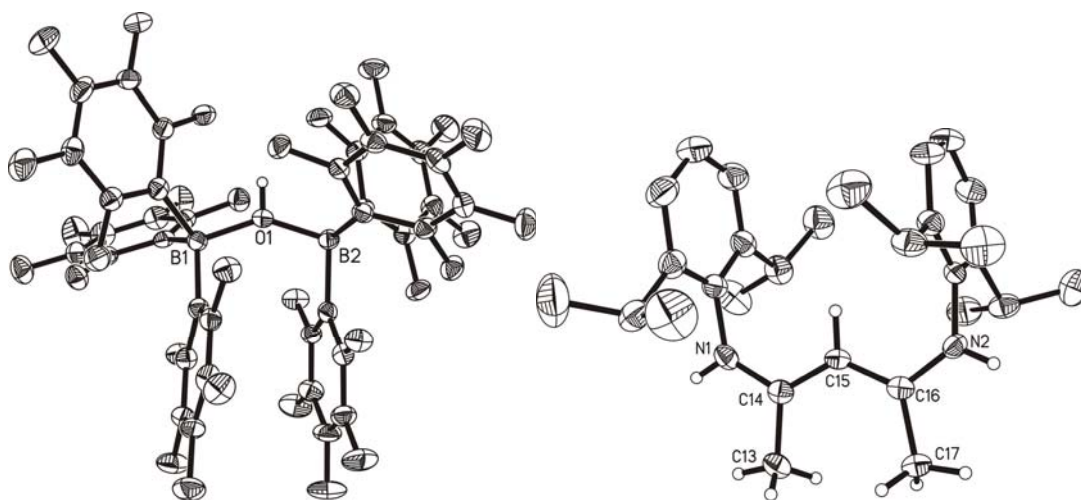
X-ray diffraction data indicate that the Ge-O bond length is shorter than those in Ge-O-Zr and Ge-O-Hf. Moreover the  $X_{Cp1}-Yb-X_{Cp2}$  angle is narrower when compared with those in Al-O-Yb compounds.

Complex  $LGe(\mu-O)Y(THF)Cp_2$  (**12**) was prepared following a similar procedure. In complex **12**, the Ge-O bond is shorter but the Y-O bond is longer.

**Structure of complex 12**

This structural feature is attributable to the formation of strong bonds between the high Lewis acidic ytterbium and yttrium elements and the hard donor oxygen, which in turn strengthens the interaction between the germanium atom and the oxygen donor.

Reaction of the strong Brønsted acid  $(C_6F_5)_3B \cdot OH_2$  with 1 equiv. of LAI: resulted in a organocation together with  $Ar_3B-(\mu-OH)-BAR_3$  anion giving complex **(13)**



**Structure of anion and cation in complex 13**

Complex **13** was characterized by X-ray structural analysis. The further investigation indicated there was an oxidation-reduction reaction between  $Al^{+1}$  and  $H^{+1}$ .

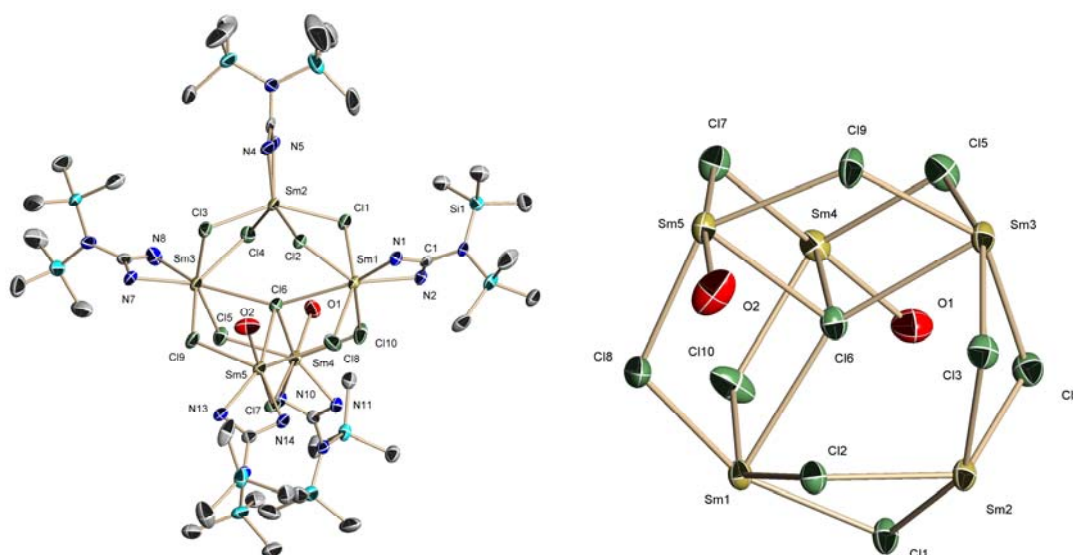
In order to investigate the reaction between a lanthanide precursor and  $Cp^*_2ZrMe(OH)$ ,  $Cp^*_2Zr(Me)OLi$  (**14**) and  $Cp^*_2PrN(SiMe_3)_2$  (**15**) were prepared. However, further reactions with **14** and **15** did not lead to satisfactory results due to their high sensitivity towards heat and moisture.

9-Oxidophenalenone and (trimethylsilylamino)naphthalene were used as ligands to modify the activity of the resulting complexes.  $(9\text{-Oxidophenalenone})_3Yb$  (**16**) was obtained as one of the products.

Guanidinato ligand was chosen to modify the structure and reactivity of lanthanide complexes.  $SmBr_3$  reacted with 2 equiv. of  $[(Me_3Si)_2NC(NCy)_2]Li$  which resulted in  $[(Me_3Si)_2NC(NCy)_2]_2SmBr_2Li(THF)_2$  (**17**). Complex **17** is a stable compound of room temperature. However, when Br atom was substituted by a  $-CH_2SiMe_3$  group, the product became highly sensitive and reacted with  $LiAlMe(OH)$  to afford the  $Al-(\mu-O)-Sm$  skeleton (**18**).

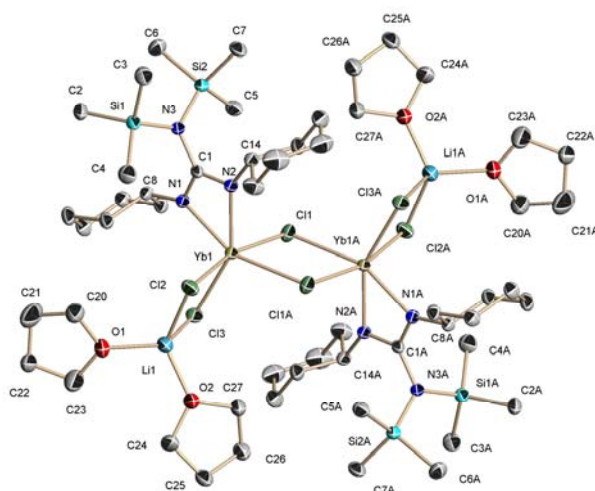
Efforts were also made to prepare  $L'LnCl_2(LiCl)_n(THF)_m$  derivatives. ( $L' = (Me_3Si)_2NC(NCy)_2$ ,  $Ln = Sm$ , **19**;  $Yb$ , **20**).

X-ray diffraction analysis of complex **19** indicates that the bulky guanidinato ligands within **19** are arranged on a sphere consisting of samarium and chlorine atoms, which leads to a basket-like cage.



**Structure of complex 19 and the the center cage**

Using a similar procedure, complex **20** was obtained. X-ray structure analysis indicated that a dimer was formed that crystallizes in the triclinic  $P-1$  space group with a  $s$  center of symmetry.



**Structure of complex 20**

## 3.2 Outlook

The dissertation presented here has emphasized on the preparation of heterobimetallic oxides with the  $M-(\mu-O)-M'$  skeleton, especially concerned with rare earth elements. Further efforts have been made to find new ligands to modify the reactivity of lanthanide complexes effectively. New methods was also developed to prepare heterotrimetallic oxides.

An extension of this work may be the preparation of new types of organolanthanide molecules with special conformation which can be used as catalyst with high efficiency.

## 4. Experimental Section

### 4.1. General Procedures

All reactions and handling of reagents were performed under an atmosphere of dry nitrogen or argon using Schlenk techniques or a glovebox where the O<sub>2</sub> and H<sub>2</sub>O levels were usually kept below 1 ppm. All glassware was oven-dried at 140 °C for at least 24 h, assembled hot and cooled under high vacuum prior to use. Toluene (Na/benzophenone ketyl and diphenylether), benzene (K/benzophenone ketyl and diphenylether), hexane (Na/K/benzophenone ketyl and diphenylether), pentane (Na/K/benzophenone ketyl and diphenylether), tetrahydrofuran (K/benzophenone ketyl), diethylether (Na/benzophenone ketyl), dichloromethane (CaH<sub>2</sub>) were dried and distilled prior to use.

### 4.2. Physical Measurements

Melting points were measured in sealed glass tubes on a Büchi B-540 melting point apparatus. NMR spectra were recorded on Bruker Avance 200, Bruker Avance 300, and Bruker Avance 500 NMR spectrometers. Chemical shifts are reported in ppm with reference to SiMe<sub>4</sub> (external) for <sup>1</sup>H, <sup>11</sup>B, <sup>13</sup>C, <sup>19</sup>F, <sup>27</sup>Al, nuclei. Downfield shifts from the reference are quoted positive, upfield shifts are assigned negative values. The NMR grade deuterated solvents were dried in following manners: C<sub>6</sub>D<sub>6</sub> and toluene –overnight stirring with Na/K alloy followed by vacuum distillation, CDCl<sub>3</sub> – 3 min. stirring with P<sub>4</sub>O<sub>10</sub> followed by filtration, THF – storing over freshly activated molecular sieves for one week. Heteroatom NMR spectra were recorded <sup>1</sup>H decoupled.

IR spectra were recorded on a Bio-Rad Digilab FTS7 spectrometer. The samples were prepared normally as Nujol mulls between KBr plates.

Mass spectra were obtained with a Finnigan MAT 8230 or a Varian MAT CH5 instrument (70 eV) by EI-MS method.



Elemental analyses were performed by the Analytisches Labor des Instituts für Anorganische Chemie der Universität Göttingen.

Crystal structure determination: Intensity data for compounds were collected on a STOE-IPDS II image-plate diffractometer. The diffraction data for the compounds were measured on a Bruker AXS instrument.<sup>[102]</sup>

The data for all the compounds were collected at low temperature (the temperatures for individual compounds are mentioned in the tables in Section 6 using graphite monochromated MoK  $\alpha$  radiation ( $\lambda = 0.71073 \text{ \AA}$ ).<sup>[101]</sup> The data reduction and space group determination were carried out using Siemens SHELXTL program. The structures were solved using SHELXS-96/97 programs. The refinement of the structures was carried out by fullmatrix least-squares method against  $F^2$  using SHELXL-97.<sup>[103-105]</sup> The various advanced features (*e.g.* restraints and constraints) of SHELXL programs were used to treat the disordered groups, lattice solvents such as THF, and the hydrogen atoms. The non-hydrogen atoms were refined anisotropically. A riding model was used for the hydrogen atoms. The crystal data for all compounds along with the final residuals and other pertaining details are listed in Section 6 in tabular form.

### 4.3 Starting Materials

Commercially available chemicals were purchased from Fluka or Aldrich and used as received. The HC[(CMe)(NAr)]<sub>2</sub> (Ar = 2,6-*i*Pr<sub>2</sub>C<sub>6</sub>H<sub>3</sub>), {HC(CMeNAr)<sub>2</sub>}Al, Cp<sub>3</sub>Ln (*n*BuC<sub>5</sub>H<sub>4</sub>)<sub>2</sub>Me<sub>2</sub>, {HC(CMeNAr)<sub>2</sub>}GeOH were synthesized using reported procedures. LiN(SiMe<sub>3</sub>)<sub>2</sub> was prepared prior to use from freshly distilled HN(SiMe<sub>3</sub>)<sub>2</sub> and MeLi in pentane. Redistilled H<sub>2</sub>O was degassed prior to use.

### 4.4 Syntheses of Compounds 1-20

#### 4.4.1 Synthesis of LAIEt(Cl) (1)

EtAlCl<sub>2</sub> (11.2 mL, 1.8 M in *n*-hexane, 20 mmol) was added drop by drop at -78 °C to LLi·OEt<sub>2</sub> (9.97 g, 20 mmol) in toluene (100 mL). The mixture was allowed to warm to room temperature and stirred for 12 h. After filtration the filtrate was concentrated (20 mL) and kept at 4 °C to afford colorless crystals. X-ray quality crystals were grown from toluene. Yield 8.05 g (79%).

M.p. 153–155 °C.

<sup>1</sup>H NMR (300.13 MHz, C<sub>6</sub>D<sub>6</sub>): δ -0.04 (q, *J* = 8.0 Hz, 2H, AlCH<sub>2</sub>CH<sub>3</sub>), 0.80 (t, *J* = 8.0 Hz, 3H, AlCH<sub>2</sub>CH<sub>3</sub>), 1.00 (d, *J* = 6.8 Hz, 6H, CH(CH<sub>3</sub>)<sub>2</sub>), 1.19 (d, *J* = 6.8 Hz, 6H, CH(CH<sub>3</sub>)<sub>2</sub>), 1.30 (d, *J* = 6.8 Hz, 6H, CH(CH<sub>3</sub>)<sub>2</sub>), 1.48 (d, *J* = 6.6 Hz, 6H, CH(CH<sub>3</sub>)<sub>2</sub>), 1.55 (s, 6H, *CMe*), 3.21 (sept, *J* = 6.8 Hz, 2H, CH(CH<sub>3</sub>)<sub>2</sub>), 3.76 (sept, *J* = 6.8 Hz, 2H, CH(CH<sub>3</sub>)<sub>2</sub>), 4.96 (s, 1H, *γ*-CH), 7.04–7.15 (m, *Ar*) ppm.

<sup>13</sup>C NMR (75.5 MHz, C<sub>6</sub>D<sub>6</sub>): δ 170.7 (CN), 146.0, 143.3, 139.7, 127.7, 125.4, 123.9 (*i*-, *o*-, *m*-, *p*-*Ar*), 98.7 (*γ*-CH), 29.2, 28.1 (CH(CH<sub>3</sub>)<sub>2</sub>), 26.9, 24.9, 24.5, 23.8 (CH(CH<sub>3</sub>)<sub>2</sub>), 23.2 (*β*-CH<sub>3</sub>), 8.5 (AlCH<sub>2</sub>CH<sub>3</sub>), -1.0 (br, AlCH<sub>2</sub>CH<sub>3</sub>) ppm.

IR (Nujol, mull, cm<sup>-1</sup>):  $\tilde{\nu}$  = 3062 (s), 1587 (m), 1558 (s), 1534 (s), 1517 (s), 1442 (s), 1344 (s), 1319 (s), 1259 (s), 1177 (m), 1101 (m), 1021 (s), 938 (m), 878 (w), 834 (w), 801 (m), 777 (w), 759 (w), 718 (w), 648 (w), 618 (m), 533 (m).

EI-MS: *m/z* (%): 479 (100) [M<sup>+</sup>-Et].

Elemental analysis for C<sub>31</sub>H<sub>46</sub>AlClN<sub>2</sub> (509.1): Calcd. C, 73.13; H, 9.11; N, 5.50. Found: C, 72.45; H, 8.86; N, 5.43.

#### 4.4.2 Synthesis of LAIEt(OH) (2)

To a mixture of LAIEt(Cl) (2.04 g, 4 mmol) and [CN(*i*Pr)C<sub>2</sub>Me<sub>2</sub>N(*i*Pr)] (:C, 0.72 g, 4 mmol) in toluene (60 mL) at 0 °C, distilled H<sub>2</sub>O (18 μL, 4 mmol) was added. The suspension was allowed to warm to room temperature and stirred for 12 h. The

insoluble solid was removed by filtration and from the filtrate all volatiles were removed in vacuo and the resulting residue was washed with *n*-pentane (5 mL) to afford a white solid. X-ray quality crystals were grown from THF at 4 °C. Yield 1.43 g (73%).

M.p. 163 °C.

<sup>1</sup>H NMR (500.13MHz, C<sub>6</sub>D<sub>6</sub>): δ -0.23 (q, *J* = 8.2 Hz, 2H, AlCH<sub>2</sub>CH<sub>3</sub>), 0.63 (s, 1H, OH), 0.71 (t, *J* = 8.2 Hz, 3H, AlCH<sub>2</sub>CH<sub>3</sub>), 1.06 (d, *J* = 6.8 Hz, 6H, CH(CH<sub>3</sub>)<sub>2</sub>), 1.21 (d, *J* = 7.0 Hz, 6H, CH(CH<sub>3</sub>)<sub>2</sub>), 1.32 (d, *J* = 7.0 Hz, 6H, CH(CH<sub>3</sub>)<sub>2</sub>), 1.34 (d, *J* = 6.6 Hz, 6H, CH(CH<sub>3</sub>)<sub>2</sub>), 1.58 (s, 6H, CMe), 3.22 (sept, *J* = 6.8 Hz, 2H, CH(CH<sub>3</sub>)<sub>2</sub>), 3.68 (sept, *J* = 6.8 Hz, 2H, CH(CH<sub>3</sub>)<sub>2</sub>), 4.93 (s, 1H, γ-CH), 7.07–7.15 (m, *Ar*) ppm.

<sup>13</sup>C NMR (125.8 MHz, C<sub>6</sub>D<sub>6</sub>): δ 169.3 (CN), 145.4, 143.4, 140.8, 127.3, 124.9, 123.9 (*i*-, *o*-, *m*-, *p*-*Ar*), 97.3 (γ-CH), 28.9, 27.8 (CH(CH<sub>3</sub>)<sub>2</sub>), 26.1, 24.9, 24.4, 24.0 (CH(CH<sub>3</sub>)<sub>2</sub>), 23.1 (β-CH<sub>3</sub>), 9.2 (AlCH<sub>2</sub>CH<sub>3</sub>), -2.4 (br, AlCH<sub>2</sub>CH<sub>3</sub>) ppm.

IR (Nujol, mull, cm<sup>-1</sup>): ν̃ = 3729 (m, OH), 1654 (w), 1552 (w), 1529 (w), 1319 (m), 1261 (w), 1179 (w), 1101 (w), 1059 (w), 1021 (w), 938 (w), 875 (w), 834 (w), 802 (w), 761 (w), 723 (w), 657 (w).

EI-MS: *m/z* (%): 473.3 (24) [M<sup>+</sup>-OH], 461.3 (100) [M<sup>+</sup>-Et].

Elemental analysis for C<sub>31</sub>H<sub>47</sub>AlN<sub>2</sub>O (490.7): Calcd. C, 75.88; H, 9.65; N, 5.71. Found: C, 75.24; H, 9.44; N, 5.62.

#### 4.4.3 Synthesis of LAIEt(μ-O)ZrMeCp<sub>2</sub> (3)

Toluene (40 mL) was added to the mixture of LAIEt(OH) (0.49 g, 1 mmol) and Cp<sub>2</sub>ZrMe<sub>2</sub> (0.26 g, 1 mmol). The resulting solution was stirred for 2 h at room temperature, and then continuously for 24 h at 100 °C. After concentration and keeping the solution at room temperature for 1 day, colorless crystals (0.51 g) were isolated. Yield 0.48 g (66 %).

M.p. 368–369 °C.

$^1\text{H}$  NMR (500.13 MHz,  $\text{CDCl}_3$ ):  $\delta$  0.32 (s, 3H,  $\text{ZrMe}$ ), -0.14 (q,  $J = 7.9$  Hz, 2H,  $\text{AlCH}_2\text{CH}_3$ ), 1.04 (d,  $J = 6.8$  Hz, 6H,  $\text{CH}(\text{CH}_3)_2$ ), 1.14 (t,  $J = 7.9$  Hz, 3H,  $\text{AlCH}_2\text{CH}_3$ ), 1.25 (d,  $J = 6.8$  Hz, 6H,  $\text{CH}(\text{CH}_3)_2$ ), 1.37 (d,  $J = 6.8$  Hz, 6H,  $\text{CH}(\text{CH}_3)_2$ ), 1.41 (d,  $J = 6.8$  Hz, 6H,  $\text{CH}(\text{CH}_3)_2$ ), 1.77 (s, 6H,  $\text{CMe}$ ), 3.15 (sept,  $J = 6.8$  Hz, 2H,  $\text{CH}(\text{CH}_3)_2$ ), 3.29 (sept,  $J = 6.8$  Hz, 2H,  $\text{CH}(\text{CH}_3)_2$ ), 5.02 (s, 1H,  $\gamma\text{-CH}$ ), 5.30 (s, 10H,  $\text{C}_5\text{H}_5$ ), 7.24–7.27 (m,  $\text{Ar}$ ) ppm.

$^{13}\text{C}$  NMR (125.8 MHz,  $\text{CDCl}_3$ ):  $\delta$  170.5 (CN), 144.7, 143.9, 141.2, 127.0, 124.7, 124.2 (*i*-, *o*-, *m*-, *p*- $\text{Ar}$ ), 109.9 ( $\text{C}_5\text{H}_5$ ), 97.3 ( $\gamma\text{-CH}$ ), 28.7, 27.1 ( $\text{CH}(\text{CH}_3)_2$ ), 25.3, 25.2, 24.6, 24.6 ( $\text{CH}(\text{CH}_3)_2$ ), 23.8 ( $\beta\text{-CH}_3$ ), 17.6 ( $\text{ZrMe}$ ), 9.4 ( $\text{AlCH}_2\text{CH}_3$ ), 3.4 (br,  $\text{AlCH}_2\text{CH}_3$ ) ppm.

IR (Nujol, mull,  $\text{cm}^{-1}$ ):  $\tilde{\nu} = 1734$  (m), 1653 (w), 1624 (w), 1591 (w), 1530 (m), 1396 (s), 1317 (m), 1259 (m), 1177 (m), 1099 (m), 1059 (w), 1019 (m), 940 (w), 872 (w), 839 (m), 795 (s), 759 (w), 724 (w), 643 (w), 599 (w), 587 (w), 568 (w), 530 (w), 442 (w).

EI-MS:  $m/z$  (%): 709.3 (88) [ $\text{M}^+ - \text{Me}$ ], 695.3 (100) [ $\text{M}^+ - 2\text{Me} + 1$ ].

Elemental analysis for  $\text{C}_{42}\text{H}_{59}\text{AlN}_2\text{OZr}$  (726.1): Calcd. C, 69.47; H, 8.19; N, 3.86. Found: C, 69.40; H, 8.32; N, 3.52.

#### 4.4.4 Synthesis of $\text{LAIEt}(\mu\text{-O})\text{Yb}(\text{THF})\text{Cp}_2$ (4)

THF (40 mL) was added to the mixture of  $\text{LAIEt}(\text{OH})$  (0.84 g, 1.71 mmol) and  $\text{Cp}_3\text{Yb}$  (0.63 g, 1.71 mmol) at room temperature. The resulting solution was stirred for 12 h until the color of the solution turned from dark green to brown. Finally all volatiles were removed in vacuo, and then the residual was extracted with THF (30 mL). The resulting solution was kept at room temperature for 1 day to afford yellow crystals. Yield 0.62 g (42%).

M.p. 208–210 °C.

IR (Nujol, mull,  $\text{cm}^{-1}$ ):  $\tilde{\nu} = 3063$  (m), 1624 (w), 1586 (w), 1525 (m), 1504 (m), 1314 (m), 1259 (m), 1195 (w), 1176 (w), 1100 (m), 1057 (m), 1017 (m), 949 (w), 936 (w), 907 (m), 799 (m), 776 (m), 762 (m), 722 (w), 663 (w), 643 (w), 624 (w), 597 (w), 571 (w), 447 (w).

EI-MS:  $m/z$  (%): 764.4 (100) [ $\text{M}^+$ -THF-Et], 698.3 (12) [ $\text{M}^+$ -THF-Et-Cp].

Elemental analysis for  $\text{C}_{45}\text{H}_{64}\text{AlN}_2\text{O}_2\text{Yb}$  (865.0): Calcd. C, 62.48; H, 7.46; N, 3.24. Found: C, 61.91; H, 7.30; N, 3.24.

#### 4.4.5 Synthesis of $\text{LAIEt}(\mu\text{-O})\text{Er}(\text{THF})\text{Cp}_2$ (5)

THF (40 mL) was added to the mixture of  $\text{LAIEt}(\text{OH})$  (0.49 g, 1 mmol) and  $\text{Cp}_3\text{Er}$  (0.36 g, 1 mmol) at room temperature. The resulting solution was stirred for 12 h until the color of the solution turned from pink to yellow. Finally all volatiles were removed in vacuo, and then the residual was extracted with THF (30 mL). The resulting solution was kept at room temperature for 1 day to afford yellow crystals. Yield 0.18 g (21%).

M.p. 235 °C.

IR (Nujol, mull,  $\text{cm}^{-1}$ ):  $\tilde{\nu} = 3063$  (w), 1585 (w), 1525 (w), 1313 (w), 1254 (w), 1195 (w), 1175 (w), 1100 (w), 1057 (w), 1015 (w), 936 (w), 903 (m), 799 (w), 772 (m), 762 (m), 722 (w).

EI-MS:  $m/z$  (%): 758.3 (100) [ $\text{M}^+$ -THF-Et], 693.3 (6) [ $\text{M}^+$ -THF-Et-Cp].

Elemental analysis for  $\text{C}_{45}\text{H}_{64}\text{AlErN}_2\text{O}_2$  (859.2): Calcd. C, 62.90; H, 7.51; N, 3.26. Found: C, 61.40; H, 7.36; N, 3.08.

#### 4.4.6 Synthesis of $\text{LAIEt}(\mu\text{-O})\text{Dy}(\text{THF})\text{Cp}_2$ (6)

THF (40 mL) was added to the mixture of  $\text{LAIEt}(\text{OH})$  (0.49 g, 1 mmol) and  $\text{Cp}_3\text{Dy}$  (0.36 g, 1 mmol) at room temperature. The resulting solution was stirred for

12 h until the color of the solution turned from yellow to light yellow. Finally all volatiles were removed in vacuo, and then the residual was extracted with THF (30 mL). The resulting solution was kept at room temperature for 1 day to afford yellow crystals. Yield 0.24 g (28%).

M.p. 208–210 °C.

IR (Nujol, mull,  $\text{cm}^{-1}$ ):  $\tilde{\nu}$  = 1623 (w), 1585 (w), 1528 (w), 1314 (w), 1260 (w), 1175 (w), 1099 (w), 1058 (w), 1018 (w), 936 (w), 898 (w), 799 (w), 772 (w), 761 (w), 722 (w), 664 (w).

EI-MS:  $m/z$  (%): 754.3(100) [ $\text{M}^+$ -THF-Et], 688.3 (20) [ $\text{M}^+$ -THF-Et-Cp].

Elemental analysis for  $\text{C}_{45}\text{H}_{64}\text{AlDyN}_2\text{O}_2$  (854.5): Calcd. C, 63.25; H, 7.55; N, 3.28. Found: C, 62.71; H, 7.61; N, 3.26.

#### 4.4.7 Synthesis of $\text{LAIEt}(\mu\text{-O})\text{Y}(\text{THF})\text{Cp}_2$ (7)

THF (40 mL) was added to the mixture of  $\text{LAIEt}(\text{OH})$  (0.49 g, 1 mmol) and  $\text{Cp}_3\text{Y}$  (0.28 g, 1 mmol) at room temperature. The resulting solution was stirred for 12 h until the color of the solution turned from yellow to light yellow. Finally all volatiles were removed in vacuo, and then the residual was extracted with THF (30 mL). The resulting solution was kept at room temperature for 1 day to afford yellow crystals. Yield 0.34 g (44%).

M.p. 208–210 °C.

$^1\text{H}$  NMR (500.13 MHz,  $\text{C}_6\text{D}_6$ ):  $\delta$  0.40 (q,  $J$  = 8.0 Hz, 2H,  $\text{AlCH}_2\text{CH}_3$ ), 1.15 (d,  $J$  = 6.8 Hz, 6H,  $\text{CH}(\text{CH}_3)_2$ ), 1.31 (d,  $J$  = 6.8 Hz, 6H,  $\text{CH}(\text{CH}_3)_2$ ), 1.34 (br, 4H,  $\text{O}-(\text{CH}_2\text{CH}_2)_2$ ), 1.50 (d,  $J$  = 6.8 Hz, 6H,  $\text{CH}(\text{CH}_3)_2$ ), 1.51 (d,  $J$  = 6.8 Hz, 6H,  $\text{CH}(\text{CH}_3)_2$ ), 1.52 (s, 6H,  $\text{CMe}$ ), 1.60 (t,  $J$  = 8.0 Hz, 3H,  $\text{AlCH}_2\text{CH}_3$ ), 3.08 (br, 4H,  $\text{O}-(\text{CH}_2\text{CH}_2)_2$ ), 3.45 (sept,  $J$  = 6.8 Hz, 2H,  $\text{CH}(\text{CH}_3)_2$ ), 3.64 (sept,  $J$  = 6.8 Hz, 2H,  $\text{CH}(\text{CH}_3)_2$ ), 4.84 (s, 1H,  $\gamma\text{-CH}$ ), 5.85 (s, 10H,  $\text{C}_5\text{H}_5$ ), 7.14–7.19 (m,  $\text{Ar}$ ) ppm.

$^{13}\text{C}$  NMR (125.8 MHz,  $\text{C}_6\text{D}_6$ ):  $\delta$  170.6 (CN), 145.2, 144.0, 143.0, 126.9, 124.6, 124.5 (*i*-, *o*-, *m*-, *p*-Ar), 110.0 ( $\text{C}_5\text{H}_5$ ), 99.2 ( $\gamma$ -CH), 71.0 (br, O-( $\text{CH}_2\text{CH}_2$ ) $_2$ ), 28.8, 27.6 ( $\text{CH}(\text{CH}_3)_2$ ), 26.6, 25.6 (O-( $\text{CH}_2\text{CH}_2$ ) $_2$ ), 25.4, 24.9, 24.8 ( $\text{CH}(\text{CH}_3)_2$ ), 23.9 ( $\beta$ -CH $_3$ ), 12.2 ( $\text{AlCH}_2\text{CH}_3$ ), 6.6 (br,  $\text{AlCH}_2\text{CH}_3$ ) ppm.

IR (Nujol, mull,  $\text{cm}^{-1}$ ):  $\tilde{\nu}$  = 3060 (s), 2414 (w), 2069 (w), 1954 (w), 1930 (w), 1754 (w), 1626 (w), 1584 (w), 1524 (s), 1503 (m), 1313 (s), 1255 (s), 1194 (w), 1175 (m), 1100 (m), 1057 (m), 1015 (s), 948 (w), 936 (m), 901 (s), 799 (s), 772 (s), 761 (s), 722 (m), 642 (w), 622 (m), 597 (m), 569 (s).

EI-MS:  $m/z$  (%): 461.3 [ $\text{M}^+$ -Et-Y(THF) $\text{Cp}_2$ ] (100).

Elemental analysis for  $\text{C}_{45}\text{H}_{64}\text{AlN}_2\text{O}_2\text{Y}$  (780.9): Calcd. C, 69.21; H, 8.26; N, 3.59. Found: C, 68.76; H, 7.48; N, 3.55.

#### 4.4.8 Synthesis of $\text{LAlPh}(\mu\text{-O})\text{Yb}(\text{THF})\text{Cp}_2$ (**8**)

THF (40 mL) was added to the mixture of  $\text{LAlPh}(\text{OH})$  (0.54 g, 1 mmol) and  $\text{Cp}_3\text{Yb}$  (0.37 g, 1 mmol) at room temperature. The resulting solution was stirred for 12 h until the color of the solution turned from dark green to brown. Finally all volatiles were removed in vacuo, and then the residual was extracted with THF (30 mL). The resulting solution was kept at low temperature to afford very tiny yellow crystals. Yield: 0.30 g (33 %).

M.p. 320°C (decomp.).

IR (Nujol, mull,  $\text{cm}^{-1}$ ):  $\tilde{\nu}$  = 3055 (w), 1646 (w), 1573 (w), 1543 (w), 1322 (w), 1261 (w), 1210 (w), 1179 (w), 1124 (w), 1095 (w), 1046 (w), 1020 (w), 891 (w), 790 (w), 784 (w), 762 (w), 721 (w), 699 (w), 663 (w).

EI-MS:  $m/z$  (%): 764 (100) [ $\text{M}^+$ -THF-Ph]

Elemental analysis for  $\text{C}_{49}\text{H}_{64}\text{AlN}_2\text{O}_2\text{Yb}$  (913.07): Calcd. C, 64.46; H, 7.07; N, 3.07. Found: C, 63.92 ; H, 7.63; N, 3.14.

#### 4.4.9 Synthesis of $\text{LAlPh}(\mu\text{-O})\text{Er}(\text{THF})\text{Cp}_2$ (9)

THF (40 mL) was added to the mixture of  $\text{LAlPh}(\text{OH})$  (0.54 g, 1 mmol) and  $\text{Cp}_3\text{Er}$  (0.36 g, 1 mmol) at room temperature. The resulting solution was stirred for 12 h until the color of the solution turned from pink to brown. Finally all volatiles were removed in vacuo, and then the residual was extracted with THF (30 mL). The resulting solution was kept at low temperature to afford very tiny pink crystals. Yield: 0.22 g (24%).

M.p. 320°C (decomp).

IR (Nujol, mull,  $\text{cm}^{-1}$ ):  $\tilde{\nu}$  = 3050 (w), 1619 (w), 1575 (w), 1527 (w), 1319 (w), 1270 (w), 1214 (w), 1183 (w), 1099 (w), 1073 (w), 1046 (w), 1022 (w), 883 (w), 799 (w), 765 (w), 743 (w), 718 (w), 674 (w).

EI-MS:  $m/z$  (%): 758 (100) [ $\text{M}^+$ -THF-Ph]

Elemental analysis for  $\text{C}_{49}\text{H}_{64}\text{AlN}_2\text{O}_2\text{Er}$  (907.29): Calcd. C, 64.87; H, 7.11; N, 3.09; Found: C, 64.29 ; H, 7.04 ; N, 3.12.

#### 4.4.10 Synthesis of $\text{LAlMe}(\mu\text{-O})\text{Zr}(n\text{BuC}_5\text{H}_4)_2$ (10)

$\text{MeLi}$  (2.5 M, 2.4 mL, 6 mmol) was added drop by drop to a solution of  $(n\text{BuC}_5\text{H}_4)_2\text{ZrCl}_2$  (1.2g, 3 mmol) in THF (60 mL) at 0 °C with stirring and then warmed to room temperature overnight. The solvent was removed in vacuum and the residual was extracted with toluene and filtered to remove the  $\text{LiCl}$ . After toluene was removed, a red colored oil was obtained as  $(n\text{BuC}_5\text{H}_4)_2\text{ZrMe}_2$ .

Newly prepared  $(n\text{BuC}_5\text{H}_4)_2\text{ZrMe}_2$  was reacted with  $\text{LAlMe}(\text{OH})$  (1.4g, 3mmol) in situ in toluene (50 mL) for 2 hours at room temperature, and then continuously for 24 h at 100 °C. After concentration and keeping the solution at 4 °C, colorless crystals were isolated. Yield: 0.56g (23%)



M.p. 315°C (decomp).

$^1\text{H}$  NMR (200.13 MHz,  $\text{C}_6\text{D}_6$ ):  $\delta$  0.12 (s, 3H, *ZrMe*), -0.28 (s, 3H, *AlCH*<sub>3</sub>), 0.88 (d,  $J$  = 6.8 Hz, 6H, *CH(CH*<sub>3</sub>)<sub>2</sub>), 1.08 (d,  $J$  = 6.8 Hz, 6H, *CH(CH*<sub>3</sub>)<sub>2</sub>), 1.20 (d,  $J$  = 6.8 Hz, 6H, *CH(CH*<sub>3</sub>)<sub>2</sub>), 1.31 (d,  $J$  = 6.8 Hz, 6H, *CH(CH*<sub>3</sub>)<sub>2</sub>), 1.54 (m,  $J$  = 6.8 Hz, 18H, *Cp(n-Bu)*), 3.32 (sept,  $J$  = 6.8 Hz, 4H, *CH(CH*<sub>3</sub>)<sub>2</sub>), 2.27 (m, 6H, *CMe*), 4.80 (s, 1H,  $\gamma$ -*CH*), 5.05 (b, 2H, *C*<sub>5</sub>*H*<sub>5</sub>), 5.11 (b, 2H, *C*<sub>5</sub>*H*<sub>5</sub>), 5.26 (b, 2H, *C*<sub>5</sub>*H*<sub>5</sub>), 5.57 (b, 2H, *C*<sub>5</sub>*H*<sub>5</sub>), 7.24–7.27 (m, *Ar*) ppm.

IR (Nujol, mull,  $\text{cm}^{-1}$ ):  $\tilde{\nu}$  = 1735 (m), 1650 (w), 1619 (w), 1585 (w), 1528 (m), 1399 (s), 1315 (m), 1254 (m), 1171 (m), 1096 (m), 1050 (w), 1015 (m), 937 (w), 870 (w), 832 (m), 794 (s), 753 (w), 724 (w), 641 (w), 592 (w), 585 (w), 567 (w), 528 (w), 440 (w).

EI-MS:  $m/z$  (%): 809 (82) [ $\text{M}^+$ -Me]

Elemental analysis for  $\text{C}_{49}\text{H}_{73}\text{AlN}_2\text{OZr}$  (824.32): Calcd. C, 71.39; H, 8.93; N, 3.40; Found: C, 70.69 ; H, 9.14; N, 3.41.

#### 4.4.11 Synthesis of $\text{LGe}(\mu\text{-O})\text{Yb}(\text{THF})\text{Cp}_2$ (11)

THF (60 mL) was added to a mixture of  $\text{LGeOH}$  (0.86 g, 1.69 mmol) and  $\text{Cp}_3\text{Yb}$  (0.62 g, 1.69 mmol) at room temperature. The mixture was stirred overnight, and the color of the solution turned yellow from dark green. After the removal of all volatiles in vacuo, the residue was extracted with THF (40 mL). Partial removal of the solvent and keeping the flask at 4 °C afforded pale-yellow crystals of X-ray quality. Yield: 0.34 g (25%);

M.p. 218 °C (decomp).

IR (Nujol mull,  $\text{cm}^{-1}$ ):  $\tilde{\nu}$  = 1697 (w), 1624 (w), 1553 (w), 1533 (w), 1261 (w), 1172 (w), 1101 (w), 1058 (w), 1017 (w), 936 (w), 890 (w), 834 (w), 796 (w), 771 (m), 755 (w), 723 (w).

EI-MS:  $m/z$  (%) 491.25 (100) [ $M^+$ -OYb(THF)Cp<sub>2</sub>].

Elemental analysis for C<sub>43</sub>H<sub>59</sub>GeN<sub>2</sub>O<sub>2</sub>Yb (881.6): Calcd. C, 58.58; H, 6.75; N, 3.18.

Found C, 58.41; H, 6.78; N, 3.11.

#### 4.4.12 Synthesis of LGe( $\mu$ -O)Y(THF)Cp<sub>2</sub> (12)

THF (60 mL) was added to a mixture of LGeOH (0.51 g, 1.00 mmol) and Cp<sub>3</sub>Y (0.28 g, 1.00 mmol) at room temperature. The mixture was stirred overnight, and the color of the solution turned yellow from dark green. After the removal of all volatiles in vacuo, the residue was extracted with THF (40 mL). Partial removal of the solvent and keeping the flask at 4 °C afforded pale-yellow crystals of X-ray quality. Yield: 0.18 g (22%);

M.p. 210 °C (decomp).

<sup>1</sup>H NMR (200.13 MHz, C<sub>6</sub>D<sub>6</sub>):  $\delta$  1.20 (d,  $J$  = 6.8 Hz, 6 H, CH(CH<sub>3</sub>)<sub>2</sub>), 1.26 (d,  $J$  = 6.8 Hz, 6 H, CH(CH<sub>3</sub>)<sub>2</sub>), 1.47 (d,  $J$  = 6.8 Hz, 6 H, CH(CH<sub>3</sub>)<sub>2</sub>), 1.41 (b, 4H, O-(CH<sub>2</sub>CH<sub>2</sub>)<sub>2</sub>), 1.53 (s, 6 H, CMe), 1.58 (d,  $J$  = 6.8 Hz, 6 H, CH(CH<sub>3</sub>)<sub>2</sub>), 3.31 (b, 4H, O-(CH<sub>2</sub>CH<sub>2</sub>)<sub>2</sub>), 3.54 (sept,  $J$  = 6.8 Hz, 2 H, CH(CH<sub>3</sub>)<sub>2</sub>), 3.80 (sept,  $J$  = 6.8 Hz, 2 H, CH(CH<sub>3</sub>)<sub>2</sub>), 4.76 (s, 1 H,  $\gamma$ -CH), 5.90 (s, 10 H, (C<sub>5</sub>H<sub>5</sub>)<sub>2</sub>), 7.10-7.20(m, Ar).

IR (Nujol, mull, cm<sup>-1</sup>):  $\tilde{\nu}$  = 2416 (m), 1759 (w), 1624 (m), 1553 (s), 1514 (m), 1319 (s), 1260 (s), 1172 (m), 1100 (m), 1059 (m), 1012 (s), 932 (w), 888 (w), 861 (m), 838 (m), 795 (s), 772 (s), 756 (s), 724 (s), 664 (m).

EI-MS:  $m/z$  (%) 491.25 (100) [ $M^+$ -OY(THF)Cp<sub>2</sub>].

Elemental analysis for C<sub>43</sub>H<sub>59</sub>GeN<sub>2</sub>O<sub>2</sub>Y (797.5): Calcd. C, 64.76; H, 7.46; N, 3.51.

Found C, 64.53; H, 7.52; N, 3.43.

#### 4.4.13 Synthesis of [CH(C(Me)NH-2,6-*i*Pr<sub>2</sub>C<sub>6</sub>H<sub>3</sub>)<sub>2</sub>]<sup>+</sup>[(C<sub>6</sub>F<sub>5</sub>)<sub>3</sub>B( $\mu$ -OH)B(C<sub>6</sub>F<sub>5</sub>)<sub>3</sub>]<sup>-</sup> (13)

Freshly prepared  $(C_6F_5)_3B \cdot OH_2$  (0.53g, 1mmol) was added to a solution of  $LiAl$ : (0.44g, 1mmol) in toluene at  $-20\text{ }^\circ\text{C}$  with stirring. Then the mixture was warmed to room temperature. Color changed from red to colorless. The reaction was continued for 12 hours and then the reaction mixture filtered. The filtrate was concentrated. Colorless crystals suitable for X-ray structural analysis were obtained. Yield: 0.15g (21%)

M.p.216-218°C.

$^1\text{H}$  NMR (300.13 MHz,  $CDCl_3$ ):  $\delta$  12.39(s, 2H, *NH*) 7.59(s, 1H, *OH*), 7.02-7.05(br, 6H, *Ar*), 4.59(s, 1H,  $\gamma$ -*CH*), 2.52(sept,  $J=6.8$  Hz, 4H,  $CHMe_2$ ), 1.82 (m, 6H, *CMe*), 1.02 (d,  $J=6.8$ Hz, 12H,  $CHMe_2$ ), 0.85 (d,  $J=6.8$ Hz, 12H,  $CHMe_2$ ).

$^{19}\text{F}$  NMR (188.28 MHz,  $CDCl_3$ ):  $\delta$  27.18 (d,  $J=16.6$ Hz, *o-F*), 3.47 (br, *m-F*), -1.91(t,  $J=17.5$ Hz, *p-F*).

$^{11}\text{B}$  NMR (300.13MHz):  $\delta$  -3.79 (s)

IR (Nujol, mull,  $\text{cm}^{-1}$ ):  $\tilde{\nu}$  =3699(s), 3542 (s), 3390(s), 3066(s), 1647(s), 1592(s), 1542(s), 1519(s), 1343(s), 1316(s), 1277(d), 1260(s), 1179(s), 1089(s), 1025(s), 981(s), 938(s), 908(s), 886(d), 855(s), 788(d), 763(s),731(s), 695(s), 669(s), 626(s), 602(s), 576(s), 533(s), 512(s), 485(s), 452(s).

EI-MS:  $m/z$  (%) 512 (100) [ $(C_6F_5)_3B^+$ ], 403(88)[ $NaCNac^+ - Me$ ], 418(30)[ $NaCNac^+$ ].

Elemental analysis for  $C_{65}H_{44}B_2F_{30}N_2O$ (1460.63): Calcd. C, 53.45; H, 3.04; N, 1.92; Found: C, 53.33; H, 3.07; N, 2.01.

#### 4.4.14 Synthesis of $(Cp^*ZrMeOLi)_2(THF)_2$ (14)

To a solution of  $Cp^*ZrMe(OH)$  (0.79g, 2mmol) in THF (60mL) was added drop by drop  $LiN(SiMe_3)_2$  (0.33g, 2mmol) at  $-20\text{ }^\circ\text{C}$  with stirring. Then the mixture was warmed to room temperature. After 2 hours, the volatiles were evaporated in vacuum. The residue was extracted with hexane and filtered. The solution was concentrated

under vacuum and stored at -20 °C to give colorless crystals. Yield: 0.29g (31%)

M.p. 198 °C (decomp).

<sup>1</sup>H NMR (300.13 MHz, C<sub>6</sub>D<sub>6</sub>): δ -0.22 (s, 3H, ZrMe), 1.4(br, 4H, O-(CH<sub>2</sub>CH<sub>2</sub>)<sub>2</sub>), 1.8 (s, 30H, Cp<sup>\*</sup>), 3.2 (br, 4H, O-(CH<sub>2</sub>CH<sub>2</sub>)<sub>2</sub>)

IR (Nujol, mull, cm<sup>-1</sup>): ν̃ =2963 (s), 2910(s), 1487(m),1436 (m), 1370(m), 1260(m), 1095(m), 1021(m), 940(m), 863(m), 801(m)

EI-MS: *m/z* (%): 377(100) [1/2 M<sup>+</sup>-Me-Li]

Elemental analysis for C<sub>50</sub>H<sub>82</sub>Li<sub>2</sub>O<sub>4</sub>Zr<sub>2</sub> (943.51): Calcd. C, 63.65; H, 8.76; Found: C, 63.26 ; H, 8.11,.

#### 4.4.15 Synthesis of Cp<sup>\*</sup><sub>2</sub>PrN(SiMe<sub>3</sub>)<sub>2</sub> (15)

Cp<sup>\*</sup>Li (0.57g, 4mmol) was added drop by drop to a slurry of PrCl<sub>3</sub> (0.5g, 2mmol) in THF (60 mL) with stirring at 0 °C and then heated to reflux for 24 hours. The solvent was removed under vacuum, and the residue was extracted with toluene. Then the solution was filtered and cooled to 0 °C. LiN(SiMe<sub>3</sub>)<sub>2</sub> (0.33g, 2mmol) was slowly added to the solution in situ with stirring overnight. The volatiles were evaporated in vacuum. The residual was extracted with toluene. After filtration, the solution was concentrated and kept at -20 °C to result in dark crystals. Yield: 0.24g (21%).

M.p. 189 °C (decomp).

EI-MS: *m/z* (%) 136 (100) [Cp<sup>\*+</sup>], 160 (17) [(SiMe<sub>3</sub>)<sub>2</sub>N<sup>+</sup>]

Elemental analysis for C<sub>26</sub>H<sub>48</sub>NPrSi<sub>2</sub> (571.74): Calcd. C, 54.62; H, 8.46; N 2.45; Found: C, 53.47; H, 9.13; N, 2.01

#### 4.4.16 Synthesis of (9-Oxidophenalenone)<sub>3</sub>Yb (16)

To a solution of Yb[N(SiMe<sub>3</sub>)<sub>2</sub>]<sub>3</sub> (0.65g, 1mmol) in toluene (30 mL) was slowly

added 9-hydroxyphenalenone (9-opo) (0.59g, 3mmol). A yellow suspension appeared immediately. After stirring for 3 hours, the volatiles were evaporated in vacuum. The residual was washed with toluene (3×20 mL). Yield: 0.72g (95%).

M.p. 326°C (decomp.).

IR (Nujol, mull,  $\text{cm}^{-1}$ ):  $\tilde{\nu}$  = 1625 (s), 1571 (m), 1507 (m), 1420 (m), 1381 (br), 1265 (s), 1247 (m), 1185 (m), 1138 (s), 984 (s), 963 (v), 902 (br), 840 (br), 754 (w), 710 (s), 680 (m), 637 (s), 570 (m), 528 (m), 475 (m), 439 (w).

EI-MS:  $m/z$  (%) 195 (100) [9-opo<sup>+</sup>], 758 (35) [M<sup>+</sup>]

Elemental analysis for C<sub>39</sub>H<sub>21</sub>O<sub>6</sub>Yb (758.62): Calcd. C, 61.75; H, 2.79; Found: C, 61.23; H, 3.02.

#### 4.4.17 Synthesis of [(Me<sub>3</sub>Si)<sub>2</sub>NC(NCy)<sub>2</sub>]<sub>2</sub>SmBr<sub>2</sub>Li(THF)<sub>2</sub> (17)

To a solution of Li[N(SiMe<sub>3</sub>)<sub>2</sub>] (0.86 g, 97%, 5 mmol) in THF (60 mL) was slowly added CyN=C=NCy (1.03 g, 5 mmol) at 20 °C, and after 45 min of stirring SmBr<sub>3</sub> (0.98g, 2 mmol) was added. The reaction mixture was stirred overnight to obtain a clear solution, and then the solvent was evaporated in vacuo. The remaining solid was extracted with toluene (50 mL). After filtration, the solution was concentrated under vacuum and stored at room temperature for 2 days to give large yellow crystals. Yield: 2.46g (82%)

M.p. 256 °C (decomp.).

IR (Nujol, mull,  $\text{cm}^{-1}$ ):  $\tilde{\nu}$  =1635 (m), 1370 (m), 1294 (m), 1251 (s), 1210 (m), 1103 (m), 1050 (s), 950 (s), 920 (s), 870 (m), 831(s).

EI-MS:  $m/z$  (%) 160 (8) [(SiMe<sub>3</sub>)<sub>2</sub>N<sup>+</sup>].

Elemental analysis for C<sub>46</sub>H<sub>9</sub>Br<sub>2</sub>LiN<sub>6</sub>O<sub>2</sub>Si<sub>4</sub>Sm (1194.74): Calcd. C, 46.24; H, 8.10; N, 7.03; Found: C, 46.07; H, 8.12; N, 6.89.

**4.4.18 Synthesis of  $[(\text{Me}_3\text{Si})_2\text{NC}(\text{NCy})_2]_2\text{Sm}(\text{THF})(\mu\text{-O})\text{MeAl}$  (18)**

To a solution of  $[(\text{Me}_3\text{Si})_2\text{NC}(\text{NCy})_2]_2\text{SmBr}_2\text{Li}(\text{THF})_2$  (0.6g, 0.5mmol) in toluene (60 mL) was slowly added  $\text{LiCH}_2\text{SiMe}_3$  (0.5 mL, 1.0 M in hexane) with stirring at  $-20^\circ\text{C}$ . Then the solution was slowly warmed to  $0^\circ\text{C}$  within 45 minutes. After that, the solution was transferred to a solution of  $\text{LiAlMe}(\text{OH})$  (0.48g, 1 mmol) in toluene (10 mL) through a filter. Then the mixture was stirred over night at room temperature. The solvent was then evaporated in vacuo. The remaining solid was extracted with toluene (50 mL). After filtration, the solution was concentrated under vacuum and stored at  $-30^\circ\text{C}$ . Tiny needles were obtained after several days. Yield: 0.13g (18%)

M.p.  $247^\circ\text{C}$  (decomp).

IR (Nujol, mull,  $\text{cm}^{-1}$ ):  $\tilde{\nu} = 1635$  (m), 1595 (w), 1560 (w), 1521 (m), 1370 (m), 1295 (m), 1263 (m), 1201 (m), 1117 (m), 1044 (m), 950 (m), 928 (m), 875 (m), 831(w), 783(m)

EI-MS:  $m/z$  (%) 418(70)  $[\text{NacNac}^+]$ , 160 (18)  $[(\text{SiMe}_3)_2\text{N}^+]$ .

Elemental analysis for  $\text{C}_{72}\text{H}_{132}\text{AlN}_8\text{O}_2\text{Si}_4\text{Sm}$  (1431.55): Calcd. C, 60.45; H, 9.23; N, 7.83; Found: C, 61.12; H, 9.31; N, 7.46.

**4.4.19 Synthesis of  $[(\text{Me}_3\text{Si})_2\text{NC}(\text{NCy})_2\text{SmCl}_2]_5(\text{THF})_2$  (19)**

To a solution of  $\text{Li}[\text{N}(\text{SiMe}_3)_2]$  (0.86 g, 97%, 5 mmol) in THF (60 mL) was slowly added  $\text{CyN}=\text{C}=\text{NCy}$  (1.03 g, 5 mmol) at  $20^\circ\text{C}$ , and after 45 min of stirring  $\text{SmCl}_3$  (1.28 g, 5 mmol) was added. The reaction mixture was stirred overnight to obtain a clear solution, and the solvent was then evaporated in vacuo. The remaining solid was extracted with toluene (50 mL). After filtration, the solution was concentrated under vacuum and stored at  $0^\circ\text{C}$  in a freezer to give yellow crystals. Yield 1.33 g (43 %).

M.p.  $184^\circ\text{C}$  (decomp.).

IR (Nujol, mull,  $\text{cm}^{-1}$ ):  $\tilde{\nu} = 1633$  (m), 1377 (s), 1305 (m), 1261 (m), 1154 (m), 1093

(m), 1021 (m), 958 (m), 891 (m), 843 (m), 802 (m), 722 (m)  $\text{cm}^{-1}$ .

Elemental analysis for  $\text{C}_{103}\text{H}_{216}\text{Cl}_{10}\text{N}_{15}\text{O}_2\text{Si}_{10}\text{Sm}_5$  (3084.1): Calcd. C 40.11, H 7.06, N 6.81; found C 39.29, H 7.18, N 6.50.

#### 4.4.20 Synthesis of $[(\text{Me}_3\text{Si})_2\text{NC}(\text{NCy})_2\text{YbCl}_2]_2(\text{LiCl})_2(\text{THF})_4$ (**20**)

To a solution of  $\text{Li}[\text{N}(\text{SiMe}_3)_2]$  (0.86 g, 97%, 5 mmol) in THF (60 mL) was slowly added  $\text{CyN}=\text{C}=\text{NCy}$  (1.03 g, 5 mmol) at 20 °C, and after 45 min of stirring  $\text{YbCl}_3$  (1.4 g, 5 mmol) was added. The reaction mixture was stirred overnight to obtain a clear solution, and the solvent was evaporated in vacuo. The remaining solid was extracted with toluene (50 mL). After filtration, the solution was concentrated under vacuum and complex **20** was isolated as purple solid. Yield 1.97 g (50 %). Crystals suitable for X-ray structural analysis were obtained after storing the solution at 0 °C in a freezer.

M.p. 147 °C (decomp.).

IR (Nujol, mull,  $\text{cm}^{-1}$ ):  $\tilde{\nu} = 1629$  (m), 1402 (s), 1385 (s), 1261 (s), 1095 (s), 1025 (s), 801 (s), 722 (m)  $\text{cm}^{-1}$ .

Elemental analysis for  $\text{C}_{54}\text{H}_{112}\text{Cl}_6\text{Li}_2\text{N}_6\text{O}_4\text{Si}_4\text{Yb}_2$  (1594.53): Calcd. C 40.68, H 7.08, N 5.27; found C 39.99, H 7.04, N 5.35.

#### 4.5. Polymerization of Ethylene

On a vacuum line ( $10^{-5}$  Torr), polymerizations were carried out in a 200 mL autoclave (Büchi). In a typical experiment, 100 mL of dry toluene (from Na/K) were vacuum transferred into the polymerization flask, pre-saturated with 1.0 atm of rigorously purified ethylene. The catalyst (0.009 g in toluene; 10 mL, 12.4  $\mu\text{mol}$ ) was placed in a Schlenk flask and appropriate MAO (1.6 M in toluene) was added. The mixture was stirred for 20 min to activate the catalyst. The catalyst solution was then quickly injected into the rapidly stirred flask using a gas-tight syringe. After a

measured time interval, the polymerization was quenched by the addition of methanol (5 mL) and then the reaction mixture was poured into methanol (800 mL). The polymer was allowed to fully precipitate overnight and then collected by filtration, washed with fresh methanol, and dried.

#### **4.6. Polymer Characterization**

$^{13}\text{C}$  NMR assay of polymer microstructure was conducted in 1,1,2,2-tetrachloroethane- $\text{d}_2$  at 120 °C. Resonances were assigned according to the literature for polyethylene. Differential Scanning Calorimetric measurements of the polymer melting curves were performed on a TA instrument 2920 (Modulated Differential Scanning Calorimeter), which was calibrated against indium metal. Typically ca. 4 mg samples were used (10 °C /min).



## 5. Handling and Disposal of Solvents and Residual Waste

1 The recovered solvents were distilled or condensed into cold-traps under vacuum, collected in halogen-free or halogen-containing solvent containers, and stored for disposal.

2 Used NMR solvents were classified into halogen-free or halogen-containing solvents and were disposed as heavy metal-containing wastes and halogen-containing wastes, respectively.

3 The heavy metal residues were dissolved in nitric acid and after neutralization stored in the container for heavy metal wastes.

4 Drying agents such as KOH, CaCl<sub>2</sub>, MgCl<sub>2</sub>, MgSO<sub>4</sub>, and P<sub>4</sub>O<sub>10</sub> were hydrolyzed and disposed as acid or base wastes.

5 Wherever possible, sodium metal used for drying solvents was collected for recycling. The non-reusable sodium metal was carefully treated with cold ethanol and potassium in cold isopropanol and collected into the base-bath cleaning glassware.

6 Ethanol and acetone used for cooling baths were subsequently used for cleaning glassware.

7 The acid bath for cleaning glassware was neutralized with Na<sub>2</sub>CO<sub>3</sub> and the resulting NaCl solution was washed off in the water drainage system.

8 The residual of the base both for cleaning glassware was poured into the container for base wastes.

9 Amount of various types of disposable wastes generated during the work:

Metal containing wastes 10 L

Halogen-containing wastes 7 L

Halogen-free solvent wastes 50 L

Acid wastes 20 L

Base wastes 18 L

## 6. Crystal Data and Refinement Details

**Table CD1. Crystal data and structure refinement for 2**

Formula	$C_{39}H_{63}AlN_2O_3$
fw	634.89
$T$ (K)	133(2)
Crystal system	Orthorhombic
Space group	$P2_12_12_1$
$\lambda$ (Å)	0.71073
Unit cell dimensions	$a = 9.4622(9)$ Å $b = 15.1590(15)$ Å $c = 26.479(3)$ Å
$V$ (Å <sup>3</sup> )	3798.0(6)
$Z$	4
$\rho_{\text{calc}}$ (g/cm <sup>3</sup> )	1.110
$\mu$ (mm <sup>-1</sup> )	0.090
Crystal size (mm)	0.40 × 0.30 × 0.25
$\theta$ Range for data collection (°)	1.54 to 28.70
Index ranges	$-12 \leq h \leq 12$ , $-20 \leq k \leq 20$ , $-35 \leq l \leq 35$
Reflections collected	44236
Independent reflections [ $R_{\text{int}}$ ]	9787 [0.0414]
Data/restr./param.	9787/137/421
Goodness-of-fit on $F^2$	1.059
$R_1, wR_2$ ( $I > 2\sigma(I)$ )	0.0561, 0.1462
$R_1, wR_2$ (all data)	0.0817, 0.1656
Largest differences in peak/hole (e Å <sup>-3</sup> )	0.569/_ 0.450

**Table CD2. Crystal data and structure refinement for 3**

Formula	$C_{42}H_{59}AlN_2OZr$
fw	726.11
$T$ (K)	100(2)
Crystal system	Orthorhombic
Space group	$Pnma$
$\lambda$ (Å)	0.71073
Unit cell dimensions	$a = 18.8469(17)$ Å $b = 19.6279(17)$ Å $c = 10.2628(9)$ Å
$V$ (Å <sup>3</sup> )	3796.5(6)
$Z$	4
$\rho_{\text{calc}}$ (g/cm <sup>3</sup> )	1.270
$\mu$ (mm <sup>-1</sup> )	0.347
Crystal size (mm)	$0.27 \times 0.27 \times 0.12$
$\theta$ Range for data collection (°)	2.08 to 33.73
Index ranges	$-29 \leq h \leq 29$ $-30 \leq k \leq 30$ , $-15 \leq i \leq 16$
Reflections collected	128071
Independent reflections [ $R_{\text{int}}$ ]	7767 [0.0398]
Data/restr./param.	7767/4/240
Goodness-of-fit on $F^2$	1.040
$R_1, wR_2$ ( $I > 2\sigma(I)$ )	0.0286, 0.0734
$R_1, wR_2$ (all data)	0.0358, 0.0781
Largest differences in peak/hole (e Å <sup>-3</sup> )	0.772/_0.461

**Table CD3. Crystal data and structure refinement for LGe( $\mu$ -O)Yb(THF)Cp<sub>2</sub>(11)**

Formula	C <sub>43</sub> H <sub>59</sub> GeN <sub>2</sub> O <sub>2</sub> Yb
fw	881.55
<i>T</i> (K)	133(2)
Crystal system	triclinic
Space group	<i>P</i> -1
$\lambda$ (Å)	0.71073
Unit cell dimensions	<i>a</i> = 8.8701(6) Å, $\alpha$ = 90.055(3) ° <i>b</i> = 37.489(3) Å, $\beta$ = 98.337(3) ° <i>c</i> = 11.9890(8) Å, $\gamma$ = 89.994(3) °
<i>V</i> (Å <sup>3</sup> )	3944.5(5)
<i>Z</i>	4
$\rho_{\text{calc}}$ (g/cm <sup>3</sup> )	1.484
$\mu$ (mm <sup>-1</sup> )	3.155
<i>F</i> (000)	1796
Crystal size (mm)	0.35 × 0.35 × 0.20
$\theta$ Range for data collection (°)	0.54 to 28.70
Index ranges	-11 ≤ <i>h</i> ≤ 11 -50 ≤ <i>k</i> ≤ 50 -16 ≤ <i>l</i> ≤ 16
Reflections collected	69676
Independent reflections [ <i>R</i> <sub>int</sub> ]	19957 [0.0319]
data/restraints./params	19957/1429/904
Goodness-of-fit on <i>F</i> <sup>2</sup>	1.096
<i>R</i> <sub>1</sub> , <i>wR</i> <sub>2</sub> ( <i>I</i> > 2 $\sigma$ ( <i>I</i> ))	0.0385, 0.0682
<i>R</i> <sub>1</sub> , <i>wR</i> <sub>2</sub> (all data)	0.0497, 0.0709

**Table CD4. Crystal data and structure refinement for LGe( $\mu$ -O)Y(THF)Cp<sub>2</sub>(12)**

Formula	C <sub>43</sub> H <sub>59</sub> GeN <sub>2</sub> O <sub>2</sub> Y
fw	797.42
<i>T</i> (K)	100(2)
Crystal system	triclinic
Space group	<i>P</i> -1
$\lambda$ (Å)	0.71073
Unit cell dimensions	<i>a</i> = 8.8517(4) Å, $\alpha$ = 90.190(3) ° <i>b</i> = 37.4086(16) Å, $\beta$ = 98.071(3) ° <i>c</i> = 12.0005(5) Å, $\gamma$ = 90.000(3) °
<i>V</i> (Å <sup>3</sup> )	3934.3(3)
<i>Z</i>	4
$\rho_{\text{calc}}$ (g/cm <sup>3</sup> )	1.346
$\mu$ (mm <sup>-1</sup> )	2.269
<i>F</i> (000)	1672
Crystal size (mm)	0.23 × 0.10 × 0.10
$\theta$ Range for data collection (°)	1.63 to 26.37
Index ranges	-11 ≤ <i>h</i> ≤ 11 -46 ≤ <i>k</i> ≤ 46 -14 ≤ <i>l</i> ≤ 14
Reflections collected	84265
Independent reflections [ <i>R</i> <sub>int</sub> ]	16033 [0.0543]
data/restraints./params	16033/1429/904
Goodness-of-fit on <i>F</i> <sup>2</sup>	1.198
<i>R</i> <sub>1</sub> , <i>wR</i> <sub>2</sub> ( <i>I</i> > 2σ( <i>I</i> ))	0.0556, 0.1048
<i>R</i> <sub>1</sub> , <i>wR</i> <sub>2</sub> (all data)	0.0716, 0.1095

**Table CD5. Crystal data and structure refinement for [CH(C(Me)NH-2,6-*i*Pr<sub>2</sub>C<sub>6</sub>H<sub>3</sub>)<sub>2</sub>]<sup>+</sup>[(C<sub>6</sub>F<sub>5</sub>)<sub>3</sub>B( $\mu$ -OH)B(C<sub>6</sub>F<sub>5</sub>)<sub>3</sub>]<sup>-</sup> (13)**

Formula	C <sub>65</sub> H <sub>44</sub> B <sub>2</sub> F <sub>30</sub> N <sub>2</sub> O
fw	1460.64
<i>T</i> (K)	133(2)
Crystal system	Monoclinic
Space group	<i>P</i> 21/ <i>c</i>
$\lambda$ (Å)	0.71073
Unit cell dimensions	<i>a</i> = 11.9938(2) Å, $\alpha$ = 90° <i>b</i> = 17.0748(4) Å, $\beta$ = 90.165(2) ° <i>c</i> = 29.9829(6) Å, $\gamma$ = 90°
<i>V</i> (Å <sup>3</sup> )	6140.2(2)
<i>Z</i>	4
$\rho_{\text{calc}}$ (g/cm <sup>3</sup> )	1.580
$\mu$ (mm <sup>-1</sup> )	0.157
<i>F</i> (000)	2944
Crystal size (mm)	0.27 × 0.19 × 0.17
$\theta$ Range for data collection (°)	1.36 to 25.88
Index ranges	-14 ≤ <i>h</i> ≤ 14, -20 ≤ <i>k</i> ≤ 20, -36 ≤ <i>l</i> ≤ 36
Reflections collected	36068
Independent reflections [ <i>R</i> <sub>int</sub> ]	11821 [0.0411]
data/restraints./params	11821 / 0 / 1030
Goodness-of-fit on <i>F</i> <sup>2</sup>	1.009
<i>R</i> <sub>1</sub> , <i>wR</i> <sub>2</sub> ( <i>I</i> > 2 $\sigma$ ( <i>I</i> ))	0.0421, 0.0860
<i>R</i> <sub>1</sub> , <i>wR</i> <sub>2</sub> (all data)	0.0688, 0.0941
Largest differences in peak/hole (e Å <sup>-3</sup> )	0.648/-0.356

**Table CD6. Crystal data and structure refinement for [(Me<sub>3</sub>Si)<sub>2</sub>NC(NCy)<sub>2</sub>SmCl<sub>2</sub>]<sub>5</sub>(THF)<sub>2</sub> (19)**

Formula	C <sub>103</sub> H <sub>216</sub> Cl <sub>10</sub> N <sub>15</sub> O <sub>2</sub> Si <sub>10</sub> Sm <sub>5</sub>
fw	3084.06
<i>T</i> (K)	100(2)
Crystal system	Triclinic
Space group	<i>P</i> -1
$\lambda$ (Å)	0.71073
Unit cell dimensions	$a = 17.5764(19)$ Å, $\alpha = 74.5700(10)$ ° $b = 19.361(2)$ Å, $\beta = 70.6270(10)$ ° $c = 24.774(3)$ Å, $\gamma = 66.9270(10)$ °
$V$ (Å <sup>3</sup> )	7226.3(13)
<i>Z</i>	2
$\rho_{\text{calc}}$ (g/cm <sup>3</sup> )	1.417
$\mu$ (mm <sup>-1</sup> )	2.313
<i>F</i> (000)	3150
Crystal size (mm)	0.2 × 0.1 × 0.1
$\theta$ Range for data collection (°)	2.01 to 25.74
Index ranges	-19 ≤ <i>h</i> ≤ 21 -22 ≤ <i>k</i> ≤ 23 0 ≤ <i>l</i> ≤ 30
Reflections collected	144891
Independent reflections [ <i>R</i> <sub>int</sub> ]	27482 [0.0948]
data/restraints./params	27482/76/1441
Goodness-of-fit on <i>F</i> <sup>2</sup>	0.925
<i>R</i> <sub>1</sub> , <i>wR</i> <sub>2</sub> ( <i>I</i> > 2σ( <i>I</i> ))	0.0328, 0.0728
<i>R</i> <sub>1</sub> , <i>wR</i> <sub>2</sub> (all data)	0.0463, 0.0765
Largest differences in peak/hole (e Å <sup>-3</sup> )	0.937/-1.034

**Table CD7. Crystal data and structure refinement for [(Me<sub>3</sub>Si)<sub>2</sub>NC(NCy)<sub>2</sub>YbCl<sub>2</sub>]<sub>2</sub>(LiCl)<sub>2</sub>(THF)<sub>4</sub> (20)**

Formula	C <sub>54</sub> H <sub>112</sub> Cl <sub>6</sub> Li <sub>2</sub> N <sub>6</sub> O <sub>4</sub> Si <sub>4</sub> Yb <sub>2</sub>
fw	1594.52
<i>T</i> (K)	100(2)
Crystal system	Triclinic
Space group	<i>P</i> -1
$\lambda$ (Å)	0.71073
Unit cell dimensions	$a = 10.759(3)$ Å, $\alpha = 77.330(3)^\circ$ $b = 12.652(4)$ Å, $\beta = 71.772(3)^\circ$ $c = 14.657(4)$ Å, $\gamma = 78.326(3)^\circ$
$V$ (Å <sup>3</sup> )	1829.5(9)
<i>Z</i>	1
$\rho_{\text{calc}}$ (g/cm <sup>3</sup> )	1.447
$\mu$ (mm <sup>-1</sup> )	2.867
<i>F</i> (000)	814
Crystal size (mm)	0.2 × 0.2 × 0.1
$\theta$ Range for data collection (°)	1.67 to 27.10
Index ranges	-12 ≤ <i>h</i> ≤ 13 -15 ≤ <i>k</i> ≤ 16 0 ≤ <i>l</i> ≤ 18
Reflections collected	43553
Independent reflections [ <i>R</i> <sub>int</sub> ]	8057 [0.0251]
data/restraints./params	8057/0/377
Goodness-of-fit on <i>F</i> <sup>2</sup>	1.054
<i>R</i> <sub>1</sub> , <i>wR</i> <sub>2</sub> ( <i>I</i> > 2σ( <i>I</i> ))	0.0161, 0.0415
<i>R</i> <sub>1</sub> , <i>wR</i> <sub>2</sub> (all data)	0.0168, 0.0419
Largest differences in peak/hole (e Å <sup>-3</sup> )	1.368/-0.658



## 7. References

- [1] Copéret, C.; Chabanas, M.; Saint-Arroman, R. P.; Basset, J. -M. *Angew. Chem.* **2003**, *115*, 164-191; *Angew. Chem. Int. Ed.* **2003**, *42*, 156-181.
- [2] Cornils, B.; Herrmann, W. A. *Applied Homogeneous Catalysis with Organometallic Compounds*; Wiley-VCH, Weinheim, Germany, **1996**.
- [3] Basset, J.-M.; Gates, B. C.; Candy, J. P.; Choplin, A.; Leconte, M.; Quignard, F.; Santini, C. *Surface Organometallic Chemistry: Molecular Approaches to Surface Catalysis*; Kluwer, Dordrecht, The Netherlands, **1988**, and references therein.
- [4] Basset, J.-M.; Candy, J. P.; Choplin, A.; Didillon, B.; Quignard, F.; Théolier, A. In *Perspectives in Catalysis*; Thomas, J. P.; Zamaraev, K. (Eds) Blackwell, Oxford, **1991**, pp 125.
- [5] Roesky, H. W.; Haiduc, I.; Hosmane, N. S. *Chem. Rev.* **2003**, *103*, 2579-2595.
- [6] Kaminsky, W. *Catalysis Today* **1994**, *20*, 257-271.
- [7] Sinn, H.; Kaminski, W. *Adv. Organomet. Chem.* **1980**, *18*, 99-149.
- [8] Brintzinger, H. H.; Fischer, D.; Mülhaupt, R.; Rieger, B.; Waymouth, R. M. *Angew. Chem.* **1995**, *107*, 1255-1283; *Angew. Chem. Int. Ed. Engl.* **1995**, *34*, 1143-1170.
- [9] Andresen, A.; Cordes, H. -G.; Herwig, J.; Kaminsky, W.; Merck, A.; Mottweiler, R.; Pein, J.; Sinn, H.; Vollmer, H. -J. *Angew. Chem.* **1976**, *88*, 689-690; *Angew. Chem. Int. Ed. Engl.* **1976**, *15*, 630-632.
- [10] Gibson, V. C.; Spitzmesser, S. K. *Chem. Rev.* **2003**, *103*, 283-315.
- [11] Makio, H.; Kashiwa, N.; Fujita, T. *Adv. Synth. Catal.* **2002**, *344*, 477-493.
- [12] Janiak, C. *Metallocenes*; Togni, A.; Haltermann, R. L. (Eds.) Wiley-VCH, Weinheim, Germany, **1998**, Vols. 1 and 2.
- [13] Ittel, S. D.; Johnson, L. K.; Brookhart, M. *Chem. Rev.* **2000**, *100*, 1169-1203.
- [14] Bollmann, A.; Blann, K.; Dixon, J. T.; Hess, F. M.; Killian, E.; Maumela, H.; McGuinness, D. S.; Morgan, D. H.; Neveling, A.; Otto, S.; Overett, M.; Slawin, A. M. Z.; Wasserscheid, P.; Kuhlmann, S. *J. Am. Chem. Soc.* **2004**, *126*, 14712-14713.

- [15] Tian, J.; Hustad, P. D.; Coates, G. W. *J. Am. Chem. Soc.* **2001**, *123*, 5134-5135.
- [16] Arriola, D. J.; Carnahan, E. M.; Hustad, P. D.; Kuhlman, R. L.; Wenzel, T. T. *Science* **2006**, *312*, 714-719.
- [17] Vogt, D. *Applied Homogeneous Catalysis with Organometallic Compounds*; Cornils, B.; Herrmann, W. A. (Eds.) Wiley-VCH, Weinheim, Germany, **2002**, Vol. 1, pp 245-258.
- [18] Parshall, G. W.; Ittel, S. D. *Homogeneous Catalysis: The Applications and Chemistry of Catalysis by Soluble Transition Metal Complexes*; Wiley, New York, **1992**, pp 68-72.
- [19] Skupinska, J. *Chem. Rev.* **1991**, *91*, 613-648.
- [20] Rieger, B.; Baugh, L. S.; Kacker, S.; Striegler, S. *Late Transition Metal Polymerization Catalysis*; John Wiley & Sons: New York, **2003**, and references therein.
- [21] Blom, R.; Follestad, A.; Rytter, E.; Tilset, M.; Ystenes, M. *Organometallic Catalysts and Olefin Polymerization: Catalysts for a New Millennium*; Springer-Verlag, Berlin, Germany, **2001**, and references therein.
- [22] Galli, P.; Vecellio, G. *J. Polym. Sci. Part A: Polym. Chem.* **2004**, *42*, 396-415.
- [23] Bonnet, M. C.; Dahan, F.; Ecke, A.; Keim, W.; Schulz, R. P.; Tkatchenko, I. *J. Chem. Soc., Chem Commun.*, **1994**, 615-616.
- [24] Yanjarappa, M. J.; Sivaram, S. *Prog. Polym. Sci.* **2002**, *27*, 1347-1398.
- [25] Mecking, S.; Held, A.; Bauers, F. M. *Angew. Chem.* **2002**, *114*, 564-582; *Angew. Chem. Int. Ed.* **2002**, *41*, 544-561.
- [26] Abramo, G. P.; Li, L.; Marks, T. J. *J. Am. Chem. Soc.* **2002**, *124*, 13966-13967.
- [27] Bazan, G. C.; Rodriguez, G.; Ashe, A. J., III; Al-Ahmad, S.; Müller, C. *J. Am. Chem. Soc.* **1996**, *118*, 2291-2292.
- [28] Barnhart, R. W.; Bazan, G. C.; Mourey, T. *J. Am. Chem. Soc.* **1998**, *120*, 1082-1083.
- [29] Komon, Z. J. A.; Bazan, G. C. *Macromol. Rapid Commun.* **2001**, *22*, 467-478.
- [30] Drouin, S. D.; Zamanian, F.; Fogg, D. E. *Organometallics* **2001**, *20*, 5495-5497.
- [31] Quijada, R.; Rojas, R.; Bazan, G. C.; Komon, Z. J. A.; Mauler, R. S.; Galland, G.

- B. Macromolecules* **2001**, *34*, 2411-2417.
- [32] Denger, C.; Haase, U.; Fink, G. *Makromol. Chem., Rapid Commun.* **1991**, *12*, 697-701.
- [33] Beach, D. L.; Kissin, Y. V. *J. Polym. Sci., Polym. Chem. Ed.* **1984**, *22*, 3027-3042.
- [34] Kunrath, F. A.; de Souza, R. F.; Casagrande, O. L., Jr. *Macromol Rapid Commun.* **2000**, *21*, 277-280.
- [35] Frediani, M.; Bianchini, C.; Kaminsky, W. *Kinetics and catalysis*, **2006**, *47*, 207-212.
- [36] Wang, W-J.; Kolodka, E.; Zhu, S.; Hamielec, A. E. *J. Polym. Sci., Part A: Polym. Chem.* **1999**, *37*, 2949-2957.
- [37] Rogers, J. S.; Bazan, G. C.; Sperry, C. K. *J. Am. Chem. Soc.* **1997**, *119*, 9305-9306.
- [38] Wasilke, J.-C.; Obrey, S. J.; Baker, R. T.; Bazan, G. C. *Chem. Rev.* **2005**, *105*, 1001-1020.
- [39] McKnight, A. L.; Waymouth, R. M. *Chem. Rev.* **1998**, *98*, 2587-2598.
- [40] Komon, Z. J. A.; Diamond, G. M.; Leclerc, M. K.; Murphy, V.; Okazaki, M.; Bazan, G. C. *J. Am. Chem. Soc.* **2002**, *124*, 15280-15285.
- [41] (a) Green, M. L. H.; Popham, N. H. *J. Chem. Soc., Dalton Trans.* **1999**, 1049-1059. (b) Lindenberg, F.; Shribman, T.; Sieler, J.; Hey-Hawkins, E.; Eisen, M. S. *J. Organomet. Chem.* **1996**, *515*, 19-25. (c) Ishino, H.; Takemoto, S.; Hirata, K.; Kanaizuka, Y.; Hidai, M.; Nabika, M.; Seki, Y.; Miyatake, T.; Suzuki, N. *Organometallics* **2004**, *23*, 4544-4546. (d) Britovsek, G. J. P.; Gibson, V. C.; Wass, D. F. *Angew. Chem., Int. Ed.* **1999**, *38*, 428-447.
- [42] (a) Carofiglio, T.; Floriani, C.; Rosi, M.; Chiesi-Villa, A.; Rizzoli, C. *Inorg. Chem.* **1991**, *30*, 3245-3246. (b) Rau, M. S.; Kretz, C. M.; Geoffroy, G. L.; Rheingold, A. L.; Haggerty, B. S. *Organometallics* **1994**, *13*, 1624-1634. (c) Erker, G.; Albrecht, M.; Werner, S.; Krüger, C.; *Z. Naturforsch.* **1990**, *45b*, 1205-1209.
- [43] (a) Bai, G.; Singh, S.; Roesky, H. W.; Noltemeyer, M.; Schmidt, H.-G. *J. Am.*

- Chem. Soc.* **2005**, *127*, 3449-3455. (b) Bai, G.; Peng, Y.; Roesky, H. W.; Li, J.; Schmidt, H.-G.; Noltemeyer, M. *Angew. Chem.* **2003**, *115*, 1164-1167; *Angew. Chem. Int. Ed.* **2003**, *42*, 1132-1135. (c) Bai, G.; Roesky, H. W.; Li, J.; Noltemeyer, M.; Schmidt, H.-G. *Angew. Chem.* **2003**, *115*, 5660-5664; *Angew. Chem. Int. Ed.* **2003**, *42*, 5502-5506.
- [44] (a) Singh, S.; Jancik, V.; Roesky, H. W.; Herbst-Irmer, R. *Inorg. Chem.* **2006**, *45*, 949-951. (b) Jancik, V.; Pineda, L. W.; Stückl, A. C.; Roesky, H. W.; Herbst-Irmer, R. *Organometallics*, **2005**, *24*, 1511-1515.
- [45] Pineda, L. W.; Jancik, V.; Roesky, H. W.; Neculai, D.; Neculai, A. M. *Angew. Chem.* **2004**, *116*, 1443-1445; *Angew. Chem. Int. Ed.* **2004**, *43*, 1419-1421.
- [46] Ruspic, C.; Nembenna, S.; Hofmeister, A.; Magull, J.; Harder, S.; Roesky, H. W. *J. Am. Chem. Soc.* **2006**, *128*, 15000-15004.
- [47] Sarish, S.; Nembenna, S.; Nagendran, S.; Roesky, H. W.; Pal, A.; Herbst-Irmer, R.; Ringe, A.; Magull, J. *Inorg. Chem.* **2008**, *47*, 5971-5977.
- [48] Gurubasavaraj, P. M.; Roesky, H. W.; Sharma, P. M. Veerasha; Oswald, R. B.; Dolle, V.; Herbst-Irmer, R.; Pal, A. *Organometallics*, **2007**, *26*, 3346-3351.
- [49] Pineda, L. W.; Jancik, V.; Roesky, H. W.; Herbst-Irmer, R. *Inorg. Chem.* **2005**, *44*, 3537-3540.
- [50] Singh, S.; Roesky, H. W. *Dalton Trans.* **2007**, 1360-1370.
- [51] Bansal, S.; Singh, Y.; Singh, A. *Heteroatom Chem.* **2004**, *15*, 21-25.
- [52] Mandal, S. K.; Gurubasavaraj, P. M.; Roesky, H. W.; Oswald, R. B.; Magull, J.; Ringe, A. *Inorg. Chem.* **2007**, *46*, 7594-7600.
- [53] Nembenna, S.; Singh, S.; Jana, A.; Roesky, H. W.; Yang, Y.; Ye, H.; Ott, H.; Stalke, D. *Inorg. Chem.* **2009**, *48*, 2273-2276.
- [54] Gurubasavaraj, P. M.; Roesky, H. W.; Nekoueishahraki, B.; Pal, A.; Herbst-Irmer, R. *Inorg. Chem.* **2008**, *47*, 5324-5331.
- [55] Gurubasavaraj, P. M.; Mandal, S. K.; Roesky, H. W.; Oswald, R. B.; Pal, A.; Noltemeyer, M. *Inorg. Chem.* **2007**, *46*, 1056-1061.
- [56] Jancik, V.; Roesky, H. W. *Angew. Chem. Int. Ed.* **2005**, *44*, 6016-6018.
- [57] Nikiforov, G. B.; Roesky, H. W.; Schulz, T.; Stalke, D.; Witt, M. *Inorg. Chem.*

- 2008**, *47*, 6435-6443.
- [58] Mandal, S. K.; Gurubasavaraj, P. M.; Roesky, H. W.; Schwab, G.; Stalke, D.; Oswald, R. B.; Dolle, V. *Inorg. Chem.* **2007**, *46*, 10158-10167.
- [59] Nembenna, S; Roesky, H. W.; Mandal, S. K.; Oswald, R. B.; Pal, A.; Herbst-Irmer, R.; Noltemeyer, M.; Schmidt, H. G. *J. Am. Chem. Soc.* **2006**, *128*, 13056-13057.
- [60] (a) Fischbach, A.; Herdtweck, E.; Anwander, R.; Eickerling, G.; Scherer, W. *Organometallics* **2003**, *22*, 499-509 and references therein. (b) Giesbrecht, G. R.; Gordon, J. C.; Brady, J. T.; Clark, D. L.; Keogh, D. W.; Michalczyk, R.; Scott, B. L.; Watkin, J. G. *Eur. J. Inorg. Chem.* **2002**, 723-731.
- [61] (a) Bradley, D. C. *Chem. ReV.* **1989**, *89*, 1317-1322. (b) Bradley, D. C. *Polyhedron* **1994**, *13*, 1111-1121. (c) Mehrotra, R. C.; Singh, A. *Chem. Soc. ReV.* **1996**, 1-14.
- [62] (a) Bambirra, S.; Bouwkamp, M. W.; Meetsma, A.; Hessen, B. *J. Am. Chem. Soc.* **2004**, *126*, 9182-9183. (b) Yasuda, H.; Ihara, E. *Bull. Chem. Soc. Jpn.* **1997**, *70*, 1745-1767. (c) Yasuda, H. *J. Polym. Sci., Part A: Polym. Chem.* **2001**, *39*, 1955-1959.
- [63] (a) *Comprehensive Organometallic Chemistry*; Wilkinson, G., Stone, F. G. A., Abel, E. W., Eds.; Pergamon Press: Oxford, U.K., 1982. (b) Sinn, H.; Kaminsky, W. *Adv. Organomet. Chem.* **1980**, *18*, 99-149.
- [64] (a) Evans, W. J.; Boyle, T. J.; Ziller, J. W. *J. Am. Chem. Soc.* **1993**, *115*, 5084-5092. (b) Evans, W. J.; Ansari, M. A.; Ziller, J. W. *Inorg. Chem.* **1995**, *34*, 3079-3082. (c) Evans, W. J.; Anwander, R.; Ziller, J. W. *Organometallics* **1995**, *14*, 1107-1109. (d) Evans, W. J.; Boyle, T. J.; Ziller, J. W. *J. Organomet. Chem.* **1993**, *462*, 141-148.
- [65] Yamamoto, H.; Yasuda, H.; Yokota, K.; Nakamura, A. *Chem. Lett.* **1988**, 1963-1966.
- [66] Chai, J.; Jancik, V.; Singh, S.; Zhu, H.; He, C.; Roesky, H. W.; Schmidt, H. G.; Noltemeyer, M.; Hosmane, N. S. *J. Am. Chem. Soc.* **2005**, *127*, 7521-7528.
- [67] (a) Evans, W. J.; Gummersheimer, T. S.; Ziller, J. W. *App. OM. Chem.* **1995**,

- 437-447. (b) Evans, W. J.; Grate, J. W.; Bloom, I.; Hunter, W. E.; Atwood, J. L. *J. Am. Chem. Soc.* **1985** *107*, 405-409. (c) Schumann, H.; Palamidis E.; Loebel, J. *J. Organomet. Chem.* **1990**, *384*, C49-C52 (d) Adam, M.; Massarweh, G.; Fischer, R. D. *J. Organomet. Chem.* **1991**, *405*, C33-C37 (e) Evans, W. J.; Gonzales, S. L. *J. Organomet. Chem.* **1994**, *80*, 41-44. (f) Hao, J.; Song, H.; Cui, C. *Organometallics*, **2009**, *28*, 3100–3104 (g) Ringelberg, S. N.; Meetsma, A.; Troyanov, S. I.; Hessen, B.; Teuben, J. H. *Organometallics*, **2002**, *21*, 1759-1765.
- [68] (a) Roesky, H. W.; Haiduc, I.; Hosmane, N. S.; *Chem. Rev.* **2003**, *103*, 2579–2595; (b) Carofiglio, T.; Floriani, C.; Rosi, M.; Chiesivilla, A.; Rizzoli, C. *Inorg. Chem.* **1991**, *30*, 3245–3246.
- [69] (a) Rau, M. S.; Kretz, C. M.; Geoffroy, G. L.; Rheingold, A. L.; Haggerty, B. S. *Organometallics*, **1994**, *13*, 1624–1634. (b) Erker, G.; Albrecht, M.; Werner, S.; Krüger, C.; *Z. Naturforsch.* **1990**, *45b*, 1205–1209. (c) Li, H. L.; Eddaoudi, M.; Plevert, J.; O’Keeffe, M.; Yaghi, O. M. *J. Am. Chem. Soc.* **2000**, *122*, 12409–12410.
- [70] (a) Jancik, V.; Pineda, L. W.; Pinkas, J.; Roesky, H. W.; Neculai, D.; Neculai, A. M.; Herbst-Irmer, R. *Angew. Chem., Int. Ed.* **2004**, *43*, 2142–2145; (b) Zhu, H.; Chai, J.; He, C.; Bai, G.; Roesky, H. W.; Jancik, V.; Schmidt, H.-G.; Noltemeyer, M. *Organometallics*, **2005**, *24*, 380–384;
- [71] During the revision the preparation of LAIEt(OH) by a different route was reported: K. Leszczyńska, I. D. Madura, A. R. Kunicki, J. Zachara, M. Łoś, J. *Organomet. Chem.* **692** (2007) 3907–3913
- [72] Yang, Y.; Schulz, T.; John, M.; Yang, Z.; Jiménez-Pérez, V. M.; Roesky, H. W.; Gurubasavaraj, P. M.; Stalke, D.; Ye, H. *Organometallics* **2008**, *27*, 769–777.
- [73] Newmark, R. A.; Boardman, L. D.; Siedle, A. R. *Inorg. Chem.* **1991**, *30*, 853-856
- [74] (a) Nehete, U. N.; Anantharaman, G.; Chandrasekhar, V.; Murugavel, R.; Walawalkar, M. G.; Roesky, H. W.; Vidovic, D.; Magull, K.; Samwer, K.; Sass, B. *Angew. Chem., Int. Ed.* **2004**, *43*, 3832-3835. (b) Nehete, U. N.; Chandrasekhar,

- V.; Anantharaman, G.; Roesky, H. W.; Vidovic, D.; Magull, J. *Angew. Chem., Int. Ed.* **2004**, *43*, 3842-3844. (c) Nehete, U. N.; Chandrasekhar, V.; Roesky, H. W.; Magull, J. *Angew. Chem., Int. Ed.* **2005**, *44*, 281-284.
- [75 ] Evans, W. J.; Ansari, M. A.; Ziller, J. W. *Polyhedron*. **1997**, *16*, 3429-3434. and references therein.
- [76] Ding, Y.; Roesky, H. W.; Noltemeyer, M.; Schmidt, H.-G. *Organometallics*, **2001**, *20*, 1190-1194. (b) Ding, Y.; Hao, H.; Roesky, H. W.; Noltemeyer, M.; Schmidt, H.-G. *Organometallics*, **2001**, *20*, 4806-4811. (c) Ding, Y.; Ma, Q.; Roesky, H. W.; Herbst-Irmer, R.; Noltemeyer, M.; Schmidt, H.-G. *Organometallics* **2002**, *21*, 5216-5220.
- [77] Weinert, C. S.; Fenwick A. E.; Fanwick P. E.; Rothwell I. P. *Dalton Trans.* **2003**, 532-539.
- [78] Birmingham, J. M.; Wilkinson, G. J. *Am. Chem. Soc.* **1956**, *78*, 42-44.
- [79] (a) Hill, G. S.; Manojlovic-Muir, L.; Muir, K. W.; Puddephatt, R. J. *Organometallics*. **1997**, *16*, 525-530. (b) Stender, M.; Phillips, A. D.; Power, P. P. *Inorg. Chem.* **2001**, *40*, 5314-5315 (c) Vagedes, D.; Fröhlich, R.; Erker, G.; *Angew. Chem. Int. Ed.* **1999**, *38*, 3362-3365
- [80] (a) Danopoulos, A. A.; Galsworthy, J. R.; Green, M. L. H.; Cafferkey, S.; Doerrer L. H.; Hursthouse, M. B. *Chem. Commun.*, **1998**, 2529-2530 (b) Bergquist, C.; Bridgewater, B. M.; Harlan, C. J.; Norton, J. R.; Friesner, R. A.; Parkin, G. *J. Am. Chem. Soc.* **2000**, *122*, 10581-10590; (c) Beringhelli, T; Maggioni, D.; D'Alfonso, G. *Organometallics* **2001**, *20*, 4927-4938
- [81] Neculai, D.; Roesky, H. W.; Neculai, A. M.; Magull, J.; Walfort, B.; Stalke, D. *Angew. Chem. Int. Ed.* **2002**, *41*, 4294-4296
- [82] (a) Manastyrskyj, S.; Dubeck, M. *Inorg. Chem.* **1964**, *3*, 1647. (b) Maginn, R. E.; Manastyrskyj, S.; Dubeck, M. *J. Am. Chem. Soc.* **1963**, *85*, 672. (c) Manastyrskyj, S.; Maginn, R. E.; Dubeck, M. *Inorg. Chem.* **1963**, *2*, 904. (d) Marks, T. *Prog. Inorg. Chem.* **1978**, *24*, 51-107. (e) Marks, T.; Fischer, R. D. *NATO Adv. Study Inst. Ser., Ser. C*, **1979**, 44.
- [83] (a) Tilley, T. D.; Andersen, R. A. *Inorg. Chem.* **1981**, *20*, 3267-3270; (b) Watson,

- P. L.; Whitney, J. F.; Harlow, R. L. *Inorg. Chem.* **1981**, *20*, 3271-3278; (c) Rauoch, M. D.; Morlarty, K.J.; Atwood, J. L.; Weeks, J. A.; Hunter, W. E.; Brittain, H.O. *Organometallics* **1986**, *5*, 1281-1283
- [84] (a) Jimenez-Perez, V. M.; Munoz-Flores, B. M.; Roesky, H. W.; Schulz, T.; Pal, A.; Beck, T.; Yang, Z.; Stalke, D.; Santillan, R.; Witt, M. *Euro. J. Inorg. Chem.* **2008**, *13*, 2238-2243. (b) Yang, Z.; Ma, X.; Roesky, H. W.; Yang, Y.; Jimenez-Perez, V. M.; Magull, J.; Ringe, A.; Jones, P. G. *Euro. J. Inorg. Chem.* **2007**, *31*, 4919-4922. (c) Daniele, S.; Drost, C.; Gehrhus, B.; Hawkins, S. M.; Hitchcock, P. B.; Lappert, M. F.; Merle, P. G.; Bott, S. G. *Dalton Transactions*, **2001**, *21*, 3179-3188. (d) Galka, C. H.; Troesch, D. J. M.; Ruedenauer, I.; Gade, L. H.; Scowen, I.; McPartlin, M. *Inorg. Chem.* **2000**, *39*, 4615-4620. (e) Lee, C. H.; La, Y. H.; Park, J. W. *Organometallics*, **2000**, *19*, 344-351.
- [85] (a) Weihricha, R.; Limagea, M.H.; Parkerb, S.F.; Fillauxa, F. *J. Molecular Structure*, **2004**, *700*, 147-149; (b) Haddon, R. C.; Chichester, S. V.; Marshall, J. H. *Tetrahedron*. **1986**, *42*, 6293-6300. (c) Haddon, R. C.; Rayford, R.; Hirani, A. M. *J. Org. Chem.* **1981**, *46*, 4587-4588
- [86] (a) Pagni, R. M.; Peebles, W.; Haddon, R. C.; Chichester, S. V. *J. Org. Chem.* **1990**, *55*, 5595-5601. (b) Peebles, W.; Pagni, R. M.; Haddon, R. C. *Tetrahedron Letters* **1989**, *30*, 2727-2730. (c) Mandal, S. K.; Itkis, M. E.; Chi, X.; Samanta, S.; Lidsky, D.; Reed, R. W.; Oakley, R. T.; Tham, F. S.; Haddon, R. C. *J. Am. Chem. Soc.* **2005**, *127*, 8185-8196. (d) Franz, K. D. *Chem. Lett.* **1979**, *3*, 221-224.
- [87] Wilkinson, G. *J. Am. Chem. Soc.* **1954**, *76*, 6210.
- [88] a) Edelmann, F. T. *Coor. Chem. Rev.* **2009**, *253*, 343 -409. b) Gottfriedsen, J.; Edelmann, F. T. *Coor. Chem. Rev.* **2007**, *251*, 142-202. c) Edelmann, F. T. *Coor. Chem. Rev.* **2006**, *250*, 2511-2564. d) Gottfriedsen, J.; Edelmann, F. T. *Coor. Chem. Rev.* **2006**, *250*, 2347-2410.
- [89] a) Cui, C.; Shafir, A.; Schmidt, J. A. R.; Oliver, A. G.; Arnold, J. *Dalton Trans.* **2005**, 1387-1393. b) Yao, Y.; Zhang, Y.; Shen, Q.; Yu, K. *Organometallics* **2002**, *21*, 819-824.
- [90] a) Lu, Z.; Yap, G. P. A.; Richeson, D. S. *Organometallics* **2001**, *20*, 706-712. b)



- Zhou, Y.; Yap, G. P. A.; Richeson, D. S. *Organometallics* **1998**, *17*, 4387-4391. c) Trifonov, A. A.; Lyubov, D. M.; Fedorova, E. A.; Fukin, G. K.; Schumann, H.; Mühle, S.; Hummert, M.; Bochkarev, M. N. *Eur. J. Inorg. Chem.* **2006**, 747-756.
- [91] a) Ajellal, N.; Lyubov, D. M.; Sinenkov, M. A.; Fukin, G. K.; Cherkasov, A. V.; Thomas, C. M.; Carpentier, J. F.; Trifonov, A. A. *Chem. Eur. J.* **2008**, *14*, 5440-5448. b) Trifonov, A. A.; Lyubov, D. M.; Fedorova, E. A.; Skvortsov, G. G.; Fukin, G. K.; Kurskii, Y. A.; Bochkarev, M. N. *Russ. Chem. Bull. Int. Ed.* **2006**, *55*, 435-441. c) Trifonov, A. A.; Lyubov, D. M.; Fukin, G. K.; Baranov, E. V.; Kurskii, Yu. A. *Organometallics* **2006**, *25*, 3935-3942.
- [92] a) Neculai, A. M.; Neculai, D.; Nikiforov, G. B.; Roesky, H. W.; Schlicker, C.; Herbst-Irmer, R.; Magull, J.; Noltemeyer, M. *Eur. J. Inorg. Chem.* **2003**, 3120-3126. b) Neculai, D.; Roesky, H. W.; Neculai, A. M.; Magull, J.; Schmidt, H. G.; Noltemeyer, M. *J. Organomet. Chem.* **2002**, *643-644*, 47-52. c) Neculai, D.; Roesky, H. W.; Neculai, A. M.; Magull, J.; Herbst-Irmer, R.; Walfort, B.; Stalke, D. *Organometallics*. **2003**, *22*, 2279-2283.
- [93] Evans, W. J. *Inorg Chem*, **2007**, *46*, 3435-3449.
- [94] Li, H. X.; Xu, Q. F.; Chen, J. X.; Cheng, M. L.; Zhang, Y.; Zhang, W. H.; Lang, J. P.; Shen, Q. *J. Organomet. Chem*, **2004**, *689*, 3438-3448.
- [95] Anwander, R. *Angew. Chem.* **1998**, *110*, 619-622; *Angew. Chem. Int. Ed.* **1998**, *37*, 599-602.
- [96] Kretschmer, W. P.; Teuben, J. H.; Troyanov, S. I. *Angew. Chem.* **1998**, *110*, 92-94; *Angew. Chem. Int. Ed.* **1998**, *37*, 88-90.
- [97] Li, H. X.; Ren, Z. G.; Zhang, Y.; Zhang, W.H.; Lang, J. P.; Shen, Q. *J. Am. Chem. Soc.* **2005**, *127*, 1122-1123.
- [98] Dubé, T.; Conoci, S.; Gambarotta, S.; Glenn P.; Yap, A.; Vasapollo, G. *Angew. Chem.* **1999**, *111*, 3890-3892; *Angew. Chem. Int. Ed.* **1999**, *38*, 3657-3659.
- [99] Evans, W. J.; Champagne, T. M.; Davis, B. L.; Allen, N. T.; Nyce, G. W.; Johnston, M. A.; Lin, Y. C.; Khvostov, A.; Ziller, J. W. *J. Coord. Chem.* **2006**, *59*, 1069-1087.
- [100] Lorenz, V.; Edelmann, A.; Blaurock, S.; Freise, F.; Edelmann, F. T.

*Organometallics* **2007**, *26*, 4708-4710

[101] a) Kottke, T.; Stalke, D.J. *Appl. Crystallogr.* **1993**, *26*, 615-619. b) Stalke, D.

*Chem. Soc. Rev.* **1998**, *27*, 171-178.

[102] SAINT-NT, Bruker AXS Inc., Madison, Wisconsin (USA) **2000**.

[103] Sheldrick, G. M. *SADABS 2.0*, Universität Göttingen: Göttingen, Germany, **2000**.

[104] Sheldrick, G. M. *Acta Crystallogr. Sect. A* **1990**, *46*, 467-473.

[105] Sheldrick, G. M. *Acta Crystallogr. Sect. A* **2008**, *64*, 112-122.

## List of Publications

1. *A Chlorine-Centered Cluster of Composition  $[(Me_3Si)_2NC(NCy)_2SmCl_2]_5(thf)_2$  and a Comparison with the Heavier Ytterbium Congener  $[(Me_3Si)_2NC(NCy)_2YbCl_2]_2(LiCl)_2(thf)_4$*   
**Zhensheng Zhang**, Herbert W. Roesky, Thomas Schulz, Dietmar Stalke, Alexander Döring  
*Eur. J. Inorg. Chem.* **2009**, 4864–4869
2. *Synthesis and Structural Characterization of Monomeric Heterobimetallic Oxides with a Ge(II)-O-M Skeleton (M = Yb, Y)*  
Ying Yang, Herbert W. Roesky, Peter G. Jones, Cheuk-Wai So, **Zhensheng Zhang**, Regine Herbst-Irmer, and Hongqi Ye  
*Inorg. Chem.* **2007**, 46, 10860-10863
3. *Synthesis, structural characterization, and reactivity of the ethyl substituted aluminum hydroxide and catalytic properties of its derivative*  
Ying Yang, Prabhuodeyara M. Gurubasavaraj, Hongqi Ye, **Zhensheng Zhang**, Herbert W. Roesky, Peter G. Jones  
*J. Organomet. Chem.* **2008**, 693, 1455–1461
4. *Synthesis and Characterization of Aluminum-Containing Tin(IV) Heterobimetallic Sulfides*  
Zhi Yang, Xiaoli Ma, Vojtech Jancik, **Zhensheng Zhang**, Herbert W. Roesky, Jörg Magull, Mathias Noltemeyer, Hans-Georg Schmidt, Raymundo Cea-Olivares, Rubén A. Toscano  
*Inorg. Chem.* **2006**, 45, 3312-3315

## Lebenslauf

Name: Zhenheng Zhang  
Geboren: Tianjin, P. R. China, am April 19<sup>th</sup>, 1974  
Staatsangehörigkeit: Chinesisch  
Familienstand: ledig  
Eltern: Haiting Zhang (Vater)  
Zhiping Zhou (Mutter)

## Schulausbildung

08.1981–06.1987: Grundschule in Tianjin, China  
08.1987–06.1993: Mittelschule in Tianjin, China

## Hochschulausbildung

09/1993 - 07/1997: Studium der Chemie am Institut der Chemie, Nankai Universität,  
Tianjin, China  
07/1997: Abschluß: *Bachelor of Science*  
09/1999 – 01/2003: Studium der Organische Chemie am the Institut der Chemie,  
Nankai Universität, Tianjin, China  
01/2003: Abschluß: *Master of Science*  
04/2005 – 06/2005: Äquivalenzprüfung zum Diplomexamen – Fach Chemie, Göttingen  
07/2005 – 10/2010: Anfertigung der Dissertation unter Anleitung von Prof. Dr. Dr.  
h. c. mult. H. W. Roesky am Institut für anorganische Chemie  
der Georg-August-Universität Göttingen

## Berufstätigkeit

07/1997-08/1999: Forschungsarbeit im Tianjin Toko Ink Co., Ltd., Tianjin, China  
01/2003-03/2005: Forschungsarbeit am Institut der Chemie der Nankai Universität,  
Tianjin, China